ABSTRACT

ABDUL HALIM ZAIM. Computing Call Blocking Probabilities in LEO Satellite Networks. (Under the direction of Professor Harry G. PERROS and Professor George N. ROUSKAS.)

We present an analytical model for computing call blocking probabilities in a LEO satellite network that carries voice calls. Both satellite-fixed and earth-fixed constellations are considered. The model is analyzed approximately by decomposing it into sub-systems. Each sub-system is solved exactly in isolation using a Markov process and the individual results are combined together through an iterative method. Our model also calculates call blocking probabilities due to hand-offs. Numerical results demonstrate that our method is accurate for a wide range of traffic patterns and for constellations with a number of satellites that is representative of commercial systems. For larger systems, we also propose a method to calculate upper and lower bounds for call blocking probabilities.

Computing Call Blocking Probabilities in LEO Satellite Networks

by

Abdul Halim Zaim

A thesis submitted to the Graduate Faculty of
North Carolina State University
in partial fulfillment of the
requirements for the Degree of
Doctor of Philosophy

Electrical and Computer Engineering

Raleigh

2001

APPROVED BY:

Co-Chair of Advisory Committee	Co-Chair of Advisory Committee

BIOGRAPHY

Abdul Halim Zaim, got his M.Sc. degree from Bogazici University Computer Engineering Department in 1996, is pursuing his Ph.D. degree at North Carolina State University, Electrical and Computer Engineering Department. He worked one year at Alcatel between 1998-1999 as a co-op. He taught different courses at Istanbul University as a teaching assistant between 1993-1997. His research interests are computer performance evaluation, satellite and high speed networks, and computer network design.

Contents

List of Figures

List of Tables

Chapter 1

Introduction

The communication revolution that is currently taking place has increased the demand for a broad ranges of telecommunication services and also for wireless access solutions. Satellite Communication Systems and especially Non-Geostationary Satellite Systems are good candidates for providing communication services globally in a cost effective manner. Non-Geostationary Satellite Systems can be used for mobile telephony and data transmission without the need for complex ground-based infrastructures, a key component of existing land-based cellular schemes. The cost of the installation is fixed and there is no relationship between cost and distance. For example, linking every home to internet with fiber links costs 300 billion dollars while via satellite it costs only 9 billion dollars [1].

By using satellites at low altitudes, Low Earth Orbital Satellite Systems can reduce power requirements on-board and on the ground. This results in lightweight low power radio telephones with small low profile antennas. In addition, low altitude means minimized transmission delay nearly equal to land-based networks. A more detailed description of Mobile Satellite Communication Systems can be found in ([2]-[7]).

Satellite Communications for commercial purposes started in the mid-80s. Several U.S. corporations introduced direct-to-home (DTH) satellite broadcasting at a time when cable TV was still being established. Nowadays, there is a lot of investments in the satellite industry especially by telephone companies, and more than 200 satellites distributed over a geostationary arc at an altitude 36000 km are rotating at the same speed as the earth.

Geostationary satellites dominated for a long time long-distance communications, because of their large coverage area that permits them to connect distant telephone exchanges. These satellites were used in international telephony, especially trans-Atlantic

calls.

Technological improvements in fiber optic and switching decreased geostationary satellites' role in linking land-based telephone exchanges for international calls. Satellite communication started to be seen by telephone companies as a backup for ground links. However, it was still an important medium to broadcast television signals. Currently, geostationary satellites are seen as a good medium for non-interactive broadcast applications, but not for two way communication applications.

Starting from the early 90s telecommunication industry witnessed a lot of proposals for Low Earth Orbital Satellite Systems. Some of these proposed systems are currently in operation, such as ORBCOMM, Iridium, and Globalstar. Several others, such as LEOone, SkyBridge, and Teledesic, are scheduled to start after 2000 ([12]-[19]). These systems differ in many aspects, including the number of orbits, the number of satellites per orbit, the number of beams per satellite, their capacity, the band they operate (K-Band, Ka-Band, L-Band, etc.), and the access method employed (FDMA, TDMA, or CDMA). Also, these systems provide different services and they may or may not have on-board switching capabilities. For instance, Teledesic has on-board digital processing and switching, while other systems, such as the Globalstar, act as a bent pipe. Despite these differences, from the point of view of providing telephony-based services, the principles of operation are very similar, and thus, the analytical techniques developed in this thesis are applicable to any LEO satellite system that offers such services.

1.1 Orbit Types

In this section, we describe briefly the different orbit types. Description about orbit types can be found in ([8]-[11]).

- Low Earth Orbit (LEO) : LEO orbits are at an altitude less than 2000 km above the earth. Their orbit period is about 90 minutes. The radius of the footprint area of a LEO satellite is between 3000 km to 4000 km. The duration of a satellite in LEO orbit over the local horizon of an observer on earth is approximately 20 minutes. Propagation delay is about 25ms.

  For global connectivity in LEO type orbital systems, a large number of satellites is required in a number of different inclined orbits. Due to the relatively large movement

of a satellite in LEO orbit with respect to an observer on the Earth, satellite systems using this type of orbit need to be able to cope with large Doppler shifts. Detailed information about Doppler Shifts can be found in ([20]).

- Medium Earth Orbit (MEO) or Intermediate Circular Orbits (ICO) : MEOs are circular orbits at an altitude of around 10000 km. Their orbit period is about six hours. The duration of a satellite in MEO orbit over the local horizon of an observer on earth is a few hours. Fewer satellites on two or three orbits is enough to provide a global coverage in a MEO system. Propagation delay in a MEO system is about 125ms.

- Highly Elliptical Orbit (HEO) : As they are not circular, their perigees and apogees are not the same. (A perigee is the point of the orbit that is the nearest to the gravitational center of the earth. An apogee is the point of the orbit that is the farthest from the gravitational center of the earth). In order to provide communication services to locations at high northern latitudes, in a typical HEO, the perigee is about 500 km, while the apogee is about 50000 km. The orbits form an inclination with the equator plane of 63.4^o. The orbit period varies between eight to 24 hours.

- Geosynchronous Orbit : This is an orbit which produces a repeating ground track. The orbit period is approximately an integer multiple or sub-multiple of a sidereal day. (A sidereal day is the time required for the earth to rotate once on its axis relative to the stars. It is equal to 23 h 56 m 4 s).

- Geostationary Orbit (GEO) : This is a circular orbit in the equatorial plane with an orbital period equal to that of the earth. GEOs are at an altitude of 35786 km. A satellite in GEO orbit appears to be fixed above the earth's surface. The footprint of a GEO satellite covers nearly one third of the earth's surface (between 75^o south to 75^o north). Therefore, a near global coverage can be obtained with three satellites, but a full global coverage is not possible. Its uplink plus downlink propagation delay is 250 ms.

- Polar Orbit : This is an orbit which covers polar regions with an inclination angle of 90^o to the equator and satellites moving from south to north. This orbit is fixed in space relative to the earth, and the earth rotates underneath. A single satellite in a polar orbit can provide global coverage over a long period. During one orbit period,

it will cover some areas on the earth. Meanwhile, the earth rotates beneath the orbit and during the next passage, the same satellite will cover other areas on the earth. Therefore, after a long period the satellite will cover all areas on the earth.

Most small-LEO systems employ polar or near-polar orbits.

- Sun-Synchronous Orbit : In a sun-synchronous orbit, the orbit plane is at a constant angle with the sun plane. This results in consistent light conditions for the satellite.

In this thesis we deal with the performance of LEO satellite systems. Therefore, in Chapter 2, we review related published material such as routing, performance evaluation, and handover. In the following section, we define the various terms used in LEO satellite systems.

1.2 Architecture and Notation

1.2.1 Notations

Satellite Constellation : According to Husson [10], a constellation of satellites is a set of identical satellites, launched in several orbital planes with the orbits having the same altitudes.

Orbit Period : The time a satellite completes one full rotation around the earth within its own orbit is called the *Orbit Period*.

System Period : In a constellation, satellites move in a synchronized way in trajectories relative to the earth. The position of all the satellites in a satellite constellation at some instance of time, repeats itself after a predetermined period which is usually several days. This period is called the *System Period*. System period is calculated as an integer common multiple of the orbit period and the earth rotation time (sidereal day).

Seam : As seen in Figure 1.1. The satellite in Orbit 1 moves from north pole to south pole and then from south pole to north pole. The satellites at Orbit 1 and Orbit 6 move in opposite directions. For that reason, there is a seam in between these two orbits, and this seam indicates a change of direction. With respect to this seam, the constellation comprises two hemispherical areas of co-rotating orbits, each extending from the north to the south pole.

Intersatellite Link : This is a direct connection between two satellites using line of sight. Intersatellite Links (ISL) permit two mobile or fixed points on earth in two different

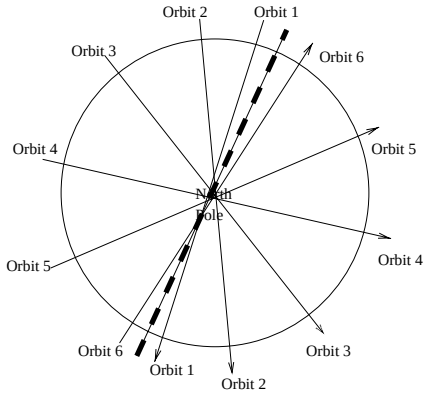

Figure 1.1: Schematic Polar View of The Iridium Satellite Constellation

footprints to communicate without the need of terrestrial systems. Of course, this feature necessitates the solution of complex handover problems. A distinction has to be made between *intraplane* ISLs which connect satellites in the same orbital plane and *interplane* ISLs which connect satellites in adjacent planes. Adding ISLs also introduces flexibility in routing, builds inherent redundancy into the network, and avoids the need for visibility of both user and gateway by each satellite in the constellation. It is easier to construct satellites with fixed intersatellite link antennas. However, for interplane ISLs, satellites change angles and distance as their orbits separate and converge. As a consequence, relative velocities between satellites increase, tracking control problems occur as antennas steer, and Doppler shift usage becomes a necessity. On the other hand, fixed antennas are possible in the intraplane ISLs in case of circular orbit constellations. The choice of circular orbits also has the advantage of allowing a relatively constant footprint size and shape. As a result of this, most proposed satellite constellations adopt circular orbits.

Footprint : The spherical area of the earth covered by a satellite with an elevation angle equal to or greater than a certain minimum elevation angle.

Elevation Angle : The angle between the line from the earth's surface to the satellite and the tangent at that point considered. This angle decreases as the satellites move further from the point on the surface of the earth. As the angle becomes smaller, so does the signal power coming from the satellite. Therefore, if the angle is smaller than a certain value which is called *minimum elevation angle*, the point on earth starts hearing another satellite from which the signals are coming stronger.

Cell : To improve the bandwidth and frequency efficiency, the satellite footprint area is divided into smaller cells. For each cell within a footprint area, a specific beam of the satellite is used.

Satellite Fixed Cell Coverage : If the satellite antenna sending beams is fixed, then as the satellite moves in its orbit, together with its footprint, the cells also move. This constellation is said to have satellite-fixed cell coverage. As satellites move, so do their footprints, and the users handover from one beam to another (*beam handover*) or from one satellite to another (*satellite handover*) whether they are fixed or mobile. The mobility of the user only effects the time of handovers. Therefore, the number of handovers during a call depends on the call duration, the beam size, the satellite footprint size and the satellite speed.

Earth-Fixed Cell Coverage : Unlike the satellite-fixed cell coverage, in earth-fixed cell coverage, the beam transponders are not fixed. The earth surface is divided into cells, as in cellular systems, and a cell is serviced by a beam of a satellite while that area is within the footprint area of that satellite. During an interval of time, which is the satellite's view time, each beam services a specific fixed cell on the earth. During the satellite handover, each beam s reassigned to the cells which is adjacent to the one it was serving. Therefore, in these systems, both beam and satellite handovers occur at the same time. Earth-fixed cell coverage satellite systems decrease the handover failure probability. However, they have some complications from the point of implementation especially at the spacecraft's payload point. The spacecraft should be capable of handling two functions: beam steering and cell switching.

Beam Steering : In order for the same beam to be fixed onto the same cell on the earth, the satellite's antenna should steer in the opposite direction of its motion. This process is illustrated in Figure 1.2. As seen in this figure, the cells numbered with 1,2 and 3 use beams c, b, and a respectively while those cells are within the footprint area of the satellite S1. Therefore, during the time interval dt, the beam-to-cell allocation remains fixed as shown in Table 1.1.

Cell Switching : When it becomes not possible for the satellite to steer the antenna, then cell switching occurs. The steering of the beam can be mechanical or electronic. In LEO systems, where the satellite motion relative to earth cells is high, electronic steering is preferable. It requires the use of active array antennas. The cell switching process is illustrated in Figures 1.3 and 1.4. After a time interval, the maximum steering angle is

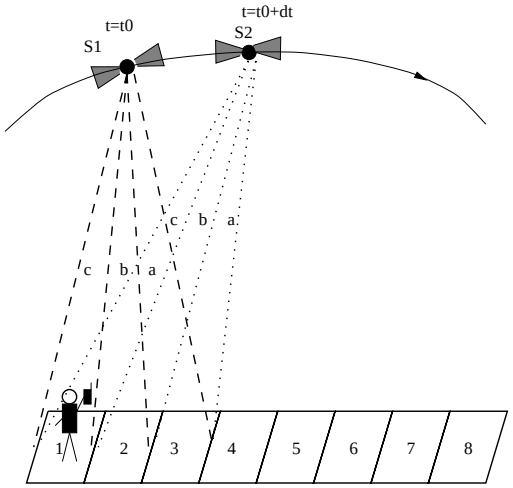

Figure 1.2: Beam Cell Steering

Cell	Beam
1	c
2	b
3	a

Table 1.1: Beam to Cell Allocation

reached, and the antenna can not steer any more. Therefore, the beam to cell allocation is changed, and this is called cell switching.

Streets-of-Coverage : A street of coverage is a line of overlapping footprints of satellites within the same orbit. This is illustrated in Figure 1.5. As seen in the figure, a street is like a strip of earth aligned along and centered about the subsatellite earth track. If enough satellites are used to cover the whole street, an overall coverage can be obtained within the orbit. The street width is smaller than the footprint diameter. For the global coverage, streets of coverage should be overlapped from different orbital planes. This may be done in two different ways:

Arbitrarily Phased Constellations : If the angles between satellites in different orbits are not maintained as the satellites orbit around the earth, then the constellation is called an arbitrarily phased constellation. This is because of the phasing angles change with time and location of satellites. Teledesic uses this kind of phasing.

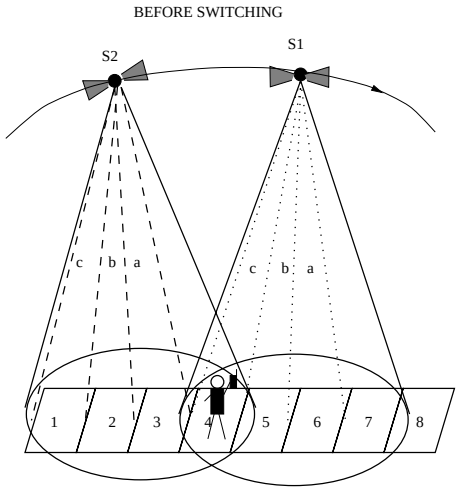

Figure 1.3: Cell Switching, before switching

Phased Constellations : In these constellations, the angles between satellites in different orbits are kept constant. As the angles are the same, the distance between two satellites in different orbits change.

1.2.2 The Architecture Of A Satellite Communication System

A satellite communication system consists of three segments; a space segment, a ground segment and a user segment.

The Space Segment

The space segment contains the satellite and all terrestrial facilities for the control and monitoring of the satellite. This includes tracking, telemetry, and command stations (TT&C) together with the satellite control center where all the operations associated with station-keeping and checking the vital functions of the satellite are performed.

The radio waves transmitted by the earth stations are received by the satellite and this process is called the *uplink*. In reverse the satellite transmits to the earth stations and this is called the *downlink*.

The satellite consists of a payload and a platform. Components of the payload are transmitting antennas and all the electronic equipment which supports the transmission of carriers. The platform consists of all the subsystems which permit the payload to operate.

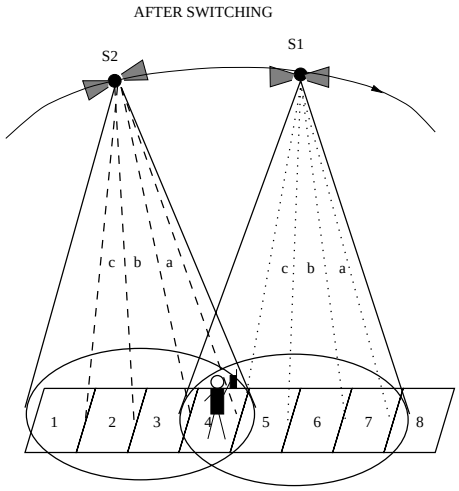

Figure 1.4: Cell Switching, after switching

These are structure, electric power supply, temperature control, attitude and orbit control, propulsion equipment, and tracking, telemetry and command equipment.

The satellite has two important roles: *1)* it amplifies the received signals for retransmission on the downlink, *2)* it changes the frequency of the signal in order to avoid reinjection of a fraction of the transmitted power into the receiver. However, today's satellites are also capable of onboard switching. That is, not only they are relaying the upcoming signals, but at the same time, they route it to the necessary Intersatellite Link according to its destination.

A satellite system must use redundant satellites to ensure a service with a specified availability. There may be two reasons for a satellite to cease its operation: a failure or end of its lifetime.

The Ground Segment

The ground segment consists of the equipment located on the ground that controls and monitors the satellites and links them into terrestrial networks. An earth station includes everything that is involved in communicating with satellites. Ground stations are mostly connected to the end-user's equipment by a terrestrial network, or in the case of small stations, they are connected directly to the end-user's equipment. They differ according to their sizes and carried traffic types.

In new LEO systems with intersatellite links, the ground segment (i.e. the gate-

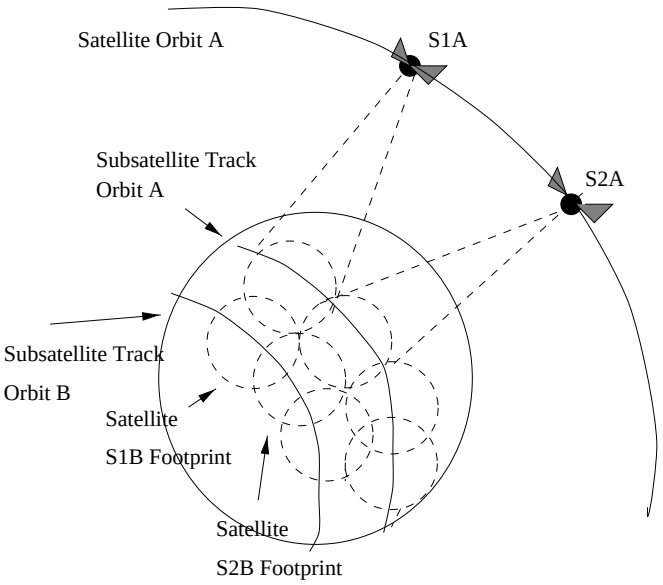

Figure 1.5: Streets of Coverage

way) is responsible for determining the route during the call set-up phase. When a user wants to make a call connection, the connection request is sent to the satellite to which that user can talk to. Afterwards, the satellite sends that request to the ground terminal, or as it is called to the Gateway, located within the same footprint area. The ground terminal locates the called user, finds the route to that user and replies to the satellite with that information. Then, the satellite sets up a connection to the destination satellite, and informs the user. Once the connection set up, the two users can start talking.

The User Segment

The user segment is made up of the equipment used by the subscribers of the satellite system. Generally, the satellite communications industry aims at reaching users in remote regions who do not have adequate local access, like in developing countries. Other prime candidates for satellite services are international business travelers, since good global communications is necessary for the success of their company. A third category of users are those requiring mobile service such as the maritime community.

In addition to the telephone services, satellite communications can provide services such as high speed data, fax, e-mail, and high speed Internet access.

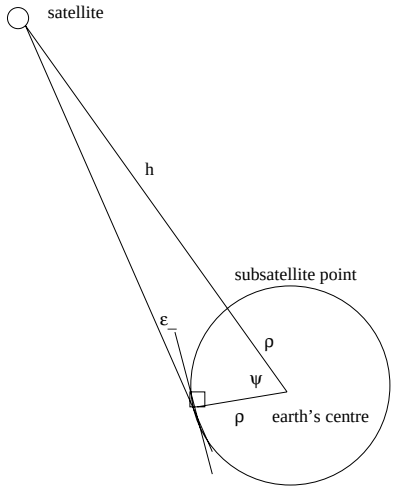

Figure 1.6: Illustration of a geometrical consideration for calculating the footprint area of a satellite

1.2.3 System Parameters

In Werner *et. al.* [21] and in Radzik and Maral [22] give a detailed explanation of how to calculate the system parameters for a LEO satellite system. In this subsection, we briefly give the results of these calculations.

Using Figure 1.6, the half sided center angle of the footprint can be calculated by the following formulae

$$\psi = \frac{\pi}{2} - \epsilon_{min} - \sin^{-1}\left(\frac{\rho}{\rho + h} * cos\left(\epsilon_{min}\right)\right) \tag{1.1}$$

From the above formula, a lower limit for the number of satellites to be used can be calculated. For an uninterrupted communication, the footprints should overlap. As each circular footprint has six neighboring footprints, the effective area for communication, is the hexagonal area formed by connecting the intersection of the circular footprints. This hexagon consists of six isosceles spherical triangles, each one with an angle of 60 degree at the center of the footprint and two identical angles

$$\alpha = \tan^{-1}\left(\frac{\sqrt{3}}{\cos\psi}\right) \tag{1.2}$$

at the periphery of the footprint.

If we calculate the spherical excess of the triangles with the following formulae

$$\xi = 2\alpha - \frac{2\pi}{3} \tag{1.3}$$

Then the area of the hexagon is

$$A = 6\rho^2\xi \tag{1.4}$$

Therefore,

$$n = \frac{4\pi\rho^2}{A} = \frac{\pi}{3\alpha - \pi} \tag{1.5}$$

satellites are necessary to cover the earth.

After calculating the number of satellites, another important system parameter is the number of orbits. To find the number of orbits, it is enough to focus on the equator. On the condition that in every orbit there are at least two satellites, each orbit covers $3\rho\psi$ of the equator. Therefore, at least

$$\Omega = \lceil \frac{2\pi}{3\psi} \rceil \tag{1.6}$$

orbits should be used. If we use this formula and first calculate the number of orbit, then a more precise formula for the number of satellites can be given as follows:

$$n' = \lceil \frac{2\pi}{\sqrt{3}\psi} \rceil \tag{1.7}$$

Chapter 2

Literature Review

Despite the importance of satellite systems, their performance has not been adequately evaluated. In satellite systems, the main concern is usually the calculation of the blocking probability of ongoing calls during satellite handovers. A call forced to terminate during a handover if it can not find empty channels on the next satellite. The blocking of calls due to handovers can severely decrease the reliability of the system. Another performance measure of interest is the blocking probability of new calls. A new call gets blocked if there is not enough capacity to carry it. Increasing new call blocking, decreases the throughput of the system. There is usually a trade off between new call blocking and handover call blocking. From the point of quality of service, it is usually preferable to decrease the handover call blocking without decreasing new call blocking drastically. Most of the studies performed about the performance of LEO satellite systems were concentrated on the calculation of handover call blocking probabilities. In this section, we review the literature related to the performance evaluation of LEO systems. For that purpose, we classify the papers reviewed in this section in two main groups. The first group deals with traffic characterization and performance evaluation issues. The second group, deals with the handover problem. In most of these papers the dependency among the amount of traffic in different cells was neglected.

2.1 Performance Analysis

Single M/M/K/K Queue Analysis: In Ganz *et al* [23] investigated the performance of low earth orbit satellite systems. Performance was expressed in terms of the

distribution of the number of handovers occurring during a single transaction time and the *average call drop probability*. Both beam to beam and satellite to satellite handovers were taken into account. The variables used in performance calculation are the system constellation, the satellite speed and direction, the cell size and the average duration of a transaction. With the assumption that the number of handover calls entering a cell is equal to the number of handover calls leaving the cell, the number of calls in a cell is the number of calls generated by the cell. Each satellite was modeled as an M/M/K/K queue. Mitra ([56]) suggested a similar extension to a classical M/M/K/K model for circuit-switched networks. However, in the system that Mitra defined, there was only one central link flooded with other links and the dependency exists only between the central link and flooding link. The connection switches are nonblocking.

Coverage and Interference Related Analysis: In Jamalipour [24] investigates the traffic characteristics of LEO based systems by defining a probability density function for the signal level. He defined three important areas: coverage or footprint area in which users communicate with the specified satellite, interference area defined by the final line of sight, and observed area consists of the coverage area of three adjacent satellites. Performance measures for the system were throughput and average delay on uplink channels.

Analysis By Simulation: In Papapetrou *et al* [25] reported on a simulator to analyze LEO systems. The simulator was designed based on Motorola's Celestri System. However, it can be modified to model other systems as well. Inputs to the simulator were orbit altitude, orbit period, number of satellites, number of orbits, inclination, intraplane ISL per satellite, interplane ISL per satellite, right ascension and phase shift. The authors used Dijkstra's shortest path algorithm (DSPA) and Werner's Dynamic Routing Algorithm which is explained in Section 2.3.1. In this simulator, they use two different traffic types, Poisson, and self-similar.

2.2 Handovers

In mobile satellite systems, channel allocation can be done either in a fixed way or dynamically. Early satellite systems used fixed channel assignment techniques, whereby channels are assigned to cells permanently. On the other hand, in dynamic channel assignment, the channels are allocated to cells according to call requests. The following two main strategies are used for channel allocation: Queueing Schemes, Channel Reservation

Schemes. The aim of these schemes is to give priority to handover requests in order to improve the quality of service. In this section, proposals related with these two techniques have been investigated. In Santos *et al.* [28] compared these techniques under fixed and dynamic channel allocation. According to Santos *et al.*, combining queueing and guard channels decreases both dropping and handover traffic while increasing the new call blocking.

Queueing Schemes: Del Re *et al.* [29]-[31] proposed an analytical model to analyze handover queueing strategies under fixed channel allocation. They compared their results with some dynamic channel allocation schemes. Their method is designed for satellite-fixed cell coverage. They modeled each footprint area as an M/M/K/K queue where the arrival and departure rates were calculated according to the footprint geometry.

In Pennoni and Ferroni [32] described an algorithm to improve the performance of LEO systems. They defined two queues for each cell, one for new calls and one for hand-off calls. The calls are held in these two queues for a maximum waiting time. If they are not served within this time, they are dropped. The queue for new calls has a maximum waiting time equal to 20 sec. The queue for hand-off calls has a maximum waiting time equal to the cross-over time of the overlapping zone of two adjacent cells. The hand-off queue has higher priority than the new calls queue.

In Dosiere *et al.* [33] used the same model as Pennoni and Ferroni to calculate the hand-off traffic rate over a street-of-coverage. Once the hand-off arrival rate was calculated, the total arrival rate was calculated as the sum of the new call arrival rate and the hand-off arrival rate. The call departure rate was defined as the sum of the call termination rate and the handover rate. These values were then put into Erlang-B formulae to calculate the blocking probability.

In Ruiz *et al* [34] used a similar technique to the one used in [32]. However, this time, they used some guard channels for handover calls and they distinguished new arrival rate from handover attempt rate.

Channel Reservation Schemes: In Respero and Maral [35] define a Guaranteed Handover mechanism for LEO satellite systems with Satellite-Fixed Cell Configuration. In this method, channel reservation is performed according to the location of the user. That is, once the user is at a critical distance from the handover point, it requests a reservation from the neighboring satellite. Reservation requests are put into a priority queue. As soon as an idle channel is found, the channel is reserved for a call from the priority queue. The advantage of this method is that the reservation is done only on the next satellite instead

of the whole call path. In that way, the number of redundant circuitry is minimized and the handover success rate is as high as in the static reservation scheme.

In Wan *et al.* [36] proposed a channel reservation algorithm for handover calls. In this algorithm, the following three queues are defined:a queue for handover requests, a queue for new call requests and a queue for available channels. Each request comes with the information indicating the position of the user within the footprint area. This information is then used to calculate the time to the next handover. The channel queue keeps track of the channels available together with the availability time of that channel. That is, if it is an idle channel, it is immediately available. If it is a channel in use, then it will become available at the time of the handover. The aim of the algorithm is to match these channels with the handover and new call request queues according to the available time criteria. A greedy algorithm is used for that purpose.

A similar approach with Wan *et al.* is proposed by Obradovic and Cigoj in [37]. They proposed a dynamic channel reservation scheme.

2.3 Routing Algorithms

The routing problem is divided into two sub problems: Up-and-Down link (UDL) routing and Intersatellite Link (ISL) routing. In UDL routing, the objective is to ensure the continuity of the connection by providing at least two end satellites, one starting and one ending satellite, through the entire connection. In ISL routing, a hitless handover between start and end satellites must be guaranteed in order to avoid forced connection termination. This task is essentially performed by a change of path translation tables in the corresponding start and end satellites. Most of the proposed routing algorithms deal with the ISL routing. User to user routing is taken into account in only a few papers.

2.3.1 Dynamic Virtual Routing

In Werner [38] and Werner *at el* [39], only a solution to the ISL routing problem is given. In Werner *et al* [40], the performance of that routing protocol is calculated using simulation.

Routing is carried out into three steps. In the first step, for each time interval for which the network topology is fixed, the momentary ISL topology is defined. This information is kept in a database. In the second step, new routes are calculated for each

pair of start and end satellites, using the ISL topologies that correspond to the time interval. The routes are produced using a modified-DSPA (M-DSPA). In that algorithm, the DSPA algorithm is applied to define a subset of least-cost paths for all satellite pairs and all time intervals. Therefore, a time dependency is formed. In [41], a neural network approach is used to calculate the path between a given OD pair. The neural network design is similar to the one used in character recognition.

The last step is the optimization. Over one constellation period, an optimization procedure is performed in terms of minimizing the occurrence of path handovers by choosing appropriate paths from each set. The result of this optimization process is a unique set of first choice paths.

2.3.2 Virtual Node Routing

In Moger and Rosenberg [42], users are mapped onto Virtual Nodes(VN), and each VN is connected directly to its neighbors with virtual connections. These VNs behave like ATM switches. Each VN can communicate with a number of cells on the earth. As a satellite within a given VN passes, the next satellite takes the place of that VN. The same cells continue to communicate with the second satellite physically, but virtually they have not changed their VN. Therefore, routing is performed according to the VN topology representing discrete network topologies. More detailed explanation of this routing scheme can be found in [42].

2.3.3 FSA-Based Link Assignment and Routing

In Chang *et al* [43], [45], and [44] the system period is divided into equal length intervals during which the visibility between satellites, that is the topology of the satellites, does not change. A link assignment algorithm is run for each interval. Therefore, the link assignment problem in LEO satellite system is simplified into a set of link assignment problems for a fixed topology network, one per interval.

A Finite State Automaton is designed to represent two different topologies. In FSA, each state represents a topology, which is stable during the time period of that state. When the FSA changes state, the topology of intersatellite links also changes.

The aim of the link assignment is to obtain the topology that maximize the minimum residual capacity, i.e. to maximize the residual capacity of the most congested link.

This objective is equivalent to minimizing the maximum link flow. Therefore, this link assignment gives the same performance with the optimal static routing. Simulated annealing is used to solve this optimization problem. More details can be found in [44] and [45].

In Chang *et al* [43], comparisons between static and dynamic routings have been performed. In dynamic routing, the routing table is updated according to the cost estimation, based on link status information, broadcasted periodically. According to these results, FSA based static routing performs better than static routing.

2.3.4 Probabilistic Routing

In Uzunalioglu *et al* [46], [47] suggested a connection handover protocol for LEO satellite systems called Footprint Handover Rerouting Protocol (FHRP). FHRP is composed of two steps: a Footprint Rerouting (FR) step and an Augmentation step. Footprint Rerouting calculates a minimum cost route between two points on the earth. FR performs this routing process each time it is called. Once a minimum cost route is found, the protocol tries to use it as long as possible using the Augmentation method. Let us imagine that, after some time, either the source or the destination satellite handovers to another satellite. If it is possible to find a direct link between that new satellite and the old route, then that link is added to the route. This method is called Augmentation. The Augmentation step repeats for a predetermined time period. This time period is calculated in such a manner so that the optimality of the route is maintained. At the end of each time period, a FR process is triggered. In Uzunalioglu [48], a routing algorithm based on these ideas is given.

It is possible to control the number of link handovers by choosing the right links during the routing process. However, the connection handover and call termination events are totally out of control and random. Therefore, the aim of Probabilistic Routing Protocol (PRP) is to use a routing algorithm, which postpones link handover to after a connection handover. In a connection handover, end satellites make a handover. In a link handover, only the links connecting end satellites make a handover.

2.3.5 An Optimized Routing Scheme and a Channel Reservation Strategy

Tam and *et al.* [49] defined a Revised Mesh Routing Algorithm(RMA) for LEO satellite systems. In the Mesh Algorithm (MA), the shortest path in three dimension is found. For that purpose, each satellite has been defined by two parameters (x,y) indicating

the satellite coordinates. Then absolute x and y coordinate differences are calculated. This shows how many hops on the x-axis and y-axis it is necessary to reach to the destination satellite. In this way, it is possible to find all candidate routes between source and destination satellites. The decision criteria is the loading on each ISL. Summing all loads on ISLs, and choosing the route with the least sum gives the best route. In MA, the call is blocked if there is not a minimum hop path between source and destination. RMA, unlike MA, uses the Minimum Cost Algorithm to choose a route in case there is not a minimum hop path between source and destination.

The authors also suggested in [49] to reserve an ISL channel for the next visibility topology before accepting a call.

2.4 Summary of the Thesis

In this thesis, we proposed an approximation method for calculating call blocking probabilities in a group of LEO satellites arranged in a single orbit. This approximation method is also applicable to MEO satellites. The approximation algorithm is for both satellite-fixed and earth-fixed types of coverage. It can be used to compute the blocking probability of new calls and also the hand-over call blocking probability. The constraints defined in Chapter 3 give us the opportunity to take into account the dependencies among different links. That makes our Markov Model different than classical M/M/K/K model. Mitra's paper can be seen as a special case of the problem studied in this thesis.

The approximation algorithm is based on decomposition. Specifically, the entire orbit is decomposed into sub-systems, each consisting of a small number of satellites. Each sub-system is analyzed exactly, by observing that its steady-state probability distribution has a product form solution. A CPU-efficient algorithm was proposed to calculate the normalizing constant associated with this product-form solution. The results obtained from each sub-system are combined together in an iterative manner in order to solve the entire orbit.

We have also generalized the above mentioned algorithm to an entire constellation of LEO satellites involving many orbits. The decomposition algorithm is further extended to take into account hand-offs.

In chapter 5, we developed a method to calculate an upper and lower bound on the call blocking probabilities. These bounds permit us to calculate blocking probabilities

in a large system with multiple orbits and multiple beams per satellite.

Chapter 3

The Single Orbit Case

In this chapter we study the problem of carrying voice calls over a LEO satellite network and we present an analytical model for computing call blocking probabilities for a single orbit of a satellite constellation. We first derive an exact Markov process, and corresponding queueing network, for a single orbit under the assumption that satellites are fixed in the sky (i.e., there are no hand-offs of voice calls). We show that the queueing network has a product-form solution, and we develop a method for computing the normalizing constant. In terms of time complexity, our method represents a significant improvement (which we quantify) over a brute-force calculation, however, it can be applied directly to orbits with at most five satellites. For a system with a larger number of satellites, we then present an approximate decomposition algorithm to compute call blocking probabilities by decomposing the system into smaller sub-systems, and solving each sub-system in isolation using the exact solution described above. This approach leads to an iterative scheme, where the individual sub-systems are solved successively until a convergence criterion is satisfied.

Next, we introduce hand-offs by considering the system of satellites as they orbit the earth. For an orbit with earth-fixed coverage, we then show that there is no blocking due to hand-offs, and thus, the solution (exact or approximate) obtained under the assumption that satellites are fixed in the sky can be used to compute call blocking probabilities in this case. For an orbit with satellite-fixed coverage, on the other hand, blocking due to hand-offs does occur. In this case, we show how the queueing network described above can be extended to model call hand-offs by allowing customers to move from one node to another, and we derive the rate of such node-to-node transitions in terms of the speed of the satellites and the shape of the footprints. We also show that the new queueing network has

a product-form solution similar to the one under the no-hand-offs assumption, and thus, the exact and approximate algorithms developed above can be applied directly to compute call blocking probabilities under the presence of hand-offs.

3.1 An Exact Model for the No Hand-Offs Case

Let us first consider the case where the position of the satellites in the single orbit is fixed in the sky, as in the case of geo-stationary satellites. The analysis of such a system is simpler, since no calls are lost due to hand-offs from one satellite to another, as when the satellites move with respect to the users on the earth. This model will be extended in the following section to account for hand-offs in constellations with both earth-fixed and satellite-fixed coverage.

Each up-and-down link of a satellite has capacity to support up to C_{UDL} calls, while each inter-satellite link has capacity equal to C_{ISL} calls. Let us assume that call requests arrive at each satellite according to a Poisson process, and that call holding times are exponentially distributed. As shown on the BCMP theorem([57]), the distribtion of the aggregate system state does not depend on the shape of the required service time distributions, but only on their means. That is, it is enough to estimate the mean arrival and departure rates to apply the model defined in this section. This idea can be emphasized by the analysis of Newell([50]) who analyzed two finite capacity nodes in tandem using diffusion approximations. Although both nodes were using different service time distributions, with the same mean, the results were insensitive to the service distributions.

We now show how to compute blocking probabilities for the 3 satellites in the single orbit of Figure 3.1. The analysis can be generalized to analyze $k > 3$ satellites in a single orbit. For simplicity, we consider only shortest-path routing, although the analysis can be applied to any fixed routing scheme whereby the path taken by a call is fixed and known in advance of the arrival of the call request.

Let n_{ij} be a random variable representing the number of active calls between satellite i and satellite j, $1 \leq i, j \leq 3$, regardless of whether the calls originated at satellite i or j. Let λ_{ij} (respectively, $1/\mu_{ij}$) denote the arrival rate (resp., mean holding time) of calls between satellites i and j. Then, the evolution of the three-satellite system in Figure 3.1

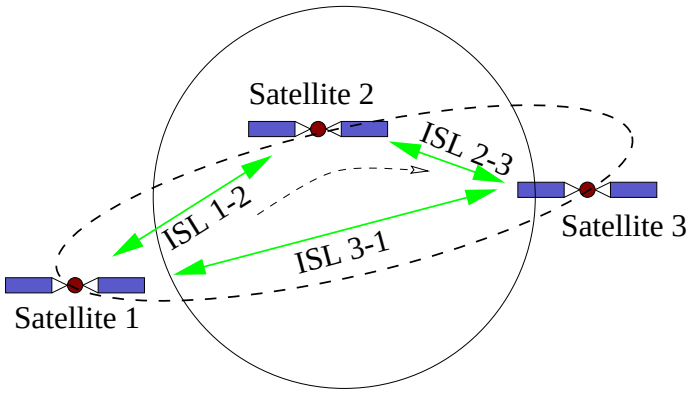

Figure 3.1: Three satellites in a single orbit

can be described by the six-dimensional Markov process:

$$\underline{n} \quad = \quad (n_{11}, n_{12}, n_{13}, n_{22}, n_{23}, n_{33}) \tag{3.1}$$

Also let $\underline{1}_{ij}$ denote a vector with zeros for all random variables except random variable n_{ij} which is 1. The state transition rates for this Markov process are given by:

$$r(\underline{n}, \underline{n} + \underline{1}_{ij}) \quad = \quad \lambda_{ij} \quad \forall\ i, j \tag{3.2}$$

$$r(\underline{n}, \underline{n} - \underline{1}_{ij}) \quad = \quad n_{ij}\ \mu_{ij} \quad \forall\ i, j,\ n_{ij} > 0 \tag{3.3}$$

The transition in (3.2) is due to the arrival of a call between satellites i and j, while the transition in (3.3) is due to the termination of a call between satellites i and j.

Due to the fact that some of the calls share common up-and-down and inter-satellite links, the following constraints are imposed on the state space:

$$2n_{11} + n_{12} + n_{13} \quad \leq \quad C_{UDL} \tag{3.4}$$

$$n_{12} + 2n_{22} + n_{23} \quad \leq \quad C_{UDL} \tag{3.5}$$

$$n_{13} + n_{23} + 2n_{33} \quad \leq \quad C_{UDL} \tag{3.6}$$

$$n_{12} \quad \leq \quad C_{ISL} \tag{3.7}$$

$$n_{13} \quad \leq \quad C_{ISL} \tag{3.8}$$

$$n_{23} \quad \leq \quad C_{ISL} \tag{3.9}$$

Constraint (3.4) ensures that the number of calls originating (equivalently, terminating) at satellite 1 is at most equal to the capacity of the up-and-down link of that satellite. Note that a call that originates and terminates within the footprint of satellite 1 captures two channels, thus the term $2n_{11}$ in constraint (3.4). Constraints (3.5) and (3.6) are similar to (3.4), but correspond to satellites 2 and 3, respectively. Finally, constraints (3.7)-(3.9) ensure that the number of calls using the link between two satellites is at most equal to the capacity of that link. Note that, because of (3.4)-(3.6), constraints (3.7)-(3.9) become redundant when $C_{ISL} \geq C_{UDL}$. In other words, there is no blocking at the inter-satellite links when the capacity of the links is at least equal to the capacity of the up-and-down links at each satellite [1].

It is straightforward to verify that the Markov process for the three-satellite system shown in Figure 3.1 has a closed-form solution which is given by:

$$P(\underline{n}) = P(n_{11}, n_{12}, n_{13}, n_{22}, n_{23}, n_{33}) = \frac{1}{G} \frac{\rho_{11}^{n_{11}}}{n_{11}!} \frac{\rho_{12}^{n_{12}}}{n_{12}!} \frac{\rho_{13}^{n_{13}}}{n_{13}!} \frac{\rho_{22}^{n_{22}}}{n_{22}!} \frac{\rho_{23}^{n_{23}}}{n_{23}!} \frac{\rho_{33}^{n_{33}}}{n_{33}!} \tag{3.10}$$

where G is the normalizing constant and $\rho_{ij} = \lambda_{ij}/\mu_{ij},\ i,j = 1,2,3$, is the offered load of calls from satellite i to satellite j. As we can see, the solution is the product of six terms of the form $\rho_{ij}^{n_{ij}}/n_{ij}!,\ i,j = 1,2,3$, each corresponding to one of the six different types of calls. Therefore, it is easily generalizable to a k-satellite system, $k > 3$.

An alternative way is to regard this Markov process as describing a network of six M/M/K/K queues, one for each type of calls between the three satellites. Since the satellites do not move, there are no hand-offs, and as a consequence customers do not move from one queue to another (we will see in Section 3.3.2 that hand-offs may be modeled by allowing customers to move between the queues). Now, the probability that there are n customers in an M/M/K/K queue is given by the familiar expression $(\rho^n/n!)/\left(\sum_{k=0}^{K} \rho^k/k!\right)$, and therefore, the probability that there are $(n_{11}, n_{12}, n_{13}, n_{22}, n_{23}, n_{33})$ customers in the six queues is given by (3.10). Unlike previous studies reported in the literature, our model takes into account the fact that the six M/M/K/K queues are not independent, since the number of customers accepted in each M/M/K/K queue depends on the number of customers in other queues, as described by the constraints (3.4)-(3.9).

Of course, the main concern in any product-form solution is the computation of

[1] When there are more than three satellites in an orbit, calls between a number of satellite pairs may share a given inter-satellite link. Consequently, the constraints of a k-satellite orbit, $k > 3$, corresponding to (3.7)-(3.9) will be similar to constraints (3.4)-(3.6), in that the left-hand side will involve a summation over a number of calls. In this case, blocking on inter-satellite links may occur even if $C_{ISL} \geq C_{UDL}$.

the normalizing constant:

$$G = \sum_{\underline{n}} \frac{\rho_{11}^{n_{11}}}{n_{11}!}\frac{\rho_{12}^{n_{12}}}{n_{12}!}\frac{\rho_{13}^{n_{13}}}{n_{13}!}\frac{\rho_{22}^{n_{22}}}{n_{22}!}\frac{\rho_{23}^{n_{23}}}{n_{23}!}\frac{\rho_{33}^{n_{33}}}{n_{33}!} \tag{3.11}$$

where the sum is taken over all vectors $\underline{n}$ that satisfy constraints (3.4) through (3.9). We now show how to compute the normalizing constant G in an efficient manner.

We can write $P(\underline{n})$ as:

$$\begin{aligned} P(n_{11}, n_{12}, n_{13}, n_{22}, n_{23}, n_{33}) &= P(n_{11}, n_{22}, n_{33} \mid n_{12}, n_{13}, n_{23}) P(n_{12}, n_{13}, n_{23}) \\ &= P(n_{11} \mid n_{12}, n_{13}, n_{23})\ P(n_{22} \mid n_{12}, n_{13}, n_{23})\ P(n_{33} \mid n_{12}, n_{13}, n_{23})\ P(n_{12}, n_{13}, n_{23}) \\ &= P(n_{11} \mid n_{12}, n_{13})\ P(n_{22} \mid n_{12}, n_{23})\ P(n_{33} \mid n_{13}, n_{23})\ P(n_{12}, n_{13}, n_{23}) \end{aligned} \tag{3.12}$$

The second step in expression (3.12) is due to the fact that, once the values of random variables n_{12}, n_{13}, n_{23}, representing the number of calls in each of the inter-satellite links, is fixed, then the random variables n_{11}, n_{22}, and n_{33} are independent of each other (refer also to Figure 3.1). The third step in (3.12) is due to the fact that random variable n_{11} depends on n_{12} and n_{13}, and it is independent of the random variable n_{23}; similarly for random variables n_{22} and n_{33}.

When we fix the values of the random variables n_{12} and n_{13}, the number of up-and-down calls in satellite 1 is described by an M/M/K/K loss system, and thus:

$$P(n_{11} \mid n_{12}, n_{13}) = \sum_{0 \le 2n_{11} \le C_{UDL} - n_{12} - n_{13}} \frac{\rho_{11}^{n_{11}}}{n_{11}!} \tag{3.13}$$

Similar expressions can be obtained for $P(n_{22} \mid n_{12}, n_{23})$ and $P(n_{33} \mid n_{13}, n_{23})$, corresponding to satellites 2 and 3, respectively. We can now rewrite expression (3.11) for the normalizing constant as follows:

$$\begin{aligned} G = \sum_{0 \le n_{12}, n_{13}, n_{23} \le \min\{C_{UDL}, C_{ISL}\}} & \frac{\rho_{12}^{n_{12}}\rho_{13}^{n_{13}}\rho_{23}^{n_{23}}}{n_{12}!n_{13}!n_{23}!} \left[\left(\sum_{0 \le 2n_{11} \le C_{UDL} - n_{12} - n_{13}} \frac{\rho_{11}^{n_{11}}}{n_{11}!} \right) \right. \\ \times & \left. \left(\sum_{0 \le 2n_{22} \le C_{UDL} - n_{12} - n_{23}} \frac{\rho_{22}^{n_{22}}}{n_{22}!} \right) \left(\sum_{0 \le 2n_{33} \le C_{UDL} - n_{13} - n_{23}} \frac{\rho_{33}^{n_{33}}}{n_{33}!} \right) \right] \end{aligned} \tag{3.14}$$

Let $C = \max\{C_{ISL}, C_{UDL}\}$. Using expression (3.14) we can see that the normalizing constant can be computed in $O(C^3)$ time rather than the $O(C^6)$ time required by a brute force enumeration of all states, a significant improvement in efficiency.

Once the value of the normalizing constant is obtained, we can compute blocking probabilities by summing up all the appropriate blocking states. Consider the 3-satellite orbit of Figure 3.1. The probability that a call which either originates or terminates at satellite 1 will be blocked on the up-and-down link of that satellite is given by:

$$P_{UDL_1} = \sum_{2n_{11}+n_{12}+n_{13}=C_{UDL}} P(\underline{n}) \tag{3.15}$$

while the probability that a call originating at satellite i (or satellite j) and terminating at satellite j (or i) will be blocked by the inter-satellite link (i, j) is:

$$P_{ISL_{ij}} = \begin{cases} 0, & C_{ISL} > C_{UDL} \\ \sum_{n_{ij}=C_{ISL}} P(\underline{n}), & \text{otherwise} \end{cases} \tag{3.16}$$

Once the blocking probabilities on all up-and-down and inter-satellite links have been obtained using expressions similar to (3.15) and (3.16), the blocking probability of calls between any two satellites can be easily obtained. We note that expressions (3.15) and (3.16) explicitly enumerate all relevant blocking states, and thus, they involve summations over appropriate parts of the state space of the Markov process for the satellite orbit. Consequently, direct computation of the link blocking probabilities using these expressions can be computationally expensive. We have been able to express the up-and-down and inter-satellite link blocking probabilities in a way that allows us to compute these probabilities as a byproduct of the computation of the normalizing G. As a result, all blocking probabilities in a satellite orbit can be computed in an amount of time that is equal to the time needed to obtain the normalizing constant, plus a constant. The derivation of the expressions for the link blocking probabilities is a straightforward generalization of the technique employed in (3.12) and is omitted.

3.2 A Decomposition Algorithm for the No Hand-Offs Case

Let k be the number of satellites in a single orbit, and N be the number of random variables in the state description of the corresponding Markov process, $N = k(k+1)/2$. Using the method described above, we can compute the normalizing constant G in time $O(C^{N-k})$ as opposed to time $O(C^N)$ needed by a brute force enumeration of all states. Although the *improvement* in the running time provided by our method for computing G

increases with k, the value of N will dominate for large values of k. Numerical experiments with the above algorithm indicate that this method is limited to $k = 5$ satellites. That is, it takes an amount of time in the order of a few minutes to compute the normalizing constant G for 5 satellites. Thus, a different method is needed for analyzing realistic constellations of LEO satellites.

In this section we present a method to analyze a single orbit with k satellites, $k > 5$, by decomposing the orbit into sub-systems of 3 or fewer satellites. Each sub-system is analyzed separately, and the results obtained by the sub-systems are combined using an iterative scheme.

In order to explain how the decomposition algorithm works, let us consider the case of a six-satellite orbit, as shown in Figure 3.2(a). This orbit is divided into two sub-systems. Sub-system 1 consists of satellites 1, 2, and 3, and sub-system 2 consists of satellites 4, 5, and 6. In order to analyze sub-system 1 in isolation, we need to have some information from sub-system 2. Specifically, we need to know the probability that a call originating at a satellite in sub-system 1 and terminating at a satellite in sub-system 2 will be blocked due to lack of capacity in a link in sub-system 2. Also, we need to know the number of calls originating from sub-system 2 and terminating in sub-system 1. Similar information is needed from sub-system 1, in order to analyze sub-system 2.

In view of this, each sub-system is augmented to include two fictitious satellites which represent the aggregate behavior of the other sub-system. In sub-system 1, we add two new satellites, which we call N1 and S1, as shown in Figure 3.2(b). A call originating at a satellite $i, i = 1, 2, 3$, and terminating at a satellite $j, j = 4, 5, 6$, will be represented by a call from i to one of the fictitious satellites (N1 or S1). Depending upon i and j, this call may be routed differently. For instance, let us assume that $i = 2$ and $j = 4$. Then, in our augmented sub-system 1, this call will be routed to satellite S1 through satellite 3. However, if $j = 6$, the call will be routed to satellite N1 through satellite 1 [2]. In other words, satellite N1 (respectively, S1) in the augmented sub-system 1 is the destination for calls of the original orbit that originate from satellite $i, i = 1, 2, 3$ and are routed to satellite $j, j = 4, 5, 6$ in the clockwise (respectively, counter-clockwise) direction in Figure 3.2(a). Similarly, calls originating from satellite $j, j = 4, 5, 6$, to satellite $i, i = 1, 2, 3$, and are routed in the counter-clockwise (respectively, clockwise) direction, are represented in sub-

[2] While this discussion assumes shortest-path routing, our model can handle any fixed-routing scheme.

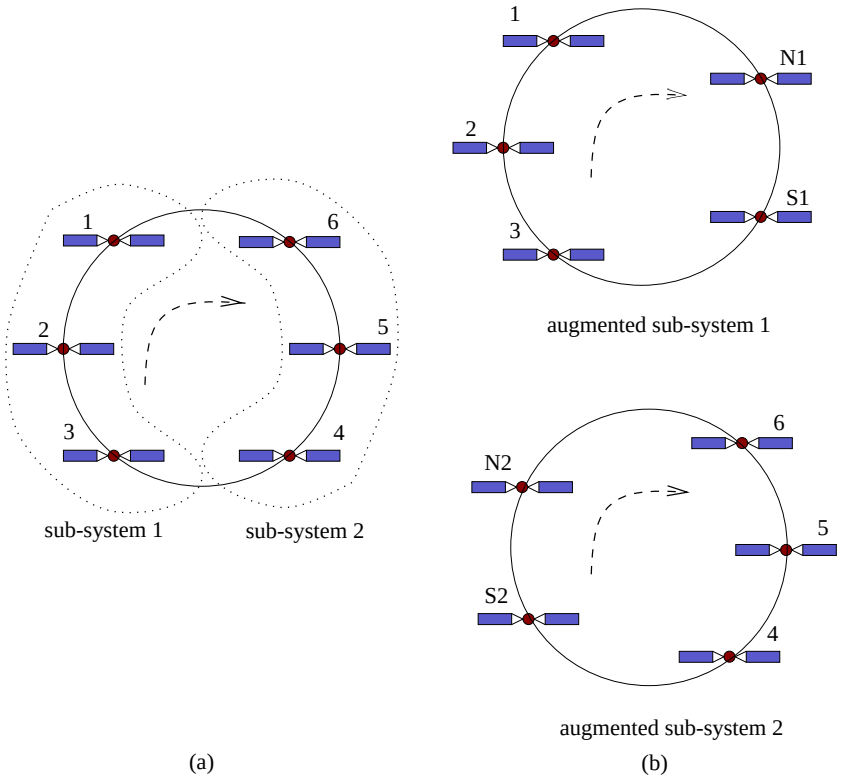

Figure 3.2: (a) Original 6-satellite orbit, (b) augmented sub-systems

system 1 as calls originating from N1 (respectively, S1) to i. Again, the originating satellite (N1 or S1) for the call depends on the values of i and j and the path the call follows in the original 6-satellite orbit.

Sub-system 2 is likewise augmented to include two fictitious satellites, N2 and S2 (see Figure 3.2(b)), which represent the aggregate behavior of sub-system 1. Satellites N2 and S2 become the origin and destination of calls traveling from sub-system 2 to sub-system 1, and vice versa, in a manner similar to N1 and S1 described above.

A summary of our iterative algorithm is provided in Figure 3.3. Below we describe the decomposition algorithm using the 6-satellite orbit shown in Figure 3.2(a). Recall that $\lambda_{ij}, 1 \leq i \leq j$, is the arrival rate of calls between satellites i and j. For analyzing the augmented sub-systems in Figure 3.2(b), we will introduce the new arrival rates $\lambda_{i,N1}$, $\lambda_{i,S1}$, $\lambda_{N2,j}$, and $\lambda_{S2,j}$, $i = 1, 2, 3$, $j = 4, 5, 6$. Specifically, $\lambda_{i,N1}$ (respectively, $\lambda_{i,S1}$) accounts for all calls between satellite $i, i = 1, 2, 3$, and a satellite in sub-system 2 that are routed in the clockwise (respectively, counter-clockwise) direction. Similarly, $\lambda_{N2,j}$ (respectively, $\lambda_{S2,j}$)

Decomposition Algorithm for A Single Orbit

A 6-satellite orbit is decomposed into two 3-satellite sub-systems as in Figure 3.2. Sub-system 1 consists of satellites 1 to 3 in the original orbit plus fictitious satellites N1 and S1, while sub-system 2 consists of satellites 4 to 6 of the original orbit plus fictitious satellites N2 and S2.

1. begin
2. $h \leftarrow 0$ //Initialization step
   // $p_{ij}(h)$ is the probability that an inter-sub-system call will be blocked in sub-system 1
   // $q_{ij}(h)$ is the probability that an inter-sub-system call will be blocked in sub-system 2
   $q_{ij}(h) \leftarrow 0, \quad 1 \leq i \leq 3 < j \leq 6$
3. $h \leftarrow h + 1$ //h-th iteration
4. $\lambda_{ij}(h) \leftarrow \lambda_{ij}, \quad 1 \leq i \leq j \leq 3$ //Sub-system 1
   $\lambda_{1,N1} = (1 - q_{16})\lambda_{16} + (1 - q_{15})\lambda_{15}$
   $\lambda_{1,S1} = (1 - q_{14})\lambda_{14}$
   $\lambda_{2,N1} = (1 - q_{26})\lambda_{26} + (1 - q_{25})\lambda_{25}$
   $\lambda_{2,S1} = (1 - q_{24})\lambda_{24}$
   $\lambda_{3,N1} = (1 - q_{36})\lambda_{36}$
   $\lambda_{3,S1} = (1 - q_{34})\lambda_{34} + (1 - q_{35})\lambda_{35}$
   Solve sub-system 1 to obtain new values for $p_{ij}(h)$
5. $\lambda_{ij}(h) \leftarrow \lambda_{ij}, \quad 4 \leq i \leq j \leq 6$ //Sub-system 2
   $\lambda_{N2,4} = 0$
   $\lambda_{S2,4} = (1 - p_{14})\lambda_{14} + (1 - p_{24})\lambda_{24} + (1 - p_{34})\lambda_{34}$
   $\lambda_{N2,5} = (1 - p_{15})\lambda_{15} + (1 - p_{25})\lambda_{25}$
   $\lambda_{S2,5} = (1 - p_{35})\lambda_{35}$
   $\lambda_{N2,6} = (1 - p_{16})\lambda_{16} + (1 - p_{26})\lambda_{26} + (1 - p_{36})\lambda_{36}$
   $\lambda_{S2,6} = 0$
   Solve sub-system 2 to obtain new values for $p_{ij}(h)$
6. Repeat from Step 3 until the blocking probabilities converge
7. end of the algorithm

Figure 3.3: Decomposition algorithm for a single orbit of a satellite constellation

accounts for all calls between sub-system 1 and satellite $j, j = 4, 5, 6$ that are routed in the clockwise (respectively, counter-clockwise) direction.

Initially, we solve sub-system 1 in isolation using:

$$\lambda_{1,N1} = (1 - q_{16})\lambda_{16} + (1 - q_{15})\lambda_{15} \tag{3.17}$$

$$\lambda_{1,S1} = (1 - q_{14})\lambda_{14} \tag{3.18}$$

$$\lambda_{2,N1} = (1 - q_{26})\lambda_{26} + (1 - q_{25})\lambda_{25} \tag{3.19}$$

$$\lambda_{2,S1} = (1 - q_{24})\lambda_{24} \tag{3.20}$$

$$\lambda_{3,N1} = (1 - q_{36})\lambda_{36} \tag{3.21}$$

$$\lambda_{3,S1} = (1 - q_{34})\lambda_{34} + (1 - q_{35})\lambda_{35} \tag{3.22}$$

Quantity $q_{ij}, 1 \leq i \leq 3 < j \leq 6$, represents the current estimate of the probability that a call between a satellite i in sub-system 1 and and satellite j in sub-system 2 will be blocked due to lack of capacity in a link of sub-system 2. For the first iteration, we use $q_{ij} = 0$ for all i and j; how these values are updated in subsequent iterations will be described shortly. Thus, the term $(1 - q_{16})\lambda_{16}$ in (4.2) represents the *effective* arrival rate of calls between satellites 1 and 6, as seen by sub-system 1; similarly for the other terms in (4.2)–(4.7).

The solution to the first sub-system yields an initial value for the probability $p_{ij}, 1 \leq i \leq 3 < j \leq 6$, that a call between a satellite i in sub-system 1 and a satellite j in sub-system 2 will be blocked due to lack of capacity in a link of sub-system 1. Therefore, the effective arrival rates of calls between, say, satellite 1 and satellite 4, that is offered to sub-system 2 can be initially estimated as $(1 - p_{16})\lambda_{16}$. We can now solve sub-system 2 in isolation using [3]:

$$\lambda_{N2,4} = 0 \tag{3.23}$$

$$\lambda_{S2,4} = (1 - p_{14})\lambda_{14} + (1 - p_{24})\lambda_{24} + (1 - p_{34})\lambda_{34} \tag{3.24}$$

$$\lambda_{N2,5} = (1 - p_{15})\lambda_{15} + (1 - p_{25})\lambda_{25} \tag{3.25}$$

$$\lambda_{S2,5} = (1 - p_{35})\lambda_{35} \tag{3.26}$$

$$\lambda_{N2,6} = (1 - p_{16})\lambda_{16} + (1 - p_{26})\lambda_{26} + (1 - p_{36})\lambda_{36} \tag{3.27}$$

[3] In (4.11) we have that $\lambda_{N2,4} = 0$ because we assume that calls between satellites in sub-system 1 and satellite 4 are routed in the counter-clockwise direction; similarly for expression (4.16).

$$\lambda_{S2,6} = 0 \tag{3.28}$$

Based on the above discussion, $\lambda_{S2,4}$ in (4.12) represents the effective arrival rate of calls between a satellite in sub-system 1 and satellite 4, as seen by sub-system 2. Expressions (4.11)–(4.16) can be explained in a similar manner. The solution to the second sub-system provides an estimate of the blocking probabilities $q_{ij}, 1 \leq i \leq 3 < j \leq 6$, that calls between satellites in the two sub-systems will be blocked due to lack of capacity in a link of sub-system 2.

The new estimates for q_{ij} are then used in expressions (4.2) to (4.7) to update the arrival rates to the two fictitious satellites of augmented sub-system 1. Sub-system 1 is then solved again, and the estimates p_{ij} are updated and used in expressions (4.11) to (4.16) to obtain new arrival rates for the fictitious satellites of sub-system 2. This leads to an iterative scheme, where the two sub-systems are solved successively until a convergence criterion (e.g., in terms of the values of the call blocking probabilities) is satisfied.

Orbits consisting of any number $k > 5$ of satellites can be decomposed into a number of sub-systems, each consisting of 3 satellites of the original orbit (the last sub-system may consist of fewer than 3 satellites). The decomposition method is similar to the one above, in that for sub-system l, the remaining satellites are aggregated to two fictitious satellites. Each sub-system is analyzed in succession as described above. The decomposition algorithm described above is similar in spirit to the decomposition algorithms developed for tandem queueing networks with finite capacity queues (see [50]). We note that when employing the decomposition algorithm, the selection of the sub-system size will depend on the number of satellites in the original orbit and how efficiently we can calculate the exact solution of the Markov process associated with each sub-system. It is well known in decomposition algorithms that the larger the individual sub-systems that have to be analyzed in isolation, the better the accuracy of the decomposition algorithm. Thus, as we mentioned above, we have decided to decompose an orbit into sub-systems of the largest size (three of the original satellites plus two fictitious ones) for which we can efficiently analyze the Markov process, plus, possibly, a sub-system of smaller size, if the number of satellites is not a multiple of three.

3.3 Modeling Hand-Offs

3.3.1 Earth-Fixed Coverage

Let us now turn to the problem of determining blocking probabilities in a single orbit of satellites with earth-fixed coverage. Let k denote the number of satellites in the orbit. In this case we assume that the earth is divided into k fixed cells (footprints) and that time is divided in intervals of length T such that, during a given interval, each satellite serves a certain cell by continuously redirecting its beams. At the end of each interval, i.e., every T time units, all satellites simultaneously redirect their beams to serve the next footprint along their orbit, and they also hand-off currently served calls to the next satellite in the orbit.

We make the following observations about this system. Hand-off events are periodic with a period of T time units, and hand-offs take place in bulk at the end of each period. Also, there is no call blocking due to hand-offs, since, at each hand-off event a satellite passes its calls to the one following it and simply inherits the calls of the satellite ahead of it. Finally, within each period T, the system can be modeled as one with no hand-offs, such as the one described in the previous subsection. Given that the period T is equal to the orbit period (approximately 90 minutes) divided by the number of satellites (e.g., 11 for the Iridium constellation) we can assume that the system reaches steady state within the period, and thus, the initial conditions (i.e., the number of calls inherited by each satellite at the beginning of the period) do not affect its behavior.

Now, since every T units of time, each satellite assumes the traffic carried by the satellite ahead, from the point of view of an observer on the earth, this system appears to be as if the satellites are permanently fixed over their footprints. Hence, we can use the decomposition algorithm presented above to analyze this system.

3.3.2 Satellite-Fixed Coverage

Consider now satellite-fixed cell coverage. As a satellite moves, its footprint on the earth (the cell served by the satellite) also moves with it. As customers move out of the footprint area of a satellite, their calls are handed off to the satellite following it from behind. In order to model hand-offs in this case, we make the assumption that potential customers are uniformly distributed over the part of the earth served by the satellites in

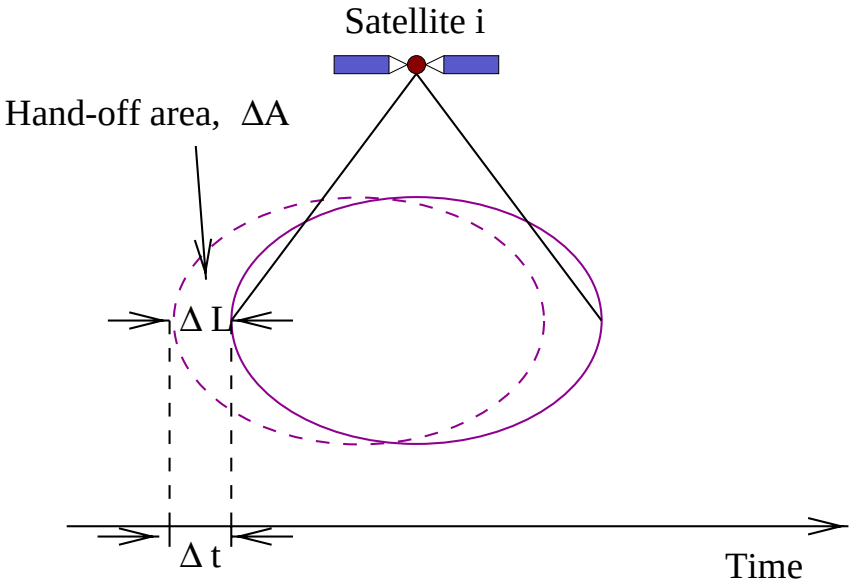

Figure 3.4: Calculation of the hand-off probability

the orbit. This assumption has the following two consequences.

- The arrival rate λ to each satellite remains constant as it moves around the earth. Then, the arrival rate of calls between satellite i and satellite j is given by $\lambda_{ij} = \lambda r_{ij}$, where r_{ij} is the probability that a call originating by a customer served by satellite i is for a customer served by satellite j.

- The active customers served by a satellite can be assumed to be uniformly distributed over the satellite's footprint. As a result, the rate of hand-offs from satellite i to satellite j that is following from behind is proportional to the number of calls at satellite i.

Clearly, the assumption that customers are uniformly distributed (even within an orbit) is an approximation. In Section 4.4 we will discuss how we are currently extending the results presented in this section to accurately model the situation when customers are not uniformly distributed.

Let A denote the area of a satellite's footprint and v denote a satellite's speed. As a satellite moves around the earth, within a time interval of length Δt, its footprint will move a distance of ΔL, as shown in Figure 3.4. Calls involving customers located in the part of the original footprint of area ΔA (the hand-off area) that is no longer served by the

satellite are handed off to the satellite following it. Let $\Delta A = A\beta\Delta L$, where β depends on the shape of the footprint. Because of the assumption that active customers are uniformly distributed over the satellite's footprint, the probability q that a customer will be handed off to the next satellite along the sky within a time interval of length Δt is

$$q = \frac{\Delta A}{A} = \beta\Delta L = \beta v\Delta t \tag{3.29}$$

Define $\alpha = \beta v$. Then, when there are n customers served by a satellite, the *rate* of hand-offs to the satellite following it will be αn.

Let us now return to the 3-satellite orbit (see Figure 3.1) and introduce hand-offs. This system can be described by a continuous-time Markov process with the same number of random variables as the no-hand-offs model of Section 3.1 (i.e., $n_{11}, \cdots, n_{33}$), the same transition rates (3.2) and (3.3), but with a number of additional transition rates to account for hand-offs. We will now derive the transition rates due to hand-offs.

Consider calls between a customer served by satellite 1 and a customer served by satellite 2. There are n_{12} such calls serving $2n_{12}$ customers: n_{12} customers on the footprint of satellite 1 and n_{12} on the footprint of satellite 2. Consider a call between customer A and customer B, served by satellite 1 and 2, respectively. The probability that customer A will be in the hand-off area of satellite 1 but B will not be in the hand-off area of satellite 2 is $q(1-q) = q - q^2$. But, from (3.29), we have that $\lim_{\Delta t \to 0} \frac{q^2}{\Delta t} = 0$, so the rate at which these calls experience a hand-off from satellite 1 to satellite 3 that follows it is αn_{12}. Let $\underline{n} = (n_{11}, n_{12}, n_{13}, n_{22}, n_{23}, n_{33})$, and define $\underline{1}_{ij}$ as a vector of zeroes for all variables except variable n_{ij} which is 1. Based on the above discussion, we thus have:

$$r(\underline{n}, \underline{n} - \underline{1}_{12} + \underline{1}_{23}) = \alpha n_{12}, \quad n_{12} > 0 \tag{3.30}$$

Similarly, the probability that customer B will be in the hand-off area of satellite 2 but A will not be in the hand-off area of satellite 1 is $q(1-q) = q - q^2$. Thus, the rate at which these calls experience a hand-off from satellite 2 to satellite 1 that follows it is again αn_{12}:

$$r(\underline{n}, \underline{n} - \underline{1}_{12} + \underline{1}_{11}) = \alpha n_{12}, \quad n_{12} > 0 \tag{3.31}$$

On the other hand, the probability that both customers A and B are in the hand-off area of their respective satellites is q^2, which, from (3.29) is $o(\Delta t)$, and thus simultaneous hand-offs are not allowed.

Now consider calls between customers that are both served by the same satellite, say, satellite 1. There are n_{11} such calls serving $2n_11$ customers. The probability that exactly one of the customers of a call is in the hand-off area of satellite 1 is $2q(1-q)$, so the rate at which these calls experience hand-offs (involving a single customer) to satellite 3 is $2\alpha n_{11}$:

$$r(\underline{n}, \underline{n} - \underline{1}_{11} + \underline{1}_{13}) = 2\alpha n_{11}, \quad n_{11} > 0 \tag{3.32}$$

As before, the probability that both customers of the call are in the hand-off area of satellite 1 is q^2, and again, no simultaneous hand-offs are allowed.

The transition rates involving the other four random variables in the state description (3.1) can be derived using similar arguments. For completeness, these transition rates are provided in (3.33)-(3.38).

$$r(\underline{n}, \underline{n} - \underline{1}_{13} + \underline{1}_{12}) = \alpha n_{13}, \quad n_{13} > 0 \tag{3.33}$$

$$r(\underline{n}, \underline{n} - \underline{1}_{13} + \underline{1}_{11}) = \alpha n_{13}, \quad n_{13} > 0 \tag{3.34}$$

$$r(\underline{n}, \underline{n} - \underline{1}_{22} + \underline{1}_{12}) = 2\alpha n_{22}, \quad n_{22} > 0 \tag{3.35}$$

$$r(\underline{n}, \underline{n} - \underline{1}_{23} + \underline{1}_{13}) = \alpha n_{23}, \quad n_{23} > 0 \tag{3.36}$$

$$r(\underline{n}, \underline{n} - \underline{1}_{23} + \underline{1}_{22}) = \alpha n_{23}, \quad n_{23} > 0 \tag{3.37}$$

$$r(\underline{n}, \underline{n} - \underline{1}_{33} + \underline{1}_{23}) = 2\alpha n_{33}, \quad n_{33} > 0 \tag{3.38}$$

From the queueing point of view, this system is the queueing network of M/M/K/K queues described in Section 3.1, where customers are allowed to move between queues according to (3.30)-(3.38). (Recall that in the queueing model of Section 3.1, customers are not allowed to move from node to node.) This queueing network has a product-form solution similar to (3.10). Let γ_{ij} denote the total arrival rate of calls between satellites i and j, including at a rate of λ_{ij}) and hand-off calls (arriving at an appropriate rate). The values of γ_{ij} can be obtained by solving the traffic equations for the queueing network. Let also $\nu_{ij} n_{ij}$ be the departure rate when there are n_{ij} of these calls, including call termination (at a rate of $\mu_{ij} n_{ij}$) and call hand-off (at a rate of $2\alpha n_{ij}$). Also, define $\rho'_{ij} = \gamma_{ij}/\nu_{ij}$. Then, the solution for this queueing network is given by:

$$P(\underline{n}) = P(n_{11}, n_{12}, n_{13}, n_{22}, n_{23}, n_{33}) =$$

$$\frac{1}{G} \frac{(\rho'_{11})^{n_{11}}}{n_{11}!} \frac{(\rho'_{12})^{n_{12}}}{n_{12}!} \frac{(\rho'_{13})^{n_{13}}}{n_{13}!} \frac{(\rho'_{22})^{n_{22}}}{n_{22}!} \frac{(\rho'_{23})^{n_{23}}}{n_{23}!} \frac{(\rho'_{33})^{n_{33}}}{n_{33}!} \tag{3.39}$$

which is identical to (3.10) except that ρ_{ij} has been replaced by ρ'_{ij}.

The product-form solution (3.39) can be generalized in a straightforward manner for any k-satellite orbit, $k > 3$. We can thus use the techniques developed in Section 3.1 to solve the system involving hand-offs exactly, or we can use the decomposition algorithm presented in Section 3.2 to solve orbits with a large number of satellites.

3.4 Numerical Results

In this section we validate both the exact model and the decomposition algorithm by comparing to simulation results. In the figures presented, simulation results are plotted along with 95% confidence intervals estimated by the method of replications. The number of replications is 30, with each simulation run lasting until each type of call has at least 15,000 arrivals. For the approximate results, the iterative decomposition algorithm terminates when all call blocking probability values have converged within 10^{-6}.

For the results presented here we consider three different traffic patterns; similar results have been obtained for several other patterns. Let r_{ij} denote the probability that a call originating by a customer served by satellite i is for a customer served by satellite j. The first pattern is a uniform traffic pattern such that:

$$r_{ij} = \frac{1}{k} \quad \forall\, i, j \qquad \text{(uniform pattern)} \tag{3.40}$$

where k is the number of satellites. The second is a pattern based on the assumption of traffic locality. Specifically, it assumes that most calls originating at a satellite i are to users in satellites $i-1$, i, and $i+1$, where addition and subtraction is modulo-k for a k-satellite orbit:

$$r_{ij} = \begin{cases} 0.3, & j = i-1, i, i+1 \\ \frac{0.1}{k-3}, & j \neq i-1, i, i+1 \end{cases} \qquad \text{(locality pattern)} \tag{3.41}$$

The third pattern is such that there are two communities of users, and most traffic is between users within a given community (e.g., satellites over different hemispheres of the earth):

$$r_{ij} = \begin{cases} \frac{0.8}{k/2}, & i, j = 1, \cdots, k/2, \text{ or } i, j = k/2+1, \cdots, k \qquad (2-\text{community pattern}) \\ \frac{0.2}{k/3}, & i = 1, \cdots, k/2, j = k/2+1, \cdots, k \text{ or } j = 1, \cdots, k/2, i = k/2+1, \cdots, k \end{cases} \tag{3.42}$$

3.4.1 Validation of the Exact Model

In this section we validate the exact Markov process model for the no hand-offs case developed in Section 3.1. Recall that we can directly compute the normalizing constant G using expression (3.14) for orbits of up to five satellites. Thus, we compare the blocking probability values obtained by solving the exact Markov process to simulation results for a 5-satellite orbit and the three traffic patterns discussed above.

Figure 3.5 plots the blocking probability against the capacity C_{UDL} of up-and-down links, when the arrival rate $\lambda = 10$ and the capacity of inter-satellite links $C_{ISL} = 10$, for the uniform traffic pattern. Three sets of plots are shown: one for calls originating and terminating at the same satellite (referred to as "local calls" in the figure), one for calls traveling over a single inter-satellite link, and one for calls traveling over two inter-satellite links [4]. Each set consists of two plots, one corresponding to blocking probability values obtained by solving the Markov process, and one corresponding to simulation results.

From the figure, we observe that, as the capacity C_{UDL} of up-and-down links increases, the blocking probability of all calls decreases. However, for calls traveling over at least one inter-satellite link, the blocking probability curve flattens out after an initial drop. This behavior is due to the fact that, for small values of C_{UDL}, the up-and-down links represent a bottleneck, thus, increasing C_{UDL} reduces the call blocking probability significantly. However, once C_{UDL} increases beyond a certain value, the inter-satellite links become the bottleneck, and the blocking probability of calls that have to travel over these links is not affected further. On the other hand, the blocking probability of calls not using inter-satellite links (i.e., those originating and terminating at the same satellite) decreases rapidly as C_{UDL} increases.

Figure 3.6 plots the blocking probability for the same calls as in Figure 3.5, against the capacity C_{ISL} of inter-satellite links; for the results presented we assume that $\lambda = 10$ and $C_{UDL} = 20$. In this figure we can see that as the value of C_{ISL} increases, the blocking probability of calls using inter-satellite links decreases, as expected. However, the blocking probability of local calls (i.e., calls originating and terminating at the same satellite which do not use inter-satellite links) increases with increasing C_{ISL}. This behavior can be explained by noting that, as C_{ISL} increases, a larger number of non-local calls (i.e., calls using inter-

[4] These are the only possible types of calls in a 5-satellite orbit and shortest path routing. Furthermore, because of symmetry, the results are the same regardless of the satellite at which the calls originate or terminate.

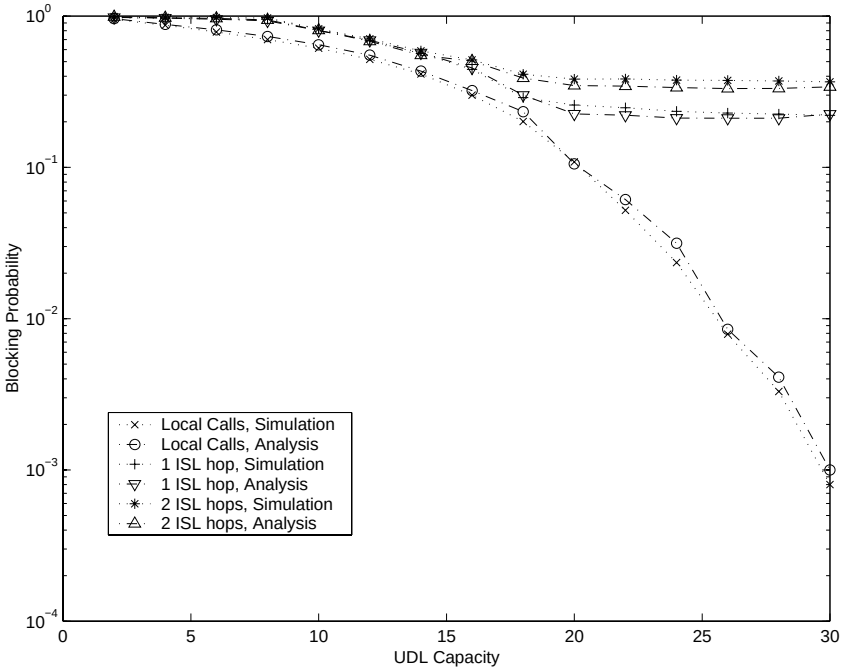

Figure 3.5: Call blocking probabilities for a 5-satellite orbit, $\lambda = 10$, $C_{ISL} = 10$, uniform pattern

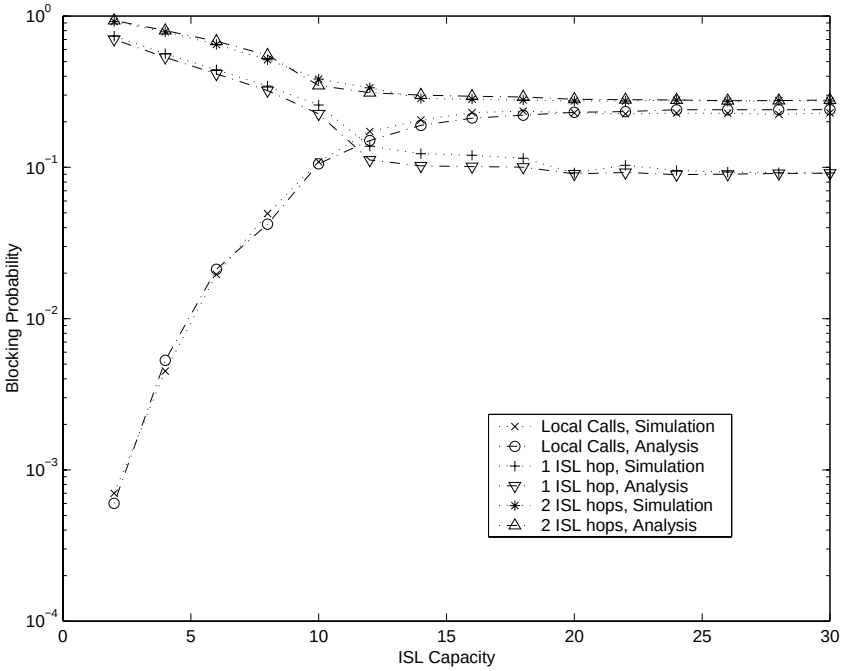

Figure 3.6: Call blocking probabilities for a 5-satellite orbit, $\lambda = 10$, $C_{UDL} = 20$, uniform pattern

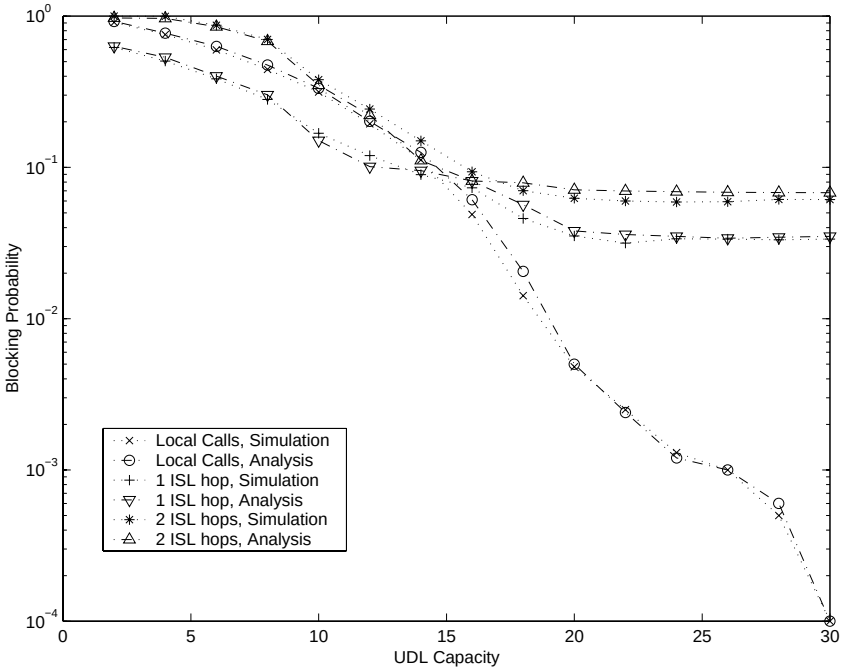

Figure 3.7: Call blocking probabilities for a 5-satellite orbit, $\lambda = 5$, $C_{ISL} = 10$, uniform pattern

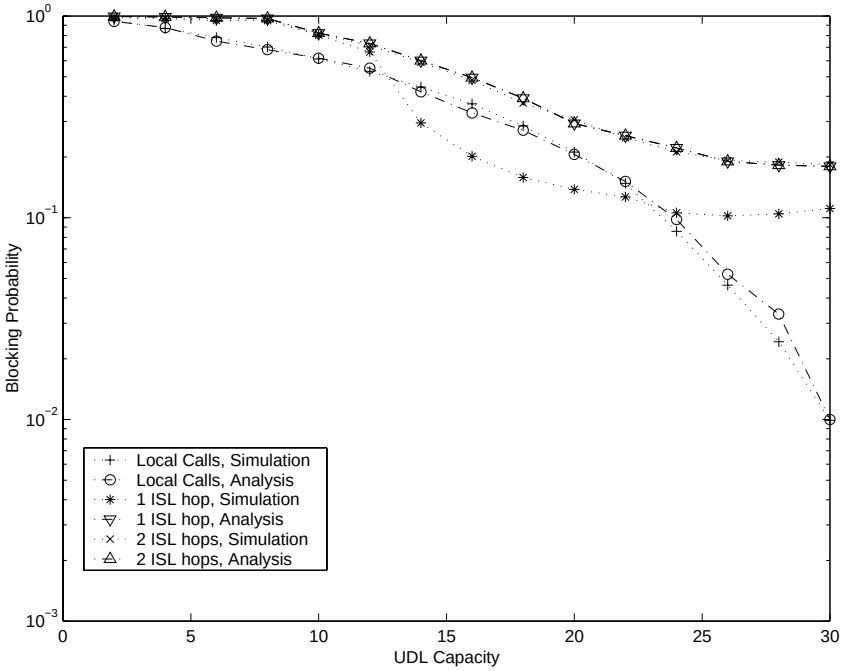

Figure 3.8: Call blocking probabilities for a 5-satellite orbit, $\lambda = 10$, $C_{ISL} = 10$, locality pattern

satellite links) is accepted (since their blocking probability decreases). Since both local and non-local calls compete for up-and-down links, an increase in the number of non-local calls accepted will result in higher blocking probability for local calls. But when the value of C_{ISL} exceeds the value of C_{UDL} (which is equal to 20 in this case), the up-and-down links become the bottleneck, and further increases in C_{ISL} have no effect on blocking probabilities.

Figure 3.7 is similar to Figure 3.5 except that the arrival rate is $\lambda = 5$ instead of 10 (all other parameters are as in Figure 3.5). The behavior of the various curves is similar to that in Figure 3.5. The main difference is that the blocking probabilities in Figure 3.7 are significantly lower, a result that is expected due to the lower arrival rate.

Finally, Figures 3.8 and 3.9 show results for the same parameters as in Figure 3.5, but correspond to the locality and 2-community traffic patterns, respectively. Again, the behavior of the curves is similar for all three figures, although the actual blocking probability values depend on the traffic pattern used.

The results in Figures 3.5–3.9 illustrate the fact that the blocking probability values obtained by solving the Markov process match the simulation results; this is expected since the Markov process model we developed is exact. Thus, this model can be used to study the interplay between various system parameters (e.g., C_{ISL}, C_{UDL}, traffic pattern, etc.) and their effect on the call blocking probabilities, in an efficient manner. We note that solving the Markov process takes only a few minutes, while running the simulation takes anywhere between 30 minutes and several hours, depending on the value of the arrival rates.

3.4.2 Validation of the Decomposition Algorithm

We now validate the decomposition algorithm developed in Section 3.2 by comparing the blocking probabilities obtained by running the algorithm to simulation results. We consider a single orbit of a satellite constellation consisting of 12 satellites, a number representative of typical commercial satellite systems. In all cases studied, we have found that the algorithms converges in only a few (less than ten) iterations, taking a few minutes to terminate. On the other hand, simulation of 12-satellite orbits is quite expensive in terms of computation time, taking several hours to complete.

Figure 3.10 plots the blocking probability against the capacity C_{UDL} of up-and-down links, when the arrival rate $\lambda = 5$ and the capacity of inter-satellite links $C_{ISL} = 20$, for the uniform traffic pattern. Six sets of calls are shown, one for local calls, and five for non-

local calls. Each set consists of two plots, one corresponding to blocking probability values obtained by running the decomposition algorithm of Section 3.2, and one corresponding to simulation results. Each non-local call for which results are shown travels over a different number of inter-satellite links, from one to five. Thus, the results in Figure 3.10 represent calls between all the different sub-systems in which the 12-satellite orbit is decomposed by the decomposition algorithm.

From the figure we observe the excellent agreement between the analytical results and simulation. The behavior of the curves can be explained by noting that, when the capacity C_{UDL} of up-and-down links is less than 20, these links represent a bottleneck. Thus, increasing the up-and-down link capacity results in a significant drop in the blocking probability for all calls. When $C_{UDL} > 20$, however, the inter-satellite links become the bottleneck, and non-local calls do not benefit from further increases in the up-and-down link capacity. We also observe that, the larger the number of inter-satellite links over which a non-local call must travel, the higher its blocking probability, as expected. The blocking probability of local calls, on the other hand, drops to zero for $C_{UDL} > 20$ since they do not have to compete for inter-satellite links.

Figures 4.7 and 3.12 are similar to Figure 3.10 but show results for the locality and 2-community traffic patterns, respectively. For the results presented we used $\lambda = 5$ and $C_{ISL} = 10$, and we varied the value of C_{UDL}. We observe that the values of the call blocking probabilities depend on the actual traffic pattern, but the behavior of the various curves is similar to that in Figure 3.10. Finally, in Figure 3.13, we fix the value of C_{UDL} to 20, and we plot the call blocking probabilities for the 2-community traffic pattern against the capacity C_{ISL} of the inter-satellite links.

Overall, the results in Figures 3.10–3.13 indicate that analytical results are in good agreement with simulation over a wide range of traffic patterns and system parameters. Thus, our decomposition algorithm can be used to estimate call blocking probabilities in LEO satellite systems in an efficient manner.

3.5 Concluding Remarks

We have presented an analytical model for computing blocking probabilities for a single orbit of a LEO satellite constellation. We have devised a method for solving the exact Markov process efficiently for up to 5-satellite orbits. For orbits consisting of a

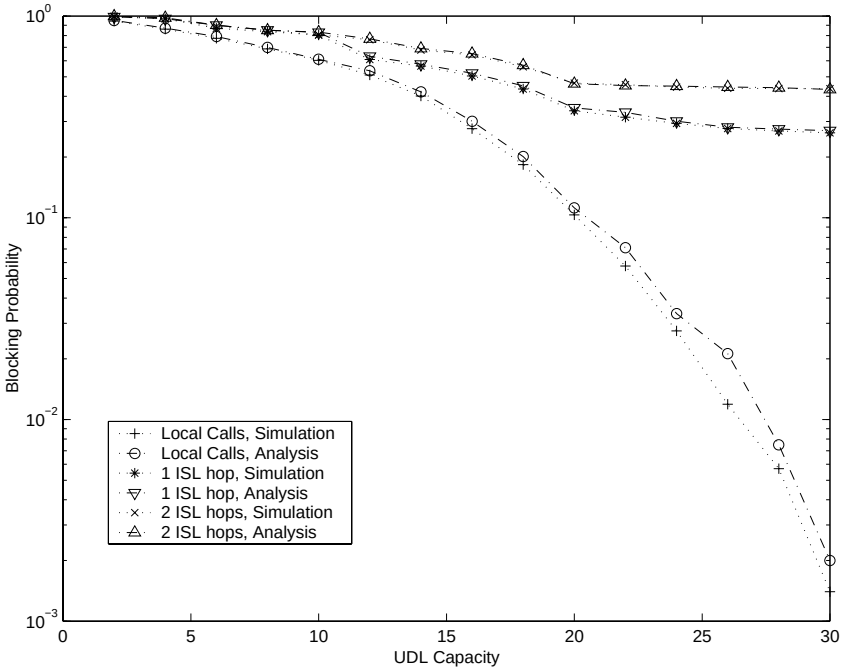

Figure 3.9: Call blocking probabilities for a 5-satellite orbit, $\lambda = 10$, $C_{ISL} = 10$, 2-community pattern

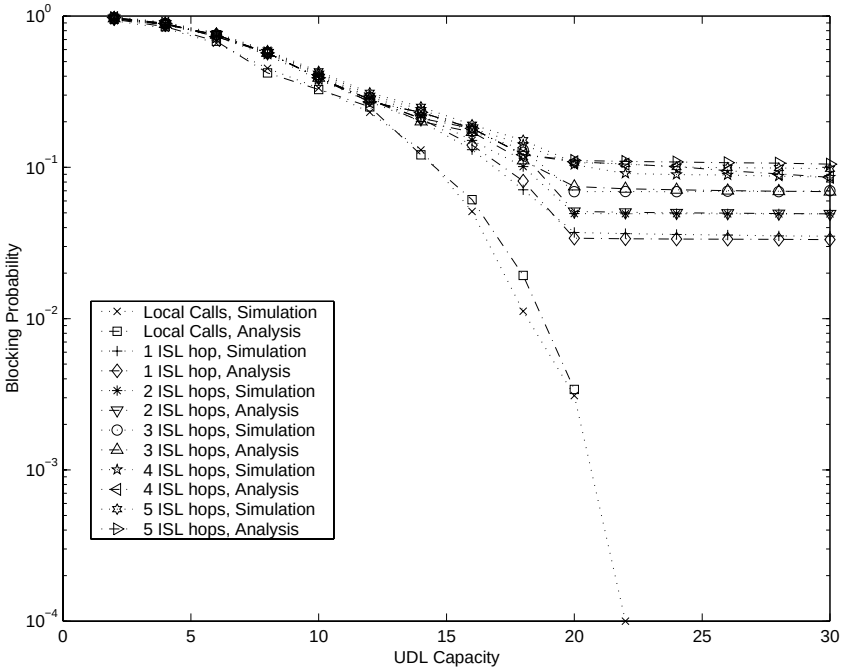

Figure 3.10: Call blocking probabilities for a 12-satellite orbit, $\lambda = 5$, $C_{ISL} = 20$, uniform pattern

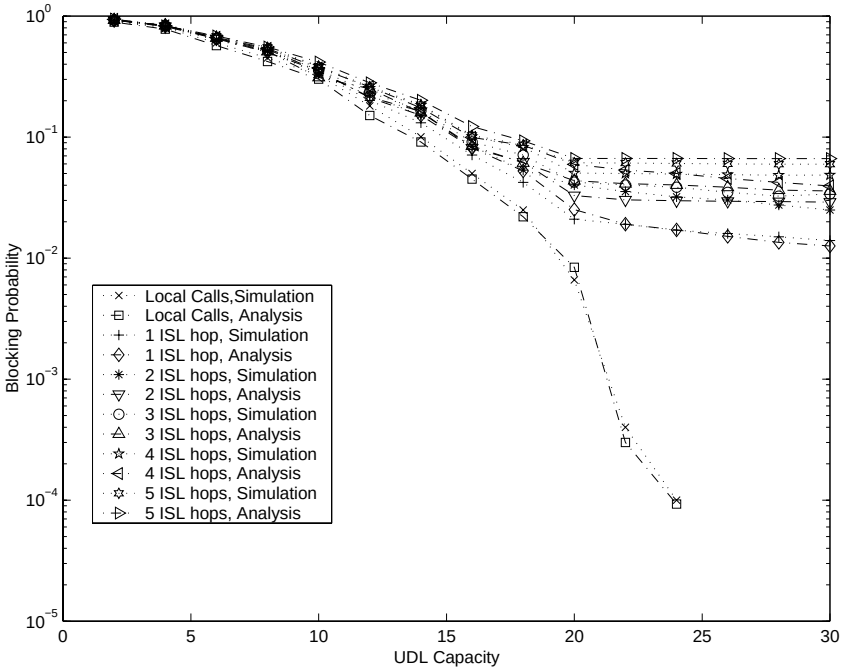

Figure 3.11: Call blocking probabilities for a 12-satellite orbit, $\lambda = 5$, $C_{ISL} = 10$, locality pattern

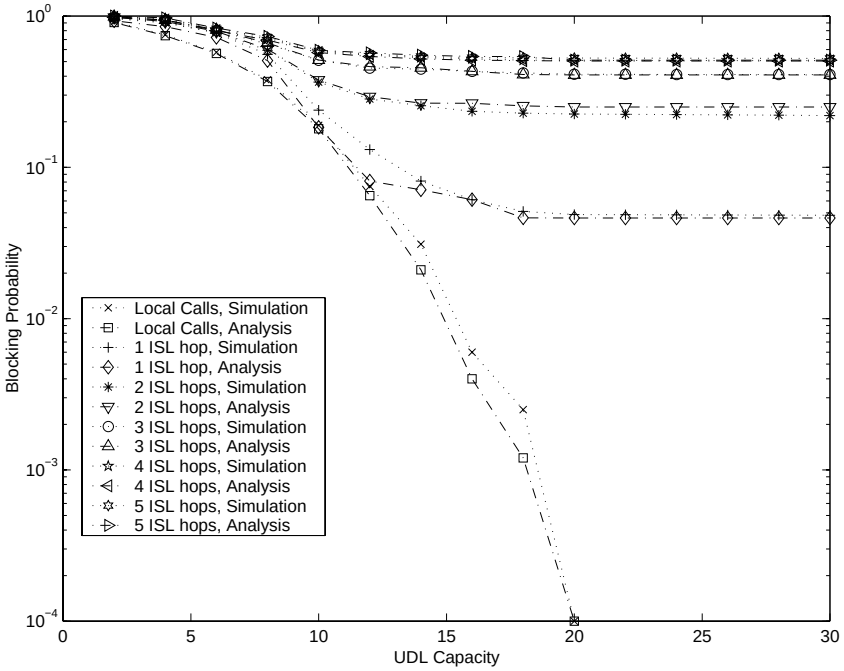

Figure 3.12: Call blocking probabilities for a 12-satellite orbit, $\lambda = 5$, $C_{ISL} = 10$, 2-community pattern

larger number of satellites, we have developed an approximate decomposition algorithm to compute the call blocking probabilities by decomposing the system into smaller sub-systems, and iteratively solving each sub-system in isolation using the exact Markov process. We have also shown how our approach can capture blocking due to hand-offs for both satellite-fixed and earth-fixed orbits.

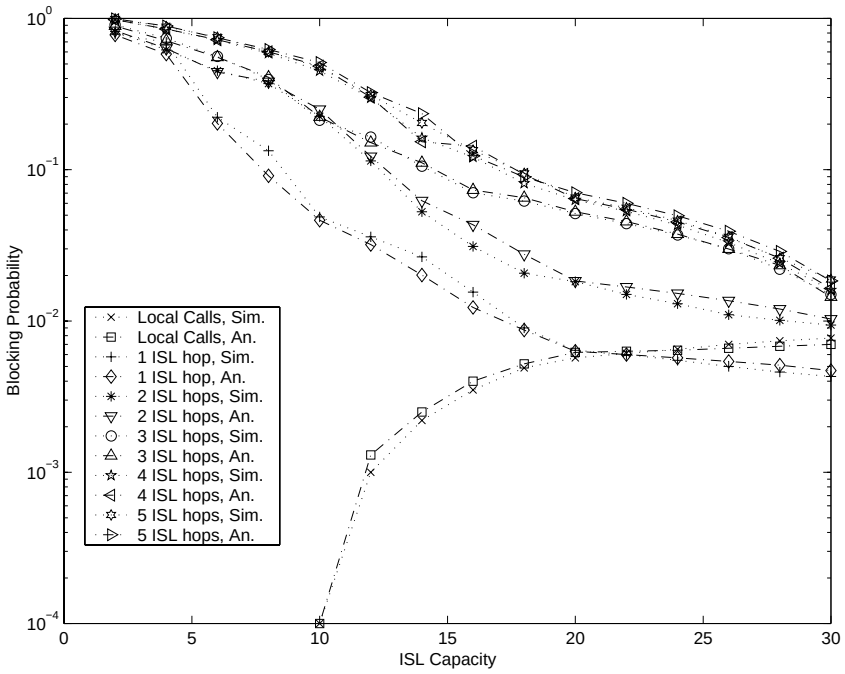

Figure 3.13: Call blocking probabilities for a 12-satellite orbit, $\lambda = 5$, $C_{UDL} = 20$, 2-community pattern

Chapter 4

The Multiple Orbits Case

In Chapter 3, we proposed an approximation method for calculating call blocking probabilities in a group of LEO satellites arranged in a single orbit. This approximation method is also applicable to MEO satellites. The approximation algorithm is for both satellite-fixed and earth-fixed types of coverage. It can be used to compute the blocking probability of new calls and also the hand-over call blocking probability.

In this chapter, we generalize the decomposition algorithm defined in Chapter 3 to an entire constellation of LEO satellites involving many orbits.

4.1 A Decomposition Algorithm for LEO Satellite Constellations

In this section, we present a decomposition method for calculating call blocking probabilities in a constellation of satellites. The constellation is decomposed into a series of sub-systems, and each sub-system is analyzed separately using the exact solution described in the previous chapter. The results obtained from the sub-systems are combined together using an iterative scheme.

As in the previous chapter, we will assume that the constellation of satellites is fixed over the earth, as in the case of geostationary satellites. That is, calls are not handed over from one satellite to another, and the call blocking probabilities due to hand-offs is zero. The decomposition algorithm presented in this section can only calculate the call blocking probabilities of new calls. In the following section, we extend the algorithm

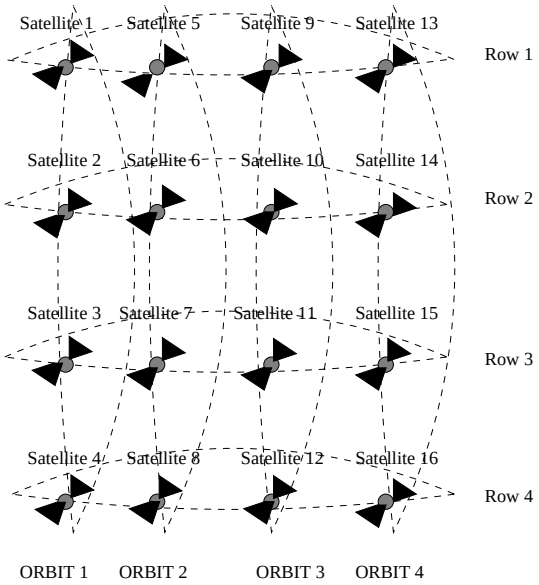

Figure 4.1: Original 16-satellite constellation

to also calculate the call blocking probabilities due to hand-offs. As before, we let λ_{ij}, $1 \leq i \leq j \leq K$, denote the arrival rate of *new* calls originating at satellite i and terminating at satellite j, in a constellation of K satellites.

In order to explain how the decomposition algorithm works, let us consider a 16 satellite constellation with 4 orbits, 4 satellites per orbit, as shown in Figure 4.1 [1]. The constellation is fixed over the earth, we assume that each satellite in the first row has an intra-plane ISL to the satellite on the same orbit located in the bottom row. For instance satellite 1 communicates with satellite 4 via an intra-plane ISL. Likewise, satellites 5 and 8, and so on. Also, each satellite in the first column communicates via an inter-plane ISL with the satellite on the fourth column that is located on the same row. For instance, satellite 1 has an inter-plane link to satellite 13, and so on.

Each orbit is divided into two sub-systems. For instance, orbit 1 is divided into sub-system 1, consisting of satellites 1 and 2, and sub-system 2, consisting of satellites 3 and 4. Orbit 2 is divided into sub-system 3, consisting of satellites 5 and 6, and sub-system 4, consisting of satellites 7 and 8. Similarly, each row of four satellites in Figure 4.1 is divided into two sub-systems. The *16* satellite constellation is thus divided into *16* sub-systems as

[1] To simplify the description of the algorithm, we used a constellation as a Torus network. With small modifications, the effect of the seam can be taken into account.

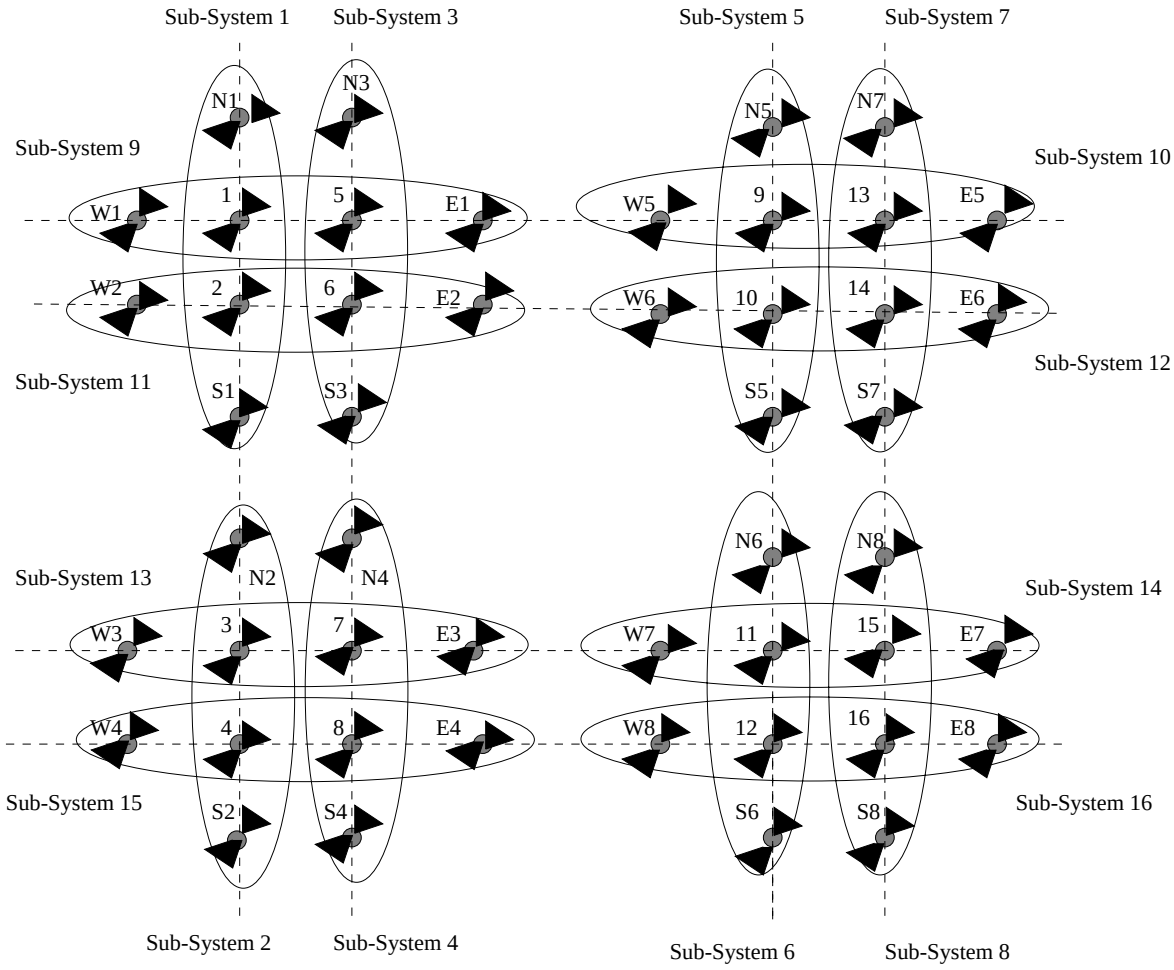

Figure 4.2: Augmented Sub-systems

shown in Figure 4.2.

In order to analyze sub-system 1 in isolation, we need to have some information from other sub-systems. Specifically, we need to know the probability that a call originating at a satellite in sub-system 1 and terminating at a satellite in sub-system j, where $j > 1$, will be blocked due to lack of capacity in a link of any sub-systems that it has to traverse, including sub-system j. Also, we need to know the number of calls that originate at other sub-systems and terminate in sub-system 1. Similar information is needed in order to analyze any other sub-system.

In view of this, each sub-system is augmented to include two fictitious satellites referred to as N and S. These two satellites are used to represent the aggregate traffic

generated by other satellites on the same orbit. For instance, sub-system 1, shown in Figure 4.2, is augmented with fictitious satellites *N1* and *S1*. A call originating at say satellite i, $i = 1, 2$ and terminating at satellite j, $j = 3, 4$ will be represented in our sub-system by a call from satellite i to one of the fictitious satellites *N1* or *S1*. Depending upon i and j, this call may be routed differently. In our augmented sub-system, a call will be routed to *S1* if the shortest-path route passes through satellites south of the sub-system. A call will be routed to *N1* if the shortest-path route goes towards the north [2]. In other words satellite N (respectively S) in the augmented sub-system is the destination satellite for all calls that originate in satellite i of sub-system 1 and routed to satellite j located outside that sub-systems in clockwise (respectively counter-clockwise) direction.

This augmented sub-system captures the traffic outside the sub-system that travels on the same orbit, i.e., on interplane ISLs. In addition, we also have to consider traffic that uses intraplane ISLs. For instance, let us consider again sub-system 1. A call originating from satellite 1 and terminating at satellite 6, will use the intraplane ISL to satellite 2 and then the interplane ISL between satellites 2 and 6. In order to account for traffic traversing intraplane ISLs, we also decompose each row of satellites into two sub-systems, each consisting of two satellites. For instance, the first row of satellites is divided to sub-system 9 consisting of satellites 1 and 5, and sub-system 10, consisting of satellites 9 and 13. The 16 satellite constellation is thus divided into an additional 8 sub-systems, as shown in Figure 4.2. Each sub-system is augmented to include two fictitious satellites, referred to as E and W. As before, E and W satellites are used to represent the aggregate traffic generated by other satellites on the same row. For instance, a call originating at say satellite i, $i = 1, 2$, and terminating at satellite j, $j = 9, 13$, will be represented in our sub-system 9 as a call from i to either $E1$ or $W1$. This call will be routed to $E1$ or $N1$ depending upon the shortest-path route. The same applies for traffic originating at satellite j, $j = 9, 13$. The aggregate satellites N and S, and E and W also represent traffic between a satellite within the sub-system and a satellite anywhere else in the constellation, which is routed through one of these aggregate satellites. For instance, let us assume that a call between satellite 5 and 11. It is routed through satellite 9 and 10. This particular call will then be represented on a call between 5 and $E1$.

Recall that $\lambda_{ij}, 1 \leq i \leq j \leq K$, be the arrival rate of calls between satellite i and

[2] We note that the algorithm can handle any fixed-routing scheme in addition to the shortest-path scheme.

j. In order to analyze the augmented sub-systems in Figure 4.2, we introduce new arrival rates $\hat{\lambda}_{ij}$, including new rates $\hat{\lambda}_{i,N}$,$\hat{\lambda}_{i,S}$ (or $\hat{\lambda}_{i,E}$, $\hat{\lambda}_{i,W}$), within each sub-system. The rate $\hat{\lambda}_{ij}$ captures the rate of calls between satellite i and satellite j, *as seen from within this sub-system*. In particular, parameter $\hat{\lambda}_{i,N}$ (or any other parameter involving any of the fictitious satellites N,S,E or W) captures the rate of calls originating at satellite i and leaving the sub-system over an ISL that goes through the fictitious satellite N. Similarly for calls leaving (or entering) the sub-system over other ISLs.

Based on this decomposition, computing the blocking probability of a call depends on whether the originating and terminating satellites of the call are within the same sub-system or not. In the former case, the blocking probability can be computed immediately after solving the sub-system. In the latter case, the blocking probability will be computed by taking into account all the sub-systems in the call's path. Returning to Figure 4.2, a call originating at satellite 1 and terminating at satellite 6 will be analyzed in two steps. At the first step, it is a call within sub-system 1 between satellite 1 and 2. This call will then leave this sub-system from satellite 2 and it will be analyzed using the sub-system 11. For sub-system 11, this is a call between satellite 2 and 6. As another example, analyzing a call between satellite 1 and satellite 8 involves three sub-systems. Within sub-system 1, it is viewed as a call between satellite 1 and (fictitious) satellite $N1$. In sub-system 2, it is considered a call between (fictitious) satellite $S2$ and satellite 4. Finally, in sub-system 15, it is a call between satellites 4 and 8.

A summary of our iterative algorithm is provided in Figure 4.3. Below we describe the decomposition algorithm using the 16 satellite constellation shown in Figure 4.2.

Initially, we solve sub-system 1 in isolation. This system in isolation is described by the following Markov process.

$$\underline{n} = (n_{11}, n_{12}, n_{1N_1}, n_{1S_1}, n_{22}, n_{2N_1}, n_{2S_1}) \tag{4.1}$$

First, we need to calculate the new arrival rates $\hat{\lambda}_{ij}$ within the sub-system using formulas (4.2)-(4.8). We now explain how we obtained equation (4.2) in more detail. The rest of the equations (as well as equations for the other sub-systems not shown here) are obtained in a similar fashion. Note that rate $\hat{\lambda}_{1,N1}$ in the left hand side of (4.2) represents the rate of calls originating at satellite 1 and leaving the sub-system over ISL 1-4 in Figure 4.1. Because of the shortest path routing we consider here, these are calls terminating at satellites

Decomposition Algorithm for Mesh Topology

Input : Network topology with N orbits and S satellites per orbit, arrival rate λ_{ij} of new calls from satellite i to satellite j, mean call holding time $1/\mu$.

Output : Call blocking probabilities $P_{s,d}$ for each source and destination satellite pair (s, d).

1. begin
2. $h \leftarrow 0$ //Initialization step
   // $p_{i,j,l}(h)$ is the probability that an inter-sub-system call entering into
   the sub-system l through satellite i and leaving
   the sub-system l from satellite j will be blocked
   $p_{i,j,l}(h) \leftarrow 0$
3. $h \leftarrow h + 1$ //h-th iteration
   S : All connections using link (i, j), $1 \leq i \leq 2$, $i \neq j$,
   $j \epsilon \{N, S, 2\}$ if $1 \leq l \leq 8$ or $j \epsilon \{W, E, 2\}$ if $9 \leq l \leq 16$
   d : Destination satellite
   $R_{i,j}$: All sub-systems visited during a connection between satellite i and j
   For each sub-system l: $\lambda_{i,j} = \sum_{\underline{S}} \lambda_{i,d} \prod_{r \epsilon R_{i,j}} (1 - p_{a,b,r})$
   Solve sub-system l to obtain new values for $p_{i,j,l}(h)$
4. Repeat Step 3 until the blocking probabilities converge
5. End of the algorithm

Figure 4.3: Decomposition algorithm for a given satellite constellation

4, 8, 12, and 16. Also, quantity p_{ij}, where $i, j \epsilon \{1, 2, ., 16, N_1, ...N_8, S_1, ...S_8, W_1, ...W_8, E_1, ...E_8\}$ represents the probability that a call between two satellites traveling through the path segment *(i,j)* in another sub-system will be blocked due to the lack of capacity in that segment.

The first term in (4.2), $(1 - p_{4,S_2})\lambda_{1,4}$ represents the *effective* arrival rate of calls between satellites 1 and 4, as seen by sub-system 1. That is the portion of calls between satellites 1 and 4 not blocked in sub-system 2 between satellites 4 and S_2. The second term is obtained similarly using the shortest path between satellites 1 and 8. The call between satellites 1 and 8 may be blocked either in sub-system 2 between satellites 4 and S_2 or

in sub-system 15 between satellites 4 and 8. Therefore, the *effective* arrival rate for a call between satellites 1 and 8 as seen by sub-system 1 is $(1-p_{4,S_2})(1-p_{4,8})\lambda_{1,8}$. This expression gives us the proportion of calls that are not blocked in sub-systems 2 and 15. The third term $(1-p_{4,S_2})(1-p_{4,E_4})(1-p_{W_8,12})\lambda_{1,12}$ shows the *effective* arrival rate between satellites 1 and 12. This expression gives us the proportion of the traffic that is not blocked between satellites 4 and S_2, 4 and E_4 and W_8 and 12. The last term of $\lambda_{1,N1}$ is similar with the previous term except it uses a different path to reach satellite 16. The rest of the terms are obtained similarly.

Equation (4.5) has a different form than the rest of the equations. In this equation, we see additional *effective* arrival rates to the arrival rate created between node 1 and 2 of that sub-system. These are due to other calls using that link. For instance, the second term indicates the *effective* rate for calls between satellite 1 and 3, that is, the proportion of calls that are not blocked between satellite 2 and $S1$ and 3 and $N2$. In order to eliminate double counting of blocking on the same link (referring to Figure 4.2 we note that the links 2-S1 and 3-N2 correspond to the same ISL 2-3), the link from satellite 2 to fictitious satellite $S1$ is assumed to have infinite capacity. That means, it is not possible for a call to get blocked between satellite 2 and $S1$ because this link is already represented between satellite 3 and $N2$. The third term shows the rate of the calls between satellite 1 and 6 that are not blocked between satellite 2 and 6. The rest of the terms are obtained similarly. Equations (4.2)-(4.8) are used to solve sub-system 1. Similar equations, not shown here are used to solve the other sub-systems in isolation. The quantities p_{ij} are updated at each iteration, as we discuss below. For the first iteration, we use $p_{ij} = 0$, for all i and j. In essence, at the beginning of each iteration, the current values of p_{ij} represent our best estimate for the value of the corresponding blocking probability.

$$\begin{aligned}\hat{\lambda}_{1,N1} = (1-p_{4,S_2})\lambda_{1,4} + (1-p_{4,S_2})(1-p_{4,8})\lambda_{1,8} + \\ (1-p_{4,S_2})(1-p_{4,E_4})(1-p_{W_8,12})\lambda_{1,12} \\ +(1-p_{4,S_2})(1-p_{4,E_4})(1-p_{W_8,16})\lambda_{1,16}\end{aligned} \tag{4.2}$$

$$\begin{aligned}\hat{\lambda}_{1,S1} = (1-p_{N_2,3})\lambda_{1,3} + (1-p_{N_2,3})(1-p_{3,7})\lambda_{1,7} + \\ (1-p_{N_2,3})(1-p_{3,E_3})(1-p_{W_7,11})\lambda_{1,11} \\ +(1-p_{N_2,3})(1-p_{3,E_3})(1-p_{W_7,15})\lambda_{1,15}\end{aligned} \tag{4.3}$$

$$\hat{\lambda}_{1,1} = \lambda_{1,1} \tag{4.4}$$

$$\begin{aligned}\hat{\lambda}_{1,2} = \lambda_{1,2} + (1-p_{2,S_1})(1-p_{N_2,3})\lambda_{1,3} + (1-p_{2,6})\lambda_{1,6} + \\ (1-p_{2,S_1})(1-p_{N_2,3})(1-p_{3,7})\lambda_{1,7} + (1-p_{2,E_2})(1-p_{W_6,10})\lambda_{1,10} + \\ (1-p_{2,S_1})(1-p_{N_2,3})(1-p_{3,E_3})(1-p_{W_7,11})\lambda_{1,11} + (1-p_{2,W_2})(1-p_{E_6,14})\lambda_{1,14} + \\ (1-p_{2,S_1})(1-p_{N_2,3})(1-p_{3,W_3})(1-p_{E_7,15})\lambda_{1,15} + (1-p_{1,N_1})(1-p_{S_2,4})\lambda_{2,4} + \\ (1-p_{1,5})\lambda_{2,5} + (1-p_{1,N_1})(1-p_{S_2,4})(1-p_{4,8})\lambda_{2,8} + (1-p_{1,E_1})(1-p_{W_5,9})\lambda_{2,9} + \\ (1-p_{1,N_1})(1-p_{S_2,4})(1-p_{4,E_4})(1-p_{W_8,12})\lambda_{2,12} + (1-p_{1,W_1})(1-p_{E_5,13})\lambda_{2,13} + \\ (1-p_{1,N_1})(1-p_{S_2,4})(1-p_{4,W_4})(1-p_{E_8,16})\lambda_{2,16}\end{aligned} \tag{4.5}$$

$$\hat{\lambda}_{2,2} = \lambda_{2,2} \tag{4.6}$$

$$\begin{aligned}\hat{\lambda}_{2,N1} = (1-p_{4,S_2})\lambda_{2,4} + (1-p_{4,S_2})(1-p_{4,8})\lambda_{2,8} + \\ (1-p_{4,S_2})(1-p_{4,E_4})(1-p_{W_8,12})\lambda_{2,12} \\ +(1-p_{4,S_2})(1-p_{4,W_4})(1-p_{E_8,16})\lambda_{2,16}\end{aligned} \tag{4.7}$$

$$\begin{aligned}\hat{\lambda}_{2,S1} = (1-p_{3,N_2})\lambda_{2,3} + (1-p_{3,N_2})(1-p_{3,7})\lambda_{2,7} + \\ (1-p_{3,N_2})(1-p_{3,E_3})(1-p_{W_7,11})\lambda_{2,11} \\ +(1-p_{3,N_2})(1-p_{3,W_3})(1-p_{E_7,15})\lambda_{2,15}\end{aligned} \tag{4.8}$$

The solution to the first sub-system gives an initial value for probabilities p_{1,N_1}, p_{1,S_1}, $p_{1,2}$, p_{2,N_1}, and p_{2,S_1}. These probabilities show that a call using sub-system 1 will be blocked due to lack of capacity in a link within sub-system 1. Using these probabilities, we will calculate *effective* arrival rates in the second sub-system. Once *effective* arrival rates are calculated, we will solve the second sub-system in isolation to find out the blocking probabilities p_{3,N_2}, p_{3,S_2}, $p_{3,4}$, p_{4,N_2}, and p_{4,S_2}. This iterative procedure continues solving each sub-system one by one until the blocking probabilities converge. Equations (4.4) and (4.6) are used only to calculate up-and-down (UDL) blocking probabilities, whether this is a UDL call only or a traversing call.

Once the blocking probabilities have converged, the blocking probability between any two satellites can be computed as follows. If both satellites are in the same sub-system,

the corresponding blocking probability is given by the solution to the sub-system. For example, the blocking probability between satellite 1 and satellite 2, both of which are in sub-system 1, is given by the value of $p_{1,2}$ obtained by the solution to this sub-system. However, the blocking probability from satellite 1 to satellite 12 in sub-system 6 is given by:

$$p_{1,12} = 1 - ((1 - p_{1,1})(1 - p_{1,N1})(1 - p_{4,S2})(1 - p_{4,E4})(1 - p_{W8,12})(1 - p_{12,12})) \qquad (4.9)$$

In the above equation, we compute the blocking probability multiplying blocking probabilities at each sub-system through the path between satellites 1 and 12. The first and the last terms $(1 - p_{1,1})$ and $(1 - p_{12,12})$ are the UDL blocking probabilities. The rest of the terms are ISL blocking probabilities.

4.2 Modeling Hand-Offs

In the previous section, we assumed that the constellation was fixed over the earth. In this section, we remove this assumption and we will let the satellites travel along their orbits. We skip the explanation of *Earth-Fixed Coverage* because it is relatively straightforward and doesn't change our calculation method as mentioned in Chapter 3, and examine the more involved case of satellite-fixed coverage.

4.2.1 Satellite-Fixed Coverage

As explained in Chapter 3, in this case a satellite moves, its footprint on the earth (the cell served by the satellite) also moves with it. As customers move out of the footprint area of a satellite, their calls are handed off to the satellites following it from behind. In order to model hand-offs in this case, we assumed in the previous chapter that potential customers are uniformly distributed over the part of the earth served by the satellites in the orbit. This assumption had two consequences, and we repeat them here for the sake of clarity.

- The arrival rate λ to each satellite remains constant as it moves around the earth. Then, the arrival rate of calls between satellite i and satellite j is given by $\lambda_{ij} = \lambda r_{ij}$, where r_{ij} is the probability that a call originating by a customer served by satellite i is for a customer served by satellite j.

- The active customers served by a satellite are assumed to be uniformly distributed over the satellite's footprint. As a result, the rate of hand-offs from satellite i to satellite j that is following from behind is proportional to the number of calls at satellite i.

As shown in Chapter 3, even for a small system there are quite a number of transitions. For a whole constellation, the number of transitions increases drastically. Therefore, it is not feasible to obtain all transition rates for a LEO satellite constellation. In order to make the problem tractable, we developed a distributed method to calculate transition rates and solve for traffic equations. That way, we can solve each sub-system in isolation, and iterate the results.

Solving Constellations with Satellite-Fixed Coverage and Hand-offs

In order to solve a constellation with satellite-fixed coverage and hand-offs, we follow the procedure described below:

- Constellation is a queueing network of M/M/K/K queues, where each queue represents the number of calls per satellites $i - j$ pair (no hand-offs case).
- Using ideas from previous section, in order to model hand-offs, we introduce additional transitions of customers moving from one queue to another.
- We solve traffic equations from Step 2 exactly to obtain the effective arrival rates.
- We apply decomposition algorithm described in Section 3.2.

A Distributed Solution for Traffic Equations

Solving the traffic equations for a whole constellation is very time-consuming ($O(N^3)$) where N is the number of states in the Markov process for the whole constellation. In order to decrease the complexity of the process, we now develop an approximate solution. Instead of defining the traffic equations for the whole system, we use a distributed approach. That is, we treat each sub-system defined in Section 4.1 separately and solve the traffic equations in isolation. Transitions between sub-systems are also taken into account.

In order to explain the distributed algorithm, we refer to Figure 4.2. Let us consider sub-system 1 in isolation. Recall that this sub-system is described by the Markov process:

$$\underline{n} = (n_{11}, n_{12}, n_{1N_1}, n_{1S_1}, n_{22}, n_{2N_1}, n_{2S_1}) \tag{4.10}$$

Consider random variable n_{12}. This random variable may represent a call originating at satellite 1 and terminating at satellite 2, a call that originates at satellite 1 (or satellite 2) and uses the ISL 1-2 but does not terminate at satellite 2 (respectively satellite 1), or a call that simply uses ISL 1-2 but does not originate or terminate at either satellite 1 or satellite 2. Based on this observation, the transitions between states of the Markov process due to hand-offs depend on the type of call.

Consider first the case where a call originates at satellite 1 and terminates at satellite 2. If the customer under satellite 1 makes a hand-off to satellite 2, this call becomes a call handled by satellite 2 alone (i.e., it both originates and terminates at satellite 2). Thus, we have the following transition:

$$r(\underline{n}, \underline{n} - \underline{1}_{12} + \underline{1}_{22}) = \alpha n_{12}, \qquad n_{12} > 0 \tag{4.11}$$

Another possibility is for the customer under satellite 2 to make a hand-off to satellite 3 (see Figure 4.1). In this case, from the point of view of sub-system 1, this call becomes a call between satellite 1 and satellite S1. Therefore, the transition is:

$$r(\underline{n}, \underline{n} - \underline{1}_{12} + \underline{1}_{1S_1}) = \alpha n_{12}, \qquad n_{12} > 0 \tag{4.12}$$

On the other hand, consider a customer in satellite 1 with a connection to satellite 10. The call is routed through satellites 2 and 6 to satellite 10. Therefore, in sub-system 1, this is a call between satellites 1 and 2. If the customer under satellite 1 makes a handover, the call leaves sub-system 1 and is treated by sub-system 11 after the handover. This transition is shown in equation (4.13).

$$r(\underline{n}, \underline{n} - \underline{1}_{12}) = \alpha n_{12}, \qquad n_{12} > 0 \tag{4.13}$$

The transition rates involving the other random variables in the state description (4.10) can be derived using similar arguments. For completeness, these transition rates are provided in (4.14)-(4.24).

$$r(\underline{n}, \underline{n} - \underline{1}_{11} + \underline{1}_{12}) = 2\alpha n_{11}, \qquad n_{11} > 0 \tag{4.14}$$

$$r(\underline{n}, \underline{n} - \underline{1}_{1N_1} + \underline{1}_{11}) = \alpha n_{1N_1}, \qquad n_{1N_1} > 0 \tag{4.15}$$

$$r(\underline{n}, \underline{n} - \underline{1}_{1N_1} + \underline{1}_{2N_1}) = \alpha n_{1N_1}, \qquad n_{1N_1} > 0 \tag{4.16}$$

$$r(\underline{n}, \underline{n} - \underline{1}_{1N_1}) = \alpha n_{1N_1}, \qquad n_{1N_1} > 0 \tag{4.17}$$

$$r(\underline{n}, \underline{n} - \underline{1}_{1S_1} + \underline{1}_{1N_1}) = \alpha n_{1S_1}, \qquad n_{1S_1} > 0 \tag{4.18}$$

$$r(\underline{n}, \underline{n} - \underline{1}_{1S_1} + \underline{1}_{2S_1}) = \alpha n_{1S_1}, \qquad n_{1S_1} > 0 \tag{4.19}$$

$$r(\underline{n}, \underline{n} - \underline{1}_{1S_1}) = \alpha n_{1S_1}, \qquad n_{1S_1} > 0 \tag{4.20}$$

$$r(\underline{n}, \underline{n} - \underline{1}_{22} + \underline{1}_{2S_1}) = 2\alpha n_{22}, \qquad n_{22} > 0 \tag{4.21}$$

$$r(\underline{n}, \underline{n} - \underline{1}_{2N_1} + \underline{1}_{12}) = \alpha n_{2N_1}, \qquad n_{2N_1} > 0 \tag{4.22}$$

$$r(\underline{n}, \underline{n} - \underline{1}_{2N_1}) = \alpha n_{2N_1}, \qquad n_{2N_1} > 0 \tag{4.23}$$

$$r(\underline{n}, \underline{n} - \underline{1}_{2S_1}) = 2\alpha n_{2S_1}, \qquad n_{2S_1} > 0 \tag{4.24}$$

Once the transition rates are known, the traffic equations for each queue can be written easily as shown in (4.25)-(4.31).

$$\gamma_{11} = \hat{\lambda}_{1,1} + \frac{\alpha}{3\alpha + \mu}\gamma_{1N_1} \tag{4.25}$$

$$\gamma_{12} = \hat{\lambda}_{1,2} + \frac{2\alpha}{2\alpha + \mu}\gamma_{11} + \frac{\alpha}{2\alpha + \mu}\gamma_{2N_1} \tag{4.26}$$

$$\gamma_{1N_1} = \hat{\lambda}_{1,N_1} + \frac{\alpha}{3\alpha + \mu}\gamma_{1S_1} \tag{4.27}$$

$$\gamma_{1S_1} = \hat{\lambda}_{1,S_1} + \frac{\alpha}{3\alpha + \mu}\gamma_{12} \tag{4.28}$$

$$\gamma_{22} = \hat{\lambda}_{2,2} + \frac{\alpha}{3\alpha + \mu}\gamma_{12} \tag{4.29}$$

$$\gamma_{2N_1} = \hat{\lambda}_{2,N_1} + \frac{\alpha}{3\alpha + \mu}\gamma_{1N_1} \tag{4.30}$$

$$\gamma_{2S_1} = \hat{\lambda}_{2,S_1} + \frac{2\alpha}{2\alpha + \mu}\gamma_{22} + \frac{\alpha}{3\alpha + \mu}\gamma_{1S_1} \tag{4.31}$$

The solution to the traffic equations above gives us the new $\rho'_{ij} = \gamma_{ij}/\nu_{ij}$. (as defined in Section 3.) At each iteration, after calculating the new *effective* arrival rates ($\hat{\lambda}_{ij}$), we compute γ_{ij}'s using Equations (4.25)-(4.31) and using these γ_{ij}'s, we calculate new ρ'_{ij}'s. This procedure repeats for each sub-system until the blocking probabilities converge.

4.3 Numerical Results

In this section we validate the accuracy of the decomposition algorithm with and without handovers by comparing the results obtained from the decomposition algorithm to simulation results as we did in Chapter 3. The parameters defined for the simulations in Chapter 3 are maintained and repeated here for easiness. The simulation results are plotted with 95% confidence intervals estimated by the method of replications. The number of replications is 30, with each simulation run lasting until each type of call has at least 15,000 arrivals. For the approximate results, the iterative decomposition algorithm terminates when all call blocking probability values have converged within 10^{-6}.

The results presented here were obtained using four different traffic patterns. Let $r_{i,j}$ denote the probability that a call originating by a customer served by satellite i is for a customer served by satellite j. The first pattern is the uniform traffic pattern, that is:

$$r_{i,j} = \frac{1}{m} \quad \forall\, i,j \qquad \text{(uniform pattern)} \tag{4.32}$$

where m is the number of satellites. The second traffic pattern is based on the notion of traffic locality. Specifically, it assumes that most calls originating at a satellite i of orbit l are to users in satellites $i-1$, i, and $i+1$ of orbit l or to users in satellites i of orbits $l-1$ and $l+1$. Let r_{i_l,j_k} denote the probability that a call originating by a customer served by satellite i of orbit l is for a customer served by satellite j of orbit k. Then, we have:

$$r_{i_l,j_k} = \begin{cases} 0.16, & j_k = (i-1)_l, i_l, (i+1)_l, i_{l-1},\ and\ i_{l+1} \\ \frac{0.2}{m-5}, & j_k \neq (i-1)_l, i_l, (i+1)_l, i_{l-1},\ and\ i_{l+1} \end{cases} \qquad \text{(locality pattern)} \tag{4.33}$$

where addition and subtraction is modulo-k for a k satellites per orbit.

The third traffic pattern assumes that there are four communities of users as shown in Figure 4.4, and most traffic is between users within a community (e.g., satellites over different continents of the earth). Let $r_{i,j}$ represent calls originating from region i and terminating at region j, we have:

$$r_{i,j} = \begin{cases} \frac{0.6}{m/4}, & i = j \qquad (4-\text{community pattern}) \\ \frac{0.133}{m/12}, & i \neq j \end{cases} \tag{4.34}$$

The fourth traffic pattern is hot spot pattern in which one of the satellites carries most of the traffic. Let $r_{i,j}$ represent calls originating from satellite i and terminating at satellite j, we have:

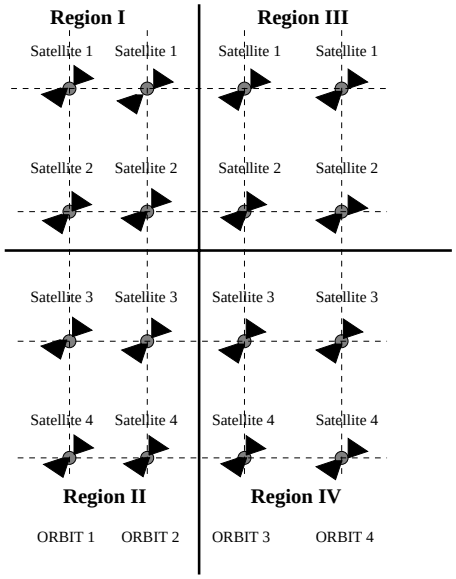

Figure 4.4: Four regions for 4-community Pattern

$$r_{i,j} = \begin{cases} 0.7, & i = 1..m, j = X \qquad \text{(hot spot pattern)} \\ \frac{0.3}{m-1}, & i, j \neq X \end{cases} \tag{4.35}$$

where X is the hot spot satellite.

4.3.1 Validation of the Decomposition Algorithm without Handovers

We now validate the decomposition algorithm developed in Section 4.1 by comparing the blocking probabilities obtained from the algorithm to simulation results. We consider a constellation of 16 satellites with four orbits and four satellites per orbit as shown in Figure 4.1. Each satellite has four ISLs; two within the same orbit and two with neighboring orbits. In this first set of tests, we assumed a system without handovers. In all cases studied, we have found that the algorithms converges in only a few (less than ten) iterations, taking a few minutes to terminate. On the other hand, simulation of 16-satellite system is quite expensive in terms of computation time, taking several hours to complete.

Figure 4.5 plots the blocking probability against the capacity C_{UDL} of up-and-down links, when the arrival rate $\lambda = 5$ and the capacity of inter-satellite links $C_{ISL} = 10$, for the uniform traffic pattern. Five sets of calls are shown, one for local calls, and four for non-local calls. Each set consists of two plots, one corresponding to blocking

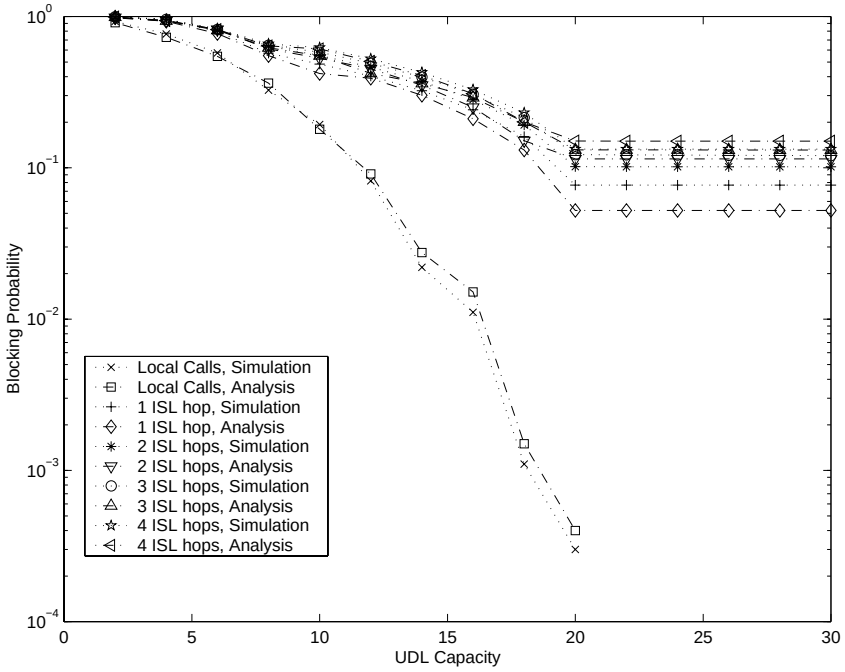

Figure 4.5: Call blocking probabilities for 16 satellites, $\lambda = 5$, $C_{ISL} = 10$, uniform pattern

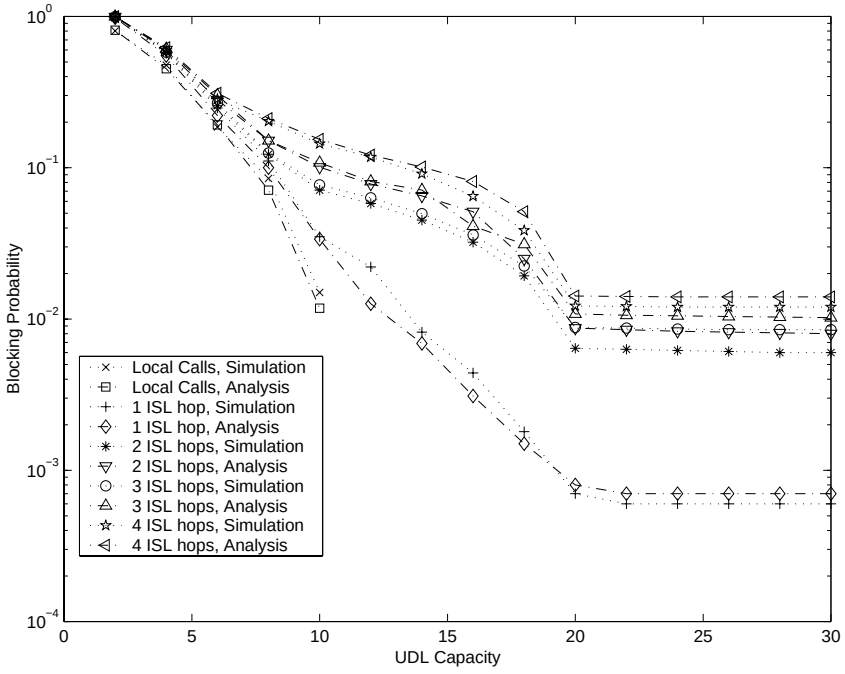

Figure 4.6: Call blocking probabilities for a 16 satellites, $\lambda = 2$, $C_{ISL} = 10$, uniform pattern

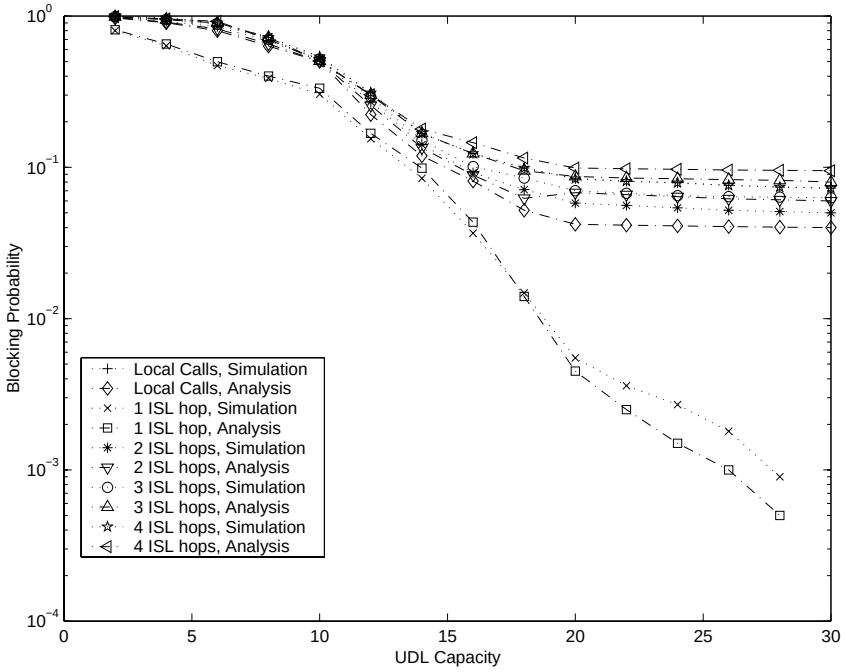

Figure 4.7: Call blocking probabilities for a 16 satellites, $\lambda = 5$, $C_{ISL} = 10$, locality pattern

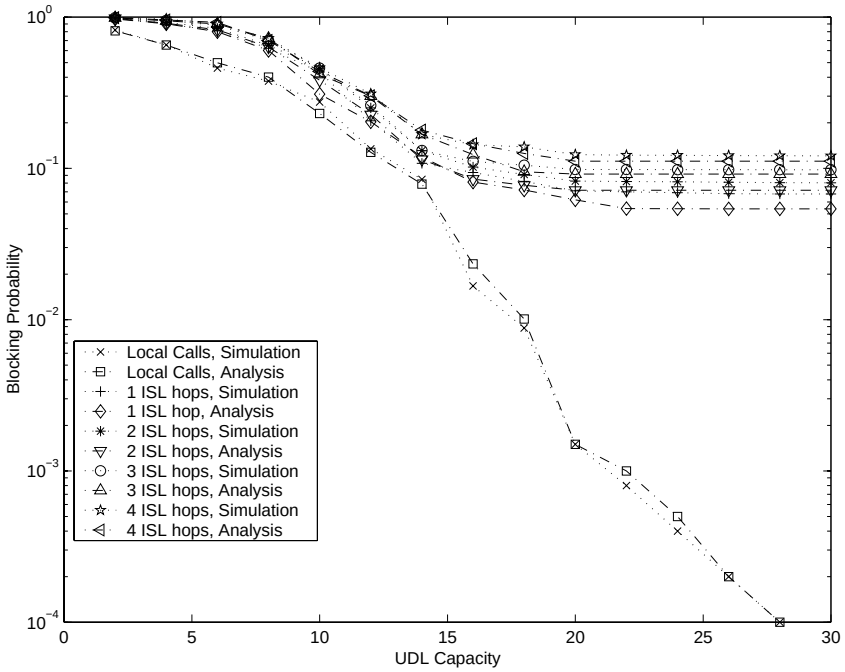

Figure 4.8: Call blocking probabilities for a 16 satellites, $\lambda = 5$, $C_{ISL} = 10$, 4-community pattern

probability values obtained by running the decomposition algorithm of Section 3.2, and one corresponding to simulation results. Each non-local call for which results are shown travels over a different number of inter-satellite links, varying from one ISL to four ISLs. Choosing the destination, we took into account the path from one sub-system to another within the same orbit, and between orbits. According to the constellation structure, four ISL is the maximum number of ISL that could be traversed between two satellites using shortest path routing. Thus, the results in Figure 4.5 represent calls between all the different sub-systems in which the 16 satellite system is decomposed by the decomposition algorithm.

From the figure we observe a very good agreement between the analytical results and simulation. Note that the y-axis uses a logarithmic scale. The behavior of the curves can be explained by noting that, when the capacity C_{UDL} of up-and-down links is less than 20, these links represent a bottleneck. Thus, increasing the up-and-down link capacity results in a significant drop in the blocking probability for all calls. When $C_{UDL} > 20$, however, the inter-satellite links become the bottleneck, and non-local calls do not benefit from further increases in the up-and-down link capacity. We also observe that, the larger the number of inter-satellite links over which a non-local call must travel, the higher its blocking probability, as expected. The blocking probability of local calls, on the other hand, drops to zero for $C_{UDL} > 20$ since they do not have to compete for inter-satellite links. The curves in this figure were obtained assuming that $\lambda = 5$ which results to a utilization of an ISL of around 65%. Therefore, the blocking probabilities are fairly high. In order to see the effect of decreased utilization, we changed the arrival rate to $\lambda = 2$, which resulted to a utilization of an ISL to 30%. The blocking probabilities are shown in Figure 4.6.

Figures 4.7 and 4.8 are similar to Figure 4.5 but show results for the locality and 4-community traffic patterns, respectively. For the results presented we used $\lambda = 5$ and $C_{ISL} = 10$, and we varied the value of C_{UDL}. We observe that the values of the call blocking probabilities depend on the actual traffic pattern, but the behavior of the various curves is similar to that in Figure 4.5.

Finally, in Figure 4.9, we see a totally different result. In this scenario, all satellites send most of their traffic to satellite 3. We observe that when the UDL capacity increases, the blocking probability on calls using 2 ISL hops decreases. This is due to the fact that these calls are between satellite 1 and 3. Therefore, increasing the UDL capacity on satellite 3 decreases the blocking probability of calls between satellite 1 and 3. On the other hand, for other calls with 1, 3 and 4 ISL hops which pass through satellite 3, the blocking probability

increases with increasing UDL capacity. This is due to the fact that increasing the UDL capacity of satellite 3 increases the loading on the ISLs of satellite 3. That is, satellite 3 can accept more calls through its ISLs. As a consequence the blocking probability on these links increase. Local call blocking probabilities go down to 0 as in other cases.

Overall, the results in Figures 4.5–4.9 indicate that analytical results are in good agreement with simulation over a wide range of traffic patterns and system parameters. The largest relative error observed was 6%, and the average relative error was 0.7%.

4.3.2 Validation of the Decomposition Algorithm with Handovers

In this section, we validate the decomposition algorithm assuming handovers. We consider the same satellite constellation with 16 satellites. We solve the traffic equations with handovers as explained in Section 4.2.1. We then used these arrival rates to calculate the new ρ's and then used our decomposition algorithm to calculate the blocking probabilities. We also included handovers in our simulation in order to test the accuracy of the algorithm.

Figure 4.10 plots the blocking probability against the capacity C_{UDL} of up-and-down links, when the arrival rate $\lambda = 5$ and the capacity of inter-satellite links $C_{ISL} = 10$, for the uniform traffic pattern. The remaining figures 4.10 to 4.13 give similar results as in the figures presented in the previous section. Five sets of calls are shown, one for local calls, and four for non-local calls.

We note that there is a good agreement between the analytical results and simulation. The results in this section are a little worse than the ones given in Section 4.3.1. This is expected, because the calculation of the arrival rates using the distributed solution for the traffic equations, introduced an additional approximation. The maximum relative error observed was 9% and the average relative error was 2%.

4.4 Concluding Remarks

We have presented an analytical model for computing blocking probabilities for LEO satellite constellations. We have developed an algorithm for decomposing the whole constellation into smaller sub-systems and then used a Markov process to solve each sub-system in isolation. In our analysis, we used sub-systems of two satellites for the sake of simplicity although it is possible to increase the sub-system sizes to three satellites plus two

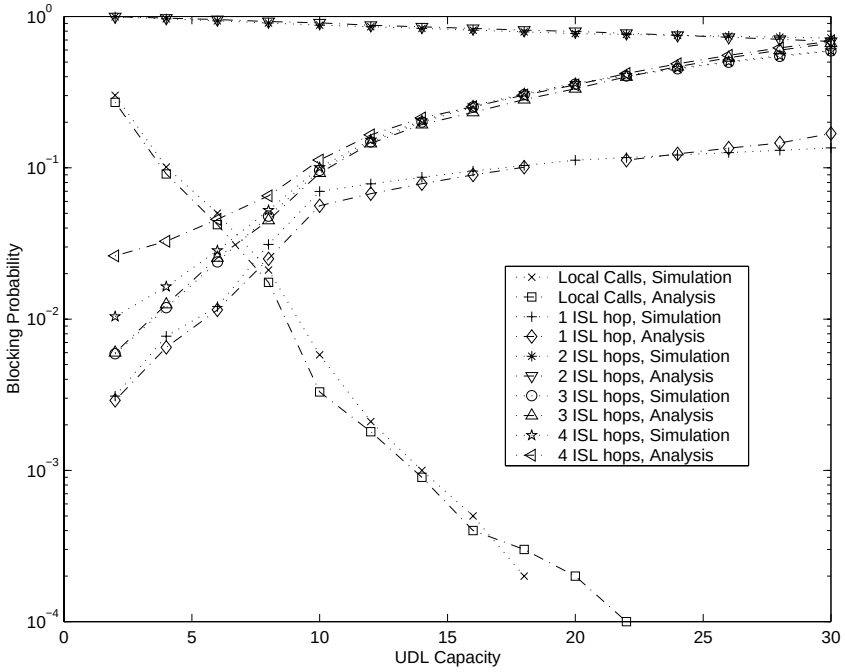

Figure 4.9: Call blocking probabilities for a 16 satellites, $\lambda = 5$, $C_{ISL} = 10$, hot-spot pattern

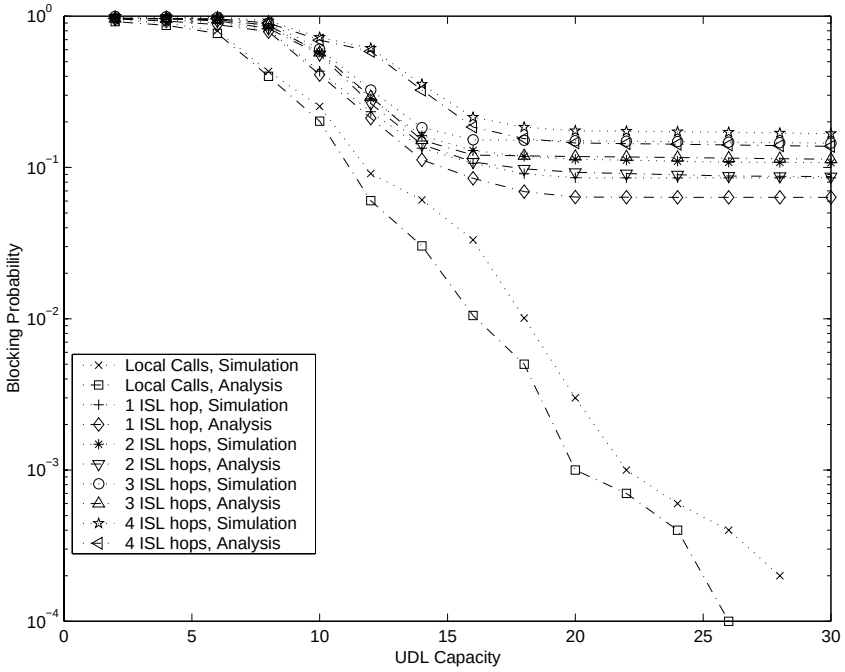

Figure 4.10: Call blocking probabilities for 16 satellites with handover, uniform pattern

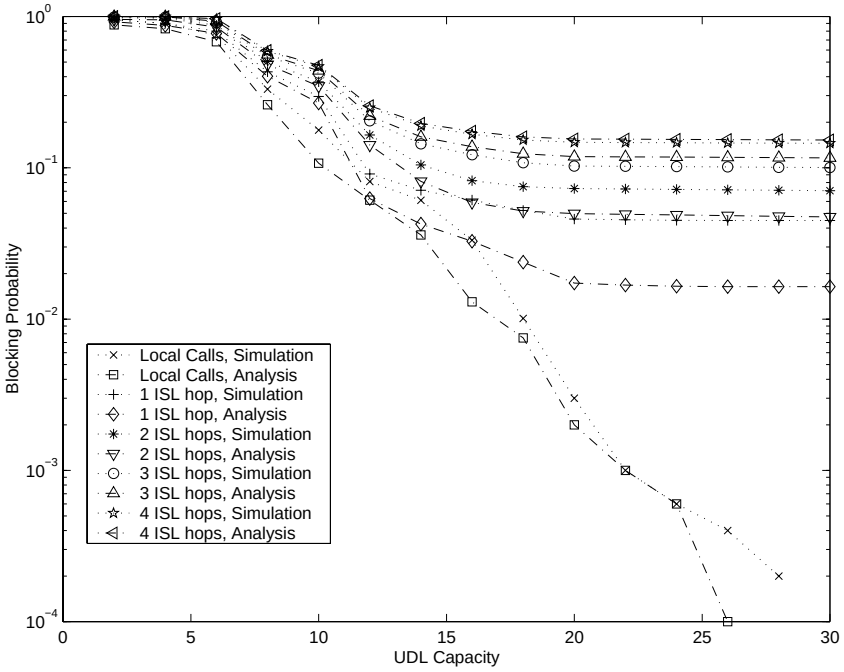

Figure 4.11: Call blocking probabilities for 16 satellites with handover, locality pattern

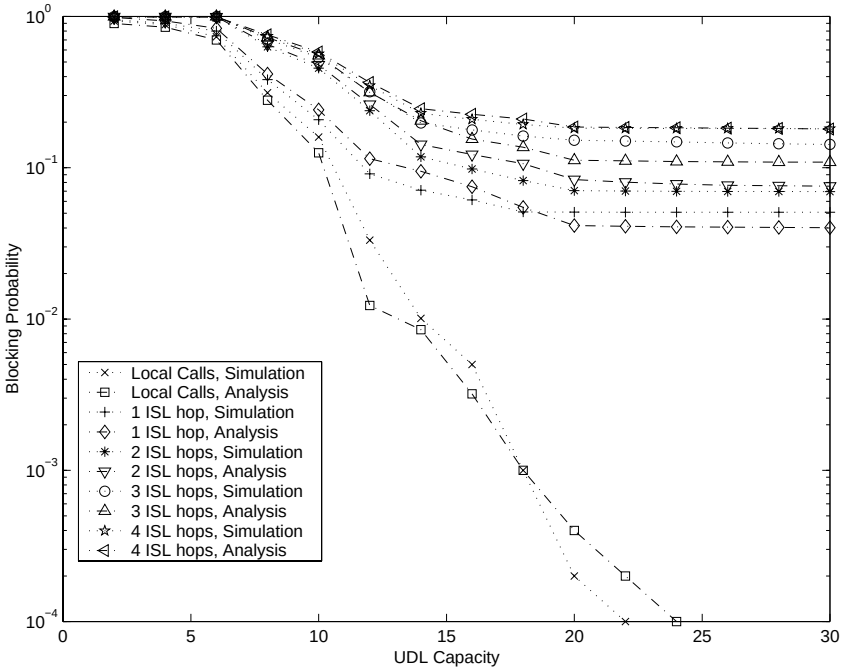

Figure 4.12: Call blocking probabilities for 16 satellites with handover, 4-community pattern

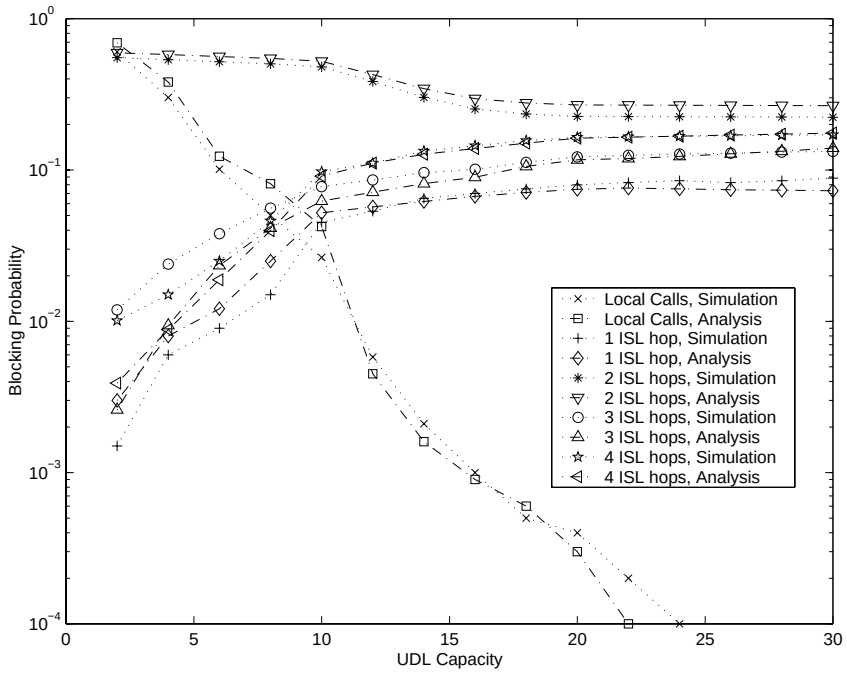

Figure 4.13: Call blocking probabilities for 16 satellites with handover, hot-spot pattern

fictitious ones. We have also shown how our approach can capture blocking due to hand-offs for both satellite-fixed and earth-fixed orbits. Finally, we have used a distributed method to solve the traffic equations.

In Figure 4.1, we didn't take into account the effect of the seam on the constellation. However, the addition of the seam does not pose a problem for our algorithm. The only change would be on our shortest-path algorithm used to define the routes that calls take. In case of a real system with seam, we need to define the seam in the definition of our constellation. In that case, our shortest-path algorithm will find the routes according to that constellation, and the constraints will be created accordingly.

Chapter 5

Bounds on the Call Blocking Probabilities

In Chapter 4, we extended the algorithm presented in Chapter 3 to systems with multiple orbits. This permitted us to analyze a whole LEO satellite constellation without a seam. LEO satellite constellations with a seam can also be analyzed by adjusting the routing paths according to the location of the seam. However, so far, we have assumed systems with a single beam per satellite. In order to remove this assumption, we need to treat each beam spot as a single satellite. That is, for a LEO constellation with 16 satellites and ten beams per satellite, we need to analyze a system with 160 satellites. This system can be analyzed using the decomposition algorithm described in Chapter 4. However, due to the large number of satellites, the complexity of the algorithm will be significantly increased especially when dealing with handoffs. In this chapter, we present an upper and lower bound on the call blocking probabilities. These bounds permit us to calculate blocking probabilities in a large system with multiple orbits and multiple beams per satellite. In order to obtain the lower bound, we treated each link independently. That is, we calculate the blocking probability at each link using only the constraint at that link. Breaking the dependency among links causes the blocking probability to decrease. This method is explained in the next section with the help of a truncated process.

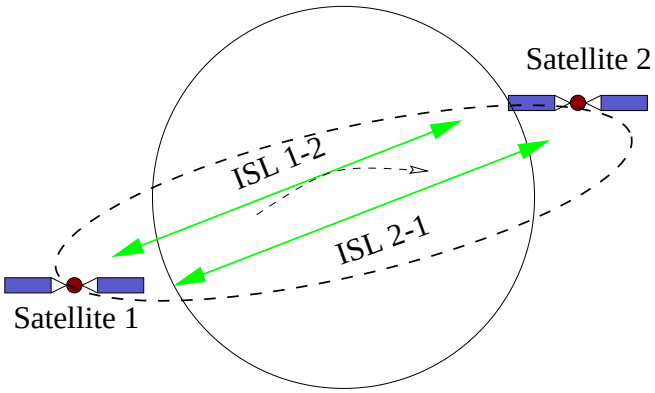

Figure 5.1: The Simplest Satellite System with 2 Satellites

5.1 The Upper and Lower Bounds: the two-satellite System

In this section, we describe a method for calculating an upper and lower bound on the call blocking probabilities using the two-satellite system shown in Figure 5.1. In this system, there are two intersatellite links, ISL1 and ISL2. Also, each satellite has an up and down link.

The Markov process for this system is :

$$\underline{n} = (n_{11}, n_{12}, n_{22}) \tag{5.1}$$

where n_{11} is the number of calls using the up and down link of satellite 1, n_{12} is the number of calls using ISL1 or ISL2, and n_{22} is the number of calls using the up and down link of satellite 2.

We recall that the constraints are:

$$2n_{11} + n_{12} \leq C_{UDL} \tag{5.2}$$

$$n_{12} + 2n_{22} \leq C_{UDL} \tag{5.3}$$

$$n_{12} \leq C_{ISL} \tag{5.4}$$

In order to obtain the upper and lower bound, we define a truncated Markov process of $\underline{n}$ for each link in the satellite system. For instance, for the up and down link of satellite *1*, we define the truncated Markov process $\underline{n}_{UDL1} = (n_{11}, n_{12})$, where $2n_{11} + n_{12} \leq C_{UDL}$. This process is obtained from $\underline{n}$ by simply setting to zero all random variables not related to the up and down link of satellite 1. In this case, only variable $n_{22} = 0$.

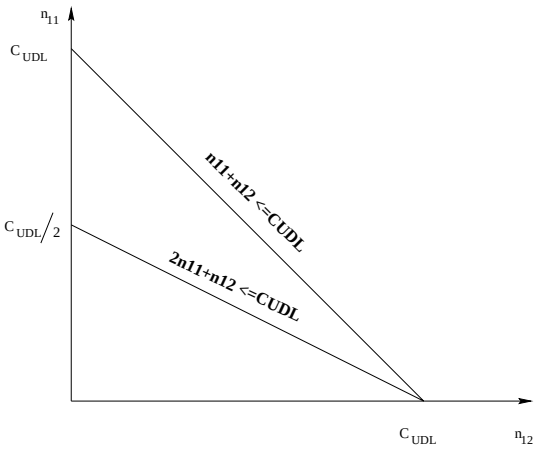

Figure 5.2: The State Spaces for $\underline{n}_{UDL1}$: original and relaxed

Likewise, for the up and down link of n_{UDL2} satellite 2, we define the truncated process of $\underline{n}$, by setting $n_{11} = 0$. We have, $n_{UDL2} = (n_{12}, n_{22})$ where $2n_{22} + n_{12} \leq C_{UDL}$. Finally, we define $n_{ISL} = (n_{22})$ by zeroing n_{11} and n_{12} where $n_{22} \leq C_{ISL}$.

Now, let us analyze the first Markov process. In order to calculate the blocking probability, we need to find the normalizing constant G_{UDL1}. For the given Markov process, the normalizing constant G_{UDL1} can be computed as follows:

$$G_{UDL1} = \sum_{0 \leq 2n_{11}+n_{12} \leq C_{UDL}} \frac{\rho_{11}^{n_{11}} \rho_{12}^{n_{12}}}{n_{11}! n_{22}!} \tag{5.5}$$

If we multiply the right-hand side of the above expression by $C_{UDL}!/C_{UDL}!$, we obtain

$$G = \frac{1}{C_{UDL}!} \sum_{0 \leq 2n_{11}+n_{12} \leq C_{UDL}} C_{UDL}! \frac{\rho_{11}^{n_{11}} \rho_{12}^{n_{12}}}{n_{11}! n_{22}!} \tag{5.6}$$

Now, instead of summing up over the state space defined by constraint 5.2, we sum up over the state space defined by the following constraint:

$$n_{11} + n_{12} \quad \leq \quad C_{UDL} \tag{5.7}$$

The resulting state space is shown in Figure 5.2. The area under the line marked $2n_{11} + n_{12} \leq C_{UDL}$ is the state space of the truncated process $\underline{n}_{UDL1}$, whereas the area under the line marked $n_{11} + n_{12} \leq C_{UDL}$ is the new state space.

Relaxing the constraint permits us to calculate the normalizing constant easier. We have

$$G_{UDL1} = \frac{1}{C_{UDL}!} \sum_{0 \leq n_{11}+n_{12} \leq C_{UDL}} C_{UDL}! \frac{\rho_{11}^{n_{11}} \rho_{12}^{n_{12}}}{n_{11}! n_{22}!} \tag{5.8}$$

For each set of values for which $n_{11} + n_{12} = K$, where $K \leq C_{UDL}$, we can write (5.8) as follows:

$$S_{n_{11}+n_{12}=K} = \frac{1}{(n_{11}+n_{12}=K)!} \sum_{n_{11}+n_{12}=K} (n_{11}+n_{12}=K)! \frac{\rho_{11}^{n_{11}} \rho_{12}^{n_{12}}}{n_{11}! n_{22}!} \tag{5.9}$$

We observe that 5.9 is in fact a multinomial distribution where $n_{11} + n_{12} = K$. Therefore, we can rewrite this equation as follows:

$$S_{n_{11}+n_{12}=K} = \frac{1}{K!}(\rho_{11}+\rho_{12})^K \tag{5.10}$$

In view of this, the normalizing constant can be calculated as follows:

$$G_{UDL_1} = \sum_{0 \leq K \leq C_{UDL}} \frac{1}{K!}(\rho_{11}+\rho_{12})^K \tag{5.11}$$

The blocking probability on UDL 1 is given by the expression:

$$P_{UDL1} = \frac{\sum_{n_{11}+n_{12}=C_{UDL}} \frac{\rho_{11}^{n_{11}} \rho_{12}^{n_{12}}}{n_{11}! n_{12}!}}{\sum_{0 \leq K \leq C_{UDL}} \frac{1}{K!}(\rho_{11}+\rho_{12})^K} \tag{5.12}$$

Multiplying the numerator by $C_{UDL}!/C_{UDL}!$ gives

$$P_{UDL1} = \frac{\frac{1}{C_{UDL}!} \sum_{n_{11}+n_{12}=C_{UDL}} C_{UDL}! \frac{\rho_{11}^{n_{11}} \rho_{12}^{n_{12}}}{n_{11}! n_{12}!}}{\sum_{0 \leq K \leq C_{UDL}} \frac{1}{K!}(\rho_{11}+\rho_{12})^K} \tag{5.13}$$

or

$$P_{UDL1} = \frac{\frac{1}{C_{UDL}!}(\rho_{11}+\rho_{12})^{C_{UDL}}}{\sum_{0 \leq K \leq C_{UDL}} \frac{1}{K!}(\rho_{11}+\rho_{12})^K} \tag{5.14}$$

This Blocking probability can be calculated easily using a recursive algorithm as shown in Figure 5.3.

We can apply the same method to calculate the blocking probabilities P_{UDL2} and P_{ISL} using the Markov process $\underline{n}_{UDL2}$ and $\underline{n}_{ISL}$ respectively (The calculation of P_{ISL} is in fact trivial). The blocking probability between satellite 1 and satellite 2 is:

$$P_{1-2} = 1 - (1 - P_{UDL_1})(1 - P_{ISL})(1 - P_{UDL_2}) \tag{5.15}$$

Since we relaxed the original constraints, the resulting blocking probability is a lower bound for the blocking probability between satellite 1 and satellite 2. A similar approach can be used to calculate upper bounds. This time, we need to tighten the constraint instead of relaxing them. That means that we will solve $\underline{n}_{UDL1}$ using the smaller state

A Recursive Algorithm to Calculate P_{UDL1}

1. begin
2. Enter C_{UDL}
3. Enter ρ_{ij}s
4. $\rho_T = \rho_{11} + \rho_{12}$
5. $P_{UDL1} = 1$ // initialization step
6. For n=1 to C_{UDL}

   $P_{UDL1} = \rho_T * P_{UDL1}/(n + \rho_T * P_{UDL1})$
7. End of the algorithm

Figure 5.3: A Recursive Algorithm to Calculate Blocking Probabilities

space defined by the constraint $n_{11} + n_{12} \leq C_{UDL}$ as shown in Figure 5.4. The choice of $C_{UDL}/2$ is based on the transformation of the formulation into multinomial distribution. That is, although it is possible to use other ratios, relaxing C_{UDL} to $C_{UDL}/2$ gives us the chance to use multinomial distribution in our calculation.

The resulting blocking probability on UDL 1 is given as follows:

$$P_{UDL_1} = \frac{\frac{1}{(C_{UDL}/2)!}(\rho_{11} + \rho_{12})^{(C_{UDL})/2}}{\sum_{0 \leq K \leq (C_{UDL}/2)} \frac{1}{K!}(\rho_{11} + \rho_{12})^K} \tag{5.16}$$

End-to-end blocking probabilities are calculated similarly with lower bounds.

We can easily verify that the lower bound described in this section is lower than the original blocking probability which is higher than the truncated process defined by the constraint 5.2. For $C_{UDL} = 2$, we can show algebraically that 5.17 holds. [1].

$$\frac{\sum_{n_{11}+n_{12}=C_{UDL}} \frac{\rho_{11}^{n_{11}} \rho_{12}^{n_{12}}}{n_{11}! n_{12}!}}{\sum_{n_{11}+n_{12} \leq C_{UDL}} \frac{\rho_{11}^{n_{11}} \rho_{12}^{n_{12}}}{n_{11}! n_{12}!}} \leq \frac{\sum_{2n_{11}+n_{12}=C_{UDL}} \frac{\rho_{11}^{n_{11}} \rho_{12}^{n_{12}}}{n_{11}! n_{12}!}}{\sum_{2n_{11}+n_{12} \leq C_{UDL}} \frac{\rho_{11}^{n_{11}} \rho_{12}^{n_{12}}}{n_{11}! n_{12}!}} \leq$$

$$\frac{\sum_{2n_{11}+n_{12}=C_{UDL}, n_{12}+2n_{22} \leq C_{UDL}, n_{12} \leq C_{ISL}} \frac{\rho_{11}^{n_{11}} \rho_{12}^{n_{12}} \rho_{22}^{n_{22}}}{n_{11}! n_{12}! n_{22}!}}{\sum_{2n_{11}+n_{12} \leq C_{UDL}, n_{12}+2n_{22} \leq C_{UDL}, n_{12} \leq C_{ISL}} \frac{\rho_{11}^{n_{11}} \rho_{12}^{n_{12}} \rho_{22}^{n_{22}}}{n_{11}! n_{12}! n_{22}!}} \tag{5.17}$$

This can be generalized to any value of C_{UDL}. The details are not given here.

[1] For $C_{UDL} = 2$, Original Blocking Probability (0.3043) > Truncated Process' Blocking Probability (0.2941) > Lower Bound (0.2). Upper Bound (0.5) is higher than all three Blocking Probabilities.

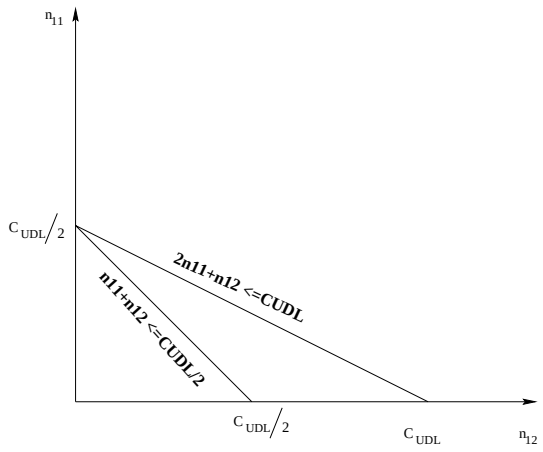

Figure 5.4: The State Spaces for $\underline{n}_{UDL1}$: original and tightened

5.2 The Upper and Lower Bound for any Satellite System

In Section 5.1, we described how to calculate an upper and a lower bound for the simplest system consisting of two satellites. In this section, we show how the upper and lower bound can be calculated for a satellite system with any number of satellites. For the sake of presentation, we will use the example in Chapter 4, shown in Figure 4.1, which consists of 16 satellites. Below, we describe how we calculate the bounds for the blocking probability of the up and down link on satellite 1, the up and down link on satellite 2, and the link between satellite 1 and 2.

For the up and down link of satellite 1, we defined a similar truncated Markov process

$$\underline{n}_{UDL1} = (n_{11}, n_{12}, n_{13}, n_{14}, ...) \tag{5.18}$$

by zeroing the remaining random variables, where

$$\begin{aligned} 2n_{11} + n_{12} + n_{13} + n_{14} + n_{15} + n_{16} + n_{17} + n_{18} + n_{19} + n_{1,10} + \\ n_{1,11} + n_{1,12} + n_{1,13} + n_{1,14} + n_{1,15} + n_{1,16} \quad \leq \quad C_{UDL} \end{aligned} \tag{5.19}$$

Likewise, we define $\underline{n}_{UDL2}$, where

$$\begin{aligned} n_{12} + 2n_{22} + n_{23} + n_{24} + n_{25} + n_{26} + n_{27} + n_{28} + n_{29} + n_{2,10} + \\ n_{2,11} + n_{2,12} + n_{2,13} + n_{2,14} + n_{2,15} + n_{2,16} \quad \leq \quad C_{UDL} \end{aligned} \tag{5.20}$$

Finally, we define $\underline{n}_{ISL}$, where

$$n_{12} + n_{13} + n_{16} + n_{17} + n_{110} + n_{111} + n_{114} + n_{115} \quad \leq \quad C_{ISL} \tag{5.21}$$

The normalizing constant for the lower bound of the up and down blocking probabilities of satellite 1 can be calculated as follows:

$$G = \sum_{0 \leq K \leq C_{UDL}} \frac{1}{K!}(\rho_{11} + \rho_{12} + \rho_{13} + \rho_{14} + \rho_{15} + \rho_{16} + \rho_{17} + \rho_{18} + \rho_{19} + \rho_{110} + \rho_{111} + \rho_{112} + \rho_{113} + \rho_{114} + \rho_{115} + \rho_{116})^K \tag{5.22}$$

where K is defined as:

$$K = \sum_{1 \leq j \leq 16} n_{1j} \tag{5.23}$$

The blocking probability on UDL of satellite 1 is as follows:

$$P_{UDL_1} = \frac{\frac{1}{C_{UDL}!}(\sum_{1 \leq j \leq 16} \rho_{1j})^{C_{UDL}}}{\sum_{0 \leq K \leq C_{UDL}} \frac{1}{K!}(\sum_{1 \leq j \leq 16} \rho_{1j})^K} \tag{5.24}$$

We can use the recursive method described in Figure **??** to calculate blocking probabilities. The lower bound of the up and down blocking probabilities is similar to 5.24 except that we set C_{UDL} equal to $C_{UDL}/2$.

We do not show the calculation for the bounds for the other blocking probabilities. Once these blocking probabilities have been calculated, we can obtain the following expressions for the lower and upper bounds.

$$P_{1-2}^{lower} = 1 - (1 - P_{UDL1}^{lower})(1 - P_{ISL}^{lower})(1 - P_{UDL2}^{lower}) \tag{5.25}$$

$$P_{1-2}^{upper} = 1 - (1 - P_{UDL1}^{upper})(1 - P_{ISL}^{upper})(1 - P_{UDL2}^{upper}) \tag{5.26}$$

5.3 Numerical Results

In this section, we compare the upper and lower bound to simulation and exact analytical results.

5.3.1 Single Orbit Case

In this section, we use the constellations that have been described in Section 3.4. We calculated upper and lower bounds for three different traffic patterns for five and 12

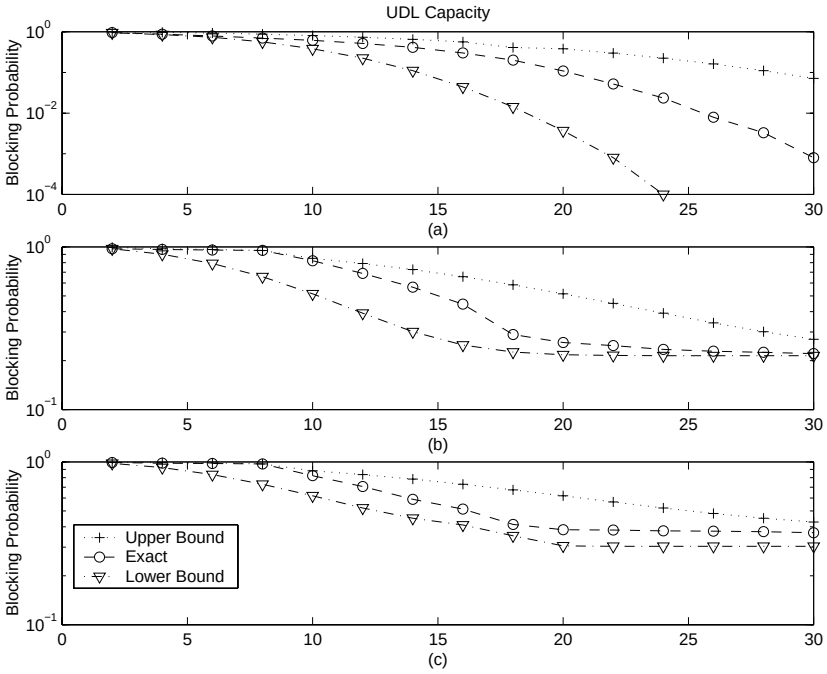

Figure 5.5: Call blocking probability, 5-satellite orbit, $\lambda = 10$, $C_{ISL} = 10$, uniform pattern

satellite systems. For five satellite system, we calculated bounds and compared them with exact results obtained in Section 3.4.1. Note that in all those figures, the y-axis is logarithmic and the x-axis show the UDL Capacity.

Figure 5.5 plots the upper and lower bounds and the exact results for the blocking probability against the capacity C_{UDL} of up-and-down links, when the arrival rate $\lambda = 10$ and the capacity of inter-satellite links $C_{ISL} = 10$, for the uniform traffic pattern. Three sets of plots are shown: (a) for calls originating and terminating at the same satellite, (b) for calls traveling over a single inter-satellite link, and (c) for calls traveling over two inter-satellite links [2]. Each set consists of three plots, one corresponding to blocking probability values obtained by solving the Markov process, and one corresponding to approximate upper bound and one corresponding to approximate lower bound.

From this figure, we observe that, as the capacity C_{UDL} of up-and-down link increases, the exact bound approach the exact values of the blocking probability. In Figure 5.5-a, the bounds appear to be far apart and getting wider. This is because, the y-axis is logarithmic and the scale goes down to 10^{-4}. In Figure 5.5-b, and c, the upper and lower

[2]Recall that these are the only possible types of calls in a 5-satellite orbit using shortest path routing.

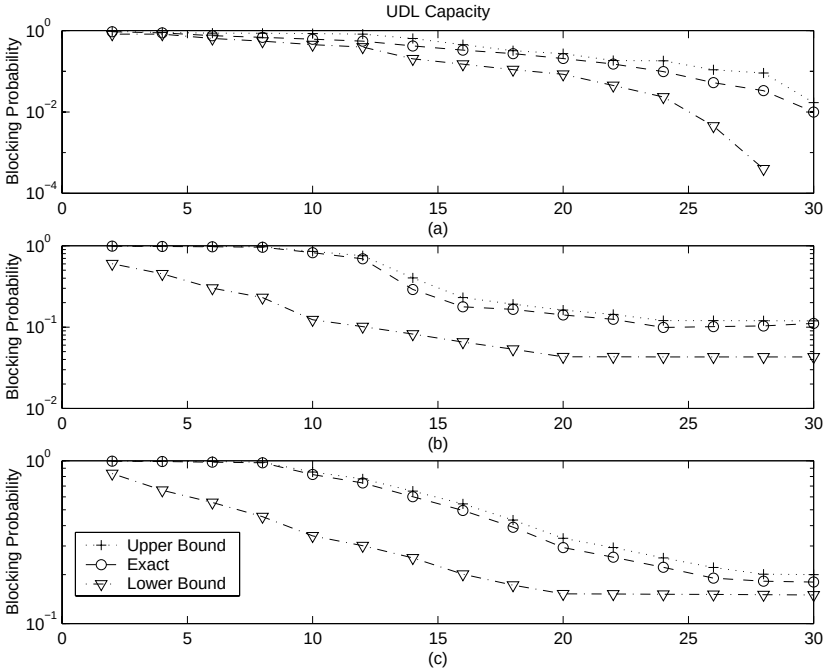

Figure 5.6: Call blocking probability, 5-satellite orbit, $\lambda = 10$, $C_{ISL} = 10$, locality pattern

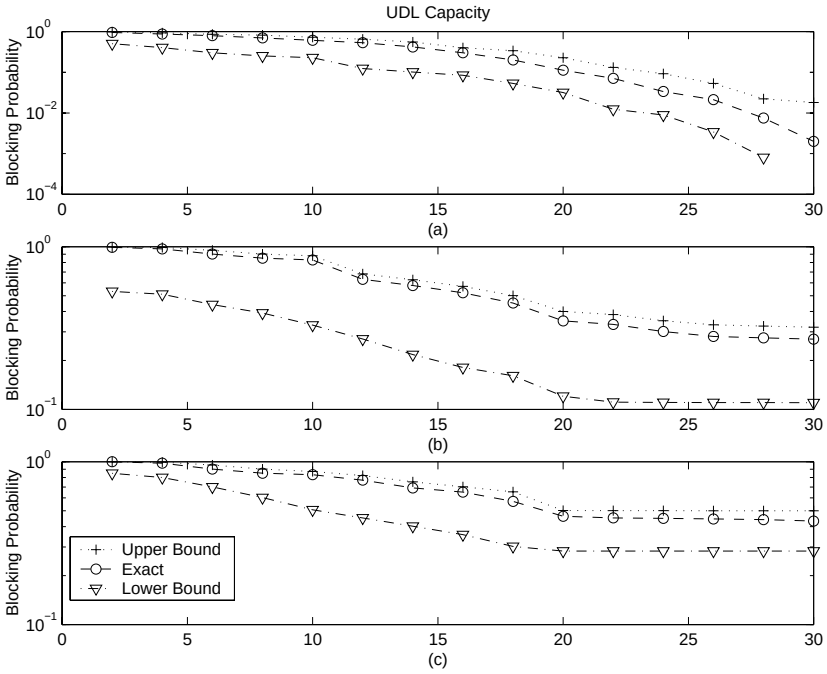

Figure 5.7: Call blocking probability, 5-satellite orbit, $\lambda = 10$, $C_{ISL} = 10$, 2-community pattern

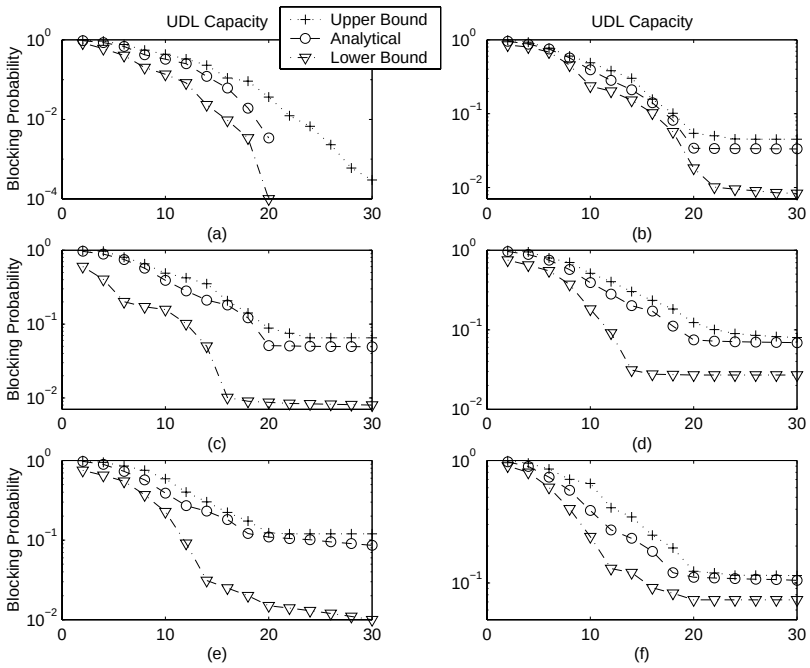

Figure 5.8: Call blocking probability, 12-satellite orbit, $\lambda = 5$, $C_{ISL} = 10$, uniform pattern

bounds converge to each other, and the exact solution stays in between them.

Figures 5.6 and 5.7 show results for the same parameters as in Figure 5.5 for the locality and 2-community traffic patterns, respectively. The curves are similar but the actual blocking probability and bound values depend on the traffic pattern used.

Figures 5.8, 5.9 and 5.10 show the results for 12 satellite orbit for uniform, locality and 2-community traffic patterns, respectively. We used the simulation results instead of exact values. Each figure gives 6 sets of plots; (a) for local calls only, (b) for calls traversing one ISL, (c) for calls traversing 2 ISLs, (d) for calls traversing 3 ISLs, (e) for calls traversing 4 ISLs, and (f) for calls traversing 5 ISLs. Five ISL is the maximum number of hops a call can make using the shortest path routing in a single orbit system with 12 satellites. The parameters used in these tests are similar to the ones in Section 3.4.2. That is $\lambda = 5$, $C_{ISL} = 10$, and C_{UDL} changes from 10 to 50. The y-axis is again logarithmic, and shows the blocking probability. As can be seen in those figures, the upper and lower bounds always stay very close to the simulation results and converge to each other as the UDL capacity increases.

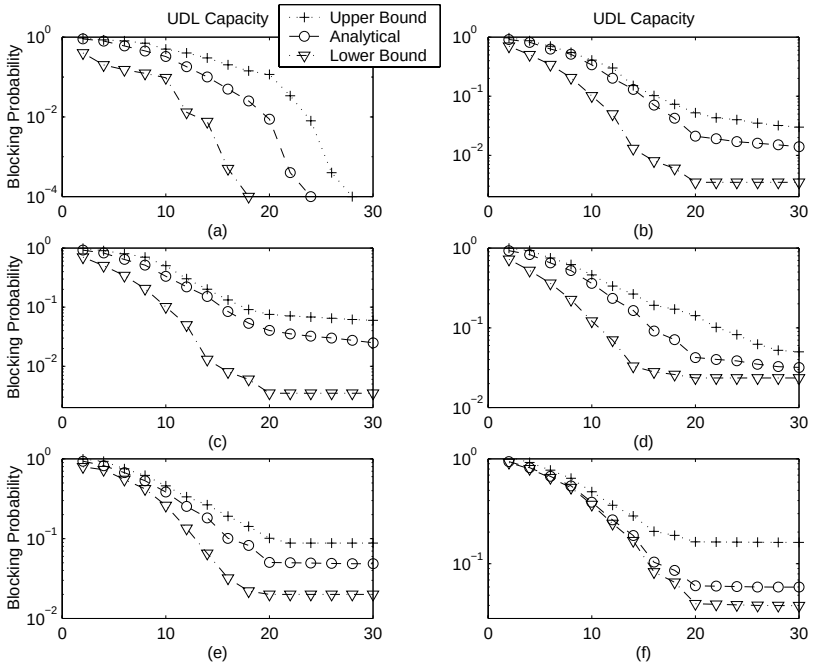

Figure 5.9: Call blocking probability, 12-satellite orbit, $\lambda = 5$, $C_{ISL} = 10$, locality pattern

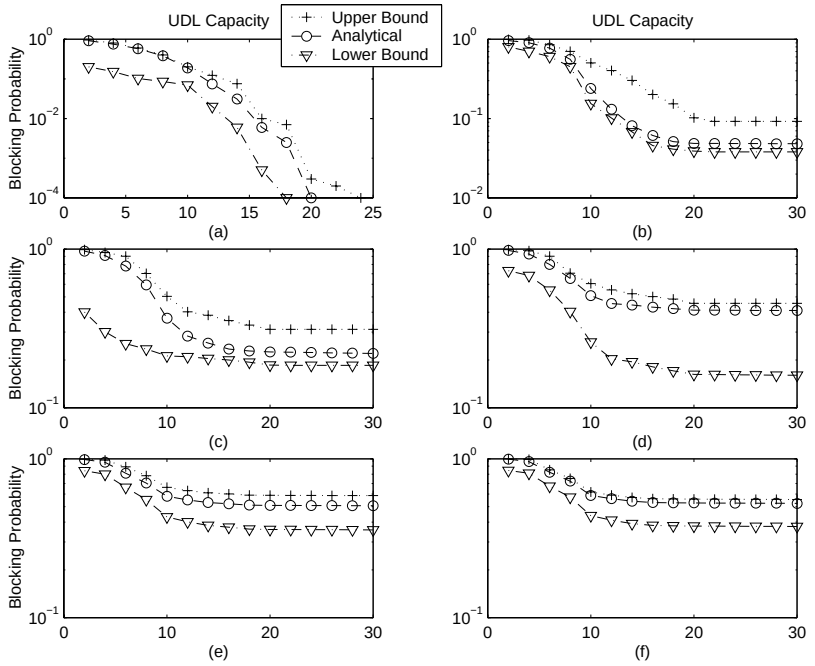

Figure 5.10: Call blocking probability, 12-satellite orbit, $\lambda = 5$, $C_{ISL} = 10$, 2-community pattern

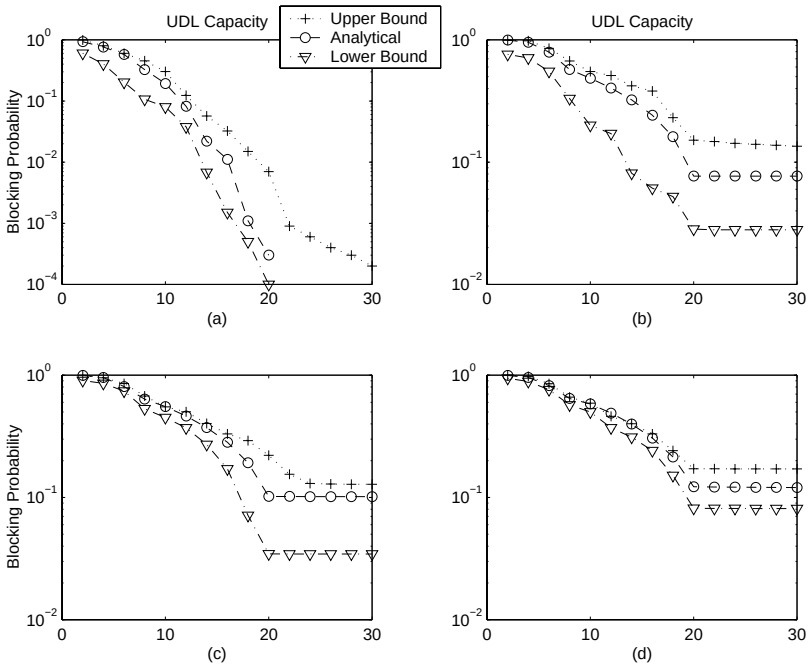

Figure 5.11: Call blocking probability, 16-satellites, $\lambda = 5$, $C_{ISL} = 10$, uniform pattern

5.3.2 Multiple Orbit Case

We used the constellation described in Section 4.1 to validate the accuracy of the bounds in a multiple orbit system. The results are shown in Figures 5.11, 5.12, 5.13, and 5.14. The figures illustrate up-and-down link only calls in (a), one ISL hop calls in (b), two ISL hop calls in (c) and three ISL hop calls in (d). As can be seen in the figures, the upper and lower bounds are very close to the simulation values obtained in Section 4.3 for four different traffic patterns.

5.4 Concluding Remarks

In this chapter, we presented an analytical model for computing upper and lower bounds on blocking probabilities for LEO satellite constellation.

This method can be used to approximate the call blocking probability on LEO satellite constellation with large number of satellites and large number of spot beams per satellite. With the aid of this method, these systems can be analyzed easily representing each spot beam with a satellite and then using the bounds described in this chapter.

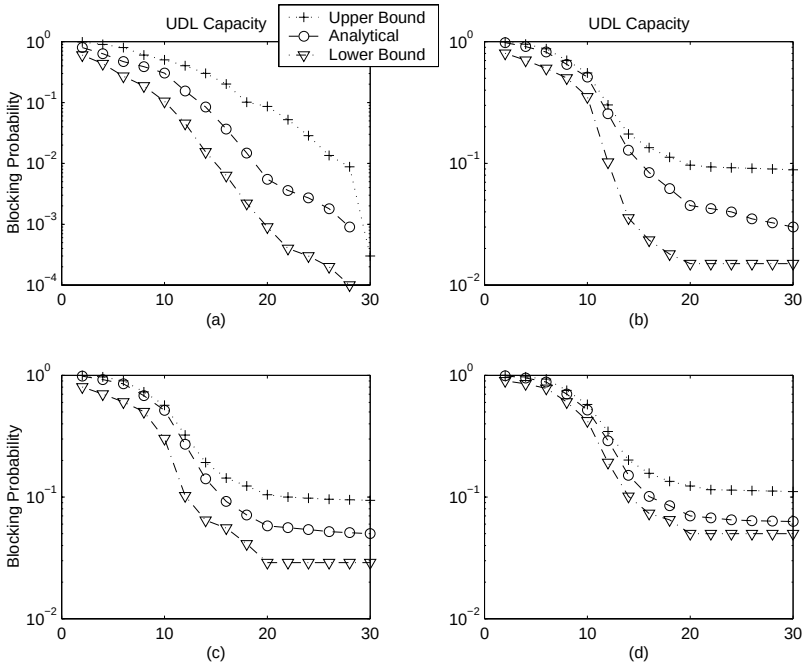

Figure 5.12: Call blocking probability, 16-satellites, $\lambda = 5$, $C_{ISL} = 10$, locality pattern

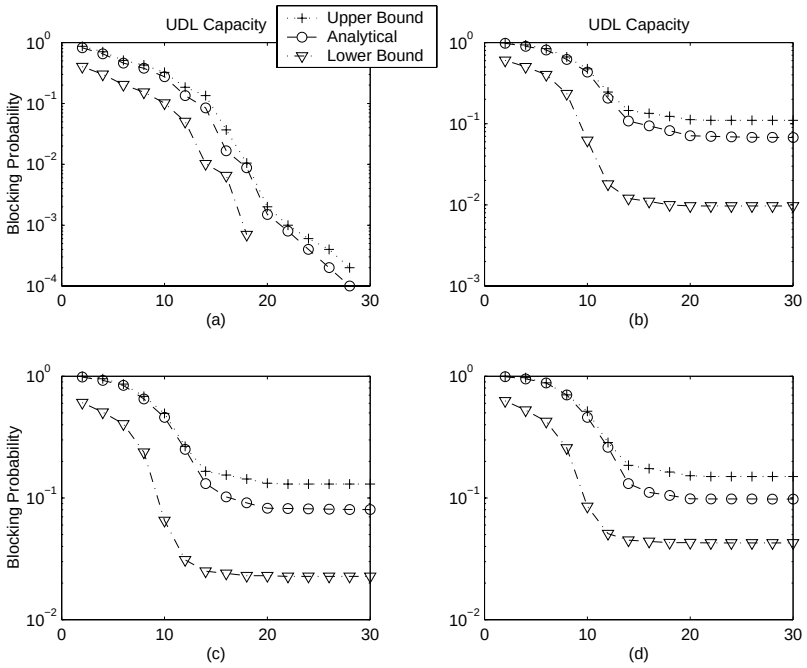

Figure 5.13: Call blocking probability, 16-satellites, $\lambda = 5$, $C_{ISL} = 10$, 4-community pattern

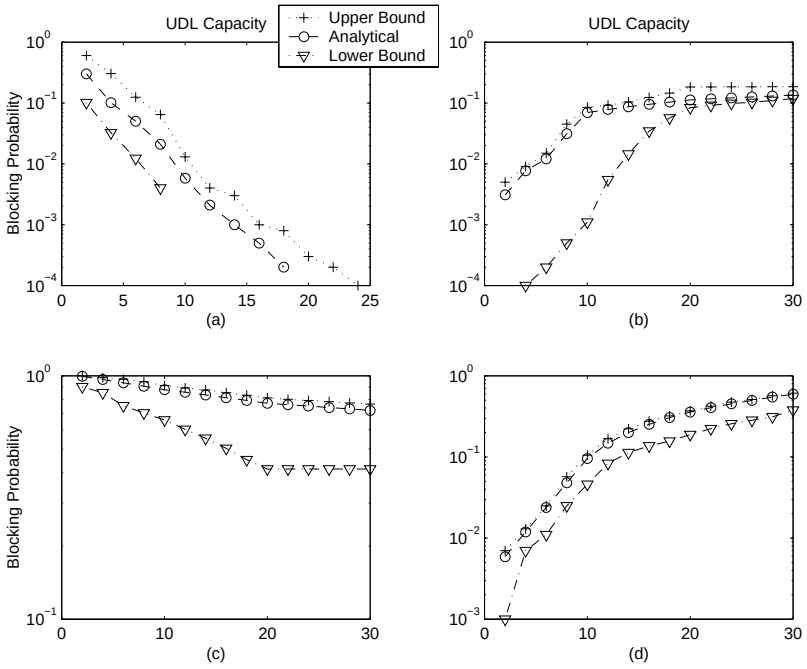

Figure 5.14: Call blocking probability, 16-satellites, $\lambda = 5$, $C_{ISL} = 10$, hot-spot pattern

Chapter 6

Conclusion

In this thesis, we have presented an analytical model for computing blocking probabilities for LEO satellite constellations. We have developed an algorithm for decomposing the whole constellation into sub-systems and then used a Markov Process to solve each sub-system in isolation. In our analysis, we used sub-systems of two satellites for the sake of simplicity although it is possible to increase the sub-system sizes to three satellites plus two fictitious ones. We have also shown how our approach can capture blocking due to hand-offs for both satellite-fixed and earth-fixed orbits. Finally, we have used a distributed method to solve the traffic equations.

In our work, we did not take the seam of a constellation into account. However, the addition of the seam does not pose a problem for our algorithm. The only change would be on the shortest-path algorithm used to define the routes that calls take.

In our models, we have assumed a single beam per satellite. It is straight-forward to extend our decomposition approach to account for multiple beams per satellite (e.g. by considering each beam as one satellite). However, the resulting system would be very complex. Therefore, we investigated an alternative approach to bound blocking probabilities for constellations with multiple beams per satellite. Calculating the upper and lower bound in a cpu-efficient manner gives us the opportunity to analyze large systems with multiple beams per satellite.

6.1 Future Work

6.1.1 Bandwidth Reservation

Our model of satellite-fixed system may be extended by introducing a bandwidth reservation scheme in order to handle hand-off calls with priority over newly generated calls. A first step would be to modify the Markov process discussed in Chapter 3 to incorporate the *guard channel* concept [51]. The guard channel scheme, proposed for cellular systems, reduces forced terminations of hand-off calls by simply reserving a fixed number of channels exclusively for hand-off calls. This reduction of call blocking due to hand-offs is achieved at the expense of the reduction of the total carried traffic, since newly generated calls have access to fewer channels. Modifying the transition rates to account for the guard channels may also produce a queueing network with an (exact or approximate) product-form solution. Once this solution has been obtained and call blocking probabilities (for hand-off or new calls) have been computed efficiently, several important issues including the appropriate number of guard channels, as well as the effectiveness of reserving channels on only the up-and-down links, the inter-satellite links, or both may be investigated.

Although the guard channel scheme is simple to implement, it does not adapt effectively to time-varying traffic conditions, since only local traffic information is considered for call admission. Consequently, a number of reservation schemes have been proposed for wireless networks that make bandwidth reservations by predicting the mobile user's movement ([52]- [55]). The main problem faced by these schemes, however, is how to predict accurately the moving direction of a mobile station. For instance, drivers are very sensitive to traffic conditions, especially in urban areas, and change their route choices accordingly. On the other hand, in a satellite network such as the one we are considering, the direction of satellite movement (equivalent to the direction of users in wireless networks) is fixed, and thus, the probability of hand-offs can be predicted with accuracy. Based on this observation, adaptive bandwidth reservation schemes for LEO satellite systems can be developed.

6.1.2 Heterogeneous traffic in satellite-fixed coverage

A very important assumption we have made for the case of satellite-fixed cells is that the rate at which new calls are issued is the same for the entire globe. Note that our

model for earth-fixed coverage makes no such assumption, and is valid for heterogeneous traffic. This, of course, is not a very realistic assumption. Another important generalization of this thesis would be to analyze the case of heterogeneous traffic. That is, the case where the arrival rates vary over different parts of the globe. This is a rather difficult problem. One way of introducing heterogeneous traffic is to utilize the per orbit decomposition, where we can easily allow a different arrival rate for each orbit. However, this approach does not solve this problem in the general case. Another approach for obtaining a general solution would be as explained below.

First a single orbit may be analyzed assuming one cell per footprint, hand-offs, and different geographic arrival rates. One way to account for the different geographic rates is to segment the street of coverage of the orbit, i.e., the band on the earth covered by the satellites in the orbit, into fixed size regions, each with a different rate of arrival of new calls. In order to analyze a single orbit, we need to know how the footprints of the satellites are related to the regions. For instance, let us consider the footprint of a single satellite, and let us assume that it is over two adjacent regions. Then, we need to know what percent of the footprint is on each region so as to calculate the combined arrival rate to the satellite. As the satellite moves, this percentage changes and the rate of arrivals also changes. In view of this, we need to introduce a variable (call it P) that will give us the position of the satellites in the orbit in relation to the regions in the street of coverage. We note that it suffices to know the position of one satellite in relation to the regions. A discretized approach can be used whereby the movement of the satellites will be done is small discrete steps. If we assume that all the regions have the same length, then each region can be traversed by a satellite in a fixed number of discrete steps. Therefore, variable P can simply assume integer values that indicate the region and the step number within the region for a single satellite.

Using this formulation, a single sub-system of a small number of satellites can be analyzed. In this case, this formulation will lead to a periodic Markov process with a state $(P, \underline{n})$, where $\underline{n}$ is a vector of random variables as in (3.1). Techniques for analyzing such a Markov process numerically by exploiting its periodic structure have been proposed in the literature.

6.1.3 Routing Algorithms and Multicast

Alternate routing and dynamic routing. The call blocking performance of new calls can be improved if alternate or dynamic routing is used. In alternate routing, a set of paths, consisting of a primary path and one or more alternate paths are selected in advance for calls between any pair of satellites. This set is searched in a fixed order when a call request arrives until a path that can accommodate the call is found. Under dynamic routing, the set of paths considered for routing a call is not fixed, but rather, it is determined by the state of the network at the time of the arrival of a call. Our decomposition algorithms may be extended to model fixed alternate routing. The main difficulty in this case is that, while call arrivals to the primary path are Poisson, arrivals to alternate paths (the overflow traffic) are not Poisson. However, for the sake of simplicity, arrivals to alternate paths may be approximated with Poisson with an appropriate rate. It is possible to analyze the system with one primary and m alternate paths by iteratively decomposing it into $m+1$ sub-systems, each corresponding to the satellite constellation using one of the $m+1$ paths, and such that the arrival rates to the l-th sub-system are obtained by the overflow rates of the $(l-1)$-sub-system. Dynamic routing is difficult to model analytically. Therefore, the focus may be to (a) investigate appropriate link metrics to be used for selecting good paths for new calls, and (b) quantify, through simulation, the improvement over alternate routing on call blocking that is possible using dynamic routing, and weight it against the cost of maintaining, updating, and exchanging the state information required for implementing dynamic routing.

Multicast. Due to their broadcast nature, satellite constellations are ideal for carrying multicast calls. For instance, consider a number of users participating in a multicast call, of which m, $m > 1$, are in the same cell. These m users may share a single satellite-to-earth channel, and, depending on the application (e.g., if we assume that at most one participant is active at any given time), they may also share a single earth-to-satellite channel, thereby increasing the call carrying capacity of the constellation. While channel sharing increases the efficiency, it also introduces new problems. Consider satellite-fixed coverage. If one of the m users in the cell must be handed off to another cell (served by another antenna or satellite), then unless another user participating in the same multicast call is already in that cell, a new channel must be assigned to the handed-off user. To the best of our knowledge, the performance of satellite constellations under multicast traffic has

not been studied adequately. In fact, based on the above discussion, modeling the behavior of multicast calls analytically may be a difficult task. However, it is possible to extend the analytical techniques described in this thesis to model a combined load of unicast and multicast traffic. The initial objective will be to efficiently compute the blocking probability of multicast calls. This may then make it appropriate to evaluate the benefits of channel sharing for multicast (as opposed to setting up multiple point-to-point calls). Lastly, it will be of interest to investigate the merits of applying existing multicast tree algorithms for routing multicast calls over a satellite constellation.

Bibliography

[1] http://www.teledesic.com.

[2] Francesco D. Priscoli. Functional Areas for Advanced Mobile Satellite Systems. *IEEE Personal Communications*, December, 1997, pp 34-40.

[3] William W. Wu, Edward F. Miller, Wilbur L. Pritchard, Raymond L. Pickholtz. Mobile Satellite Communications. *Proceedings of IEEE*, Vol.82, No.9, September, 1994, pp.1431-1447.

[4] J.B. Lagarde. Mobile Satellite Communications Services. *Alcatel Reviews*, July, 1997.

[5] John H. Lodge. Mobile Satellite Communications Systems: Toward Global Personal Communications. *IEEE Communications Magazine*, November, 1991, pp.24-30.

[6] Y. Zhang, D.D. Lucia, B.Ryu, S.K. Dao. Satellite Communications in the Global Internet: Issues, Pitfalls, and Potential. *http://info.isoc.org/isoc/whatis/conferences/inet/97/proceedings/F5/F5-1.HTM*

[7] Nils Rydbeck, Sandeep Chennakeshu, Paul Dent, Amer Hassan. Mobile-Satellite Systems: A Perspective on Technology and Trends. *IEEE Vehicular Technology Conference*, vol.2, pp. 1013-1017, 1996.

[8] B.A. Campbell, S.W. McCandless. *Introduction to Space Sciences and Spacecraft Applications.* Gulf Publishing Company, 1996, Texas.

[9] T. Logsdon. *Orbital Mechanics Theory and Applications.* John Wiley and Sons, 1998, Canada.

[10] J.C. Husson. Satellite Constellations. *Alcatel Reviews*, July, 1997.

[11] W.S. Adams, L. Rider. Circular Polar Constellations Providing Continuous Single or Multiple Coverage Above a Specified Latitude. *Journal of the Astronautical Sciences*, Vol. 35, No.2, April-June 1987, pp.155-192.

[12] M. A. Sturza. Architecture of the Teledesic Satellite System. *Proc. IMSC'95*, Ottawa, Canada, June 1995, pages 212-218.

[13] T. Hara. ORBCOMM PCS Available Now! *IEEE MILCOM'95*, vol.2, pages 874-878, 1995.

[14] J. L.Grubb. Iridium Overview: The Traveler's Dream Come True. *IEEE Communications Magazine*, Nov. 1991, pages 48-51.

[15] K.Maine, C.Devieux, P.Swan. Overview of Iridium Satellite Network. *WESCON'95*, pages 483-490.

[16] R. J.Leopold, A.Miller, J. L.Grubb. The Iridium System: A New Paradigm in Personal Communications. *Applied Microwave and Wireless*, 1993, pages 68-76.

[17] F. J. Dietrich, P.Metzen, P.Monte. The Globalstar Cellular Satellite System. *IEEE Transaction on Antennas and Propagation*, Vol. 46, No. 6, June 1998, pp.935-942.

[18] http://www.leoone.com

[19] http://www.skybridgesatellite.com

[20] J.D. Gibson. *The Communications Handbook*, CRC Press, 1997.

[21] M. Werner, A. Jahn, E. Lutz, A. Bottcher. Analysis of System Parameters For LEO/ICO Satellite Communication Networks. *IEEE Journal On Selected Areas In Communications*, Vol.13, No.2, February 1995, pp.371-381.

[22] J. Radzik, G. Maral. A Methodology For Rapidly Evaluating The Performance Of Some Low Earth Orbit Satellite Systems. *IEEE Journal On Selected Areas In Communications*, Vol.13, No.2, February 1995, pp.301-309.

[23] A.Ganz, Y.Gong, B.Li. Performance Study of Low Earth-Orbit Satellite Systems. *IEEE Transactions on Communications*, Vol.42, No:2/3/4, February/March/April, 1994.

[24] A.Jamalipour. *Low Earth Orbital Satellites For Personal Communication Networks.* Artech House Publishers, Boston, 1998.

[25] E.Papapetrou, I.Gragopoulos, F.N. Pavlidou. Performance Evaluation of LEO satellite constellations with inter-satellite links under self-similar and Poisson Traffic. *Int. Journal of Satellite Communications*,Vol.17, pp.51-64,1999.

[26] A.Halim Zaim, George N. Rouskas, Harry G.Perros. Calculation of Call Blocking Probabilities in LEO Satellite Systems: Single Orbit Case. *Technical Report*, NCSU, 2000.

[27] A.Halim Zaim, George N. Rouskas, Harry G.Perros. Calculation of Call Blocking Probabilities in LEO Satellite Systems. *Technical Report*, NCSU, 2001.

[28] V.Santos, R.Silva, M.Dinis, J.Neves. Performance Evaluation of Channel Assignment Strategies and Handover Policies for Satellite Mobile Networks. *Int.Conference on Universal Personal Communications*, 1995, pp.86 -90.

[29] E. D.Re, R.Fantacci, G.Giambene. Different Queueing Policies for Handover Requests in Low Earth Orbit Mobile Satellite Systems. *IEEE Transactions on Vehicular Technology*, Vol.48, No.2, March, 1999.

[30] E. D.Re, R.Fantacci, G.Giambene. Efficient Dynamic Channel Allocation Techniques with Handover Queueing for Mobile Satellite Networks. *IEEE Journal on Selected Areas in Communications*, Vol.13, No.2, February, 1995.

[31] E. D.Re, R.Fantacci, G.Giambene. Call Blocking Performance for Dynamic Channel Allocation Technique in Future Mobile Satellite Systems. *IEE Proc. Commun.*, Vol.143, No.5, October, 1996.

[32] G.Pennoni, A. Ferroni. Mobility Management in LEO/ICO Satellite Systems Preliminary Simulation Results. *PIMRC'94/WCN*, pp.1323-1329, 1994.

[33] F. Dosiere, T.Zein, G.Maral, J. P.Boutes. A Model for the Handover Traffic in Low Earth-Orbiting (LEO) Satellite Networks for Personal Communications. *IEEE Globecom'93*, Vol.1, 1993, pp.574-578.

[34] G.Ruiz, T. L.Doumi, J.G.Gardiner. Teletraffic Analysis and Simulation for Nongeostationary Mobile Satellite Systems. *IEEE Transactions on Vehicular technology*, vol.47, No.1, February, 1998, pp.311-320.

[35] J.Restrepo, G.Maral. Guaranteed Handover(GH) Service in a Non-Geo Constellation with "Satellite-Fixed Cell" (SFC) Systems. *Int. Mobile Satellite Conference*, 1997.

[36] P. J.Wan, V.Nguyen, H.Bai. Advance Handovers Arrangement and Channel Allocation in LEO Satellite Systems. *Global Telecommunications Conference*, Vol.1a, 1999.

[37] V.Obradovic, S.Cigoj. Performance Evaluation of Prioritized Handover Management For LEO Mobile Satellite Systems with Dynamic Channel Assignment. *Global Telecommunications Conference*, Vol.1a, 1999.

[38] M. Werner. A Dynamic Routing Concept For ATM-Based Satellite Personal Communication Networks. *IEEE Journal On Selected Areas In Communications*, Vol.15, No.8, October 1997, pp.1636-1648.

[39] M. Werner, C. Delucchi, H.J. Vogel, G. Maral, J.J. DeRidder. ATM-Based Routing in LEO/MEO Satellite Networks with Intersatellite Links. *IEEE Journal on Selected Areas in Communications*, Vol.15, No.1, January 97,pp.69-81.

[40] M. Werner, G. Berndl, B. Edmaier. Performance of Optimized Routing in LEO Intersatellite Link Networks. *IEEE Vehicular Technology Conference*, 1997, vol.1 pp.246-250.

[41] M Werner, C.Mayer, G.Maral, M.Holzbock. A Neural Network Approach to Distributed Adaptive Routing of LEO Intersatellite Link Traffic. *VTC'98*, 1998, pp.1498-1502.

[42] R. Mauger, C. Rosenberg. QoS Guarantees for Multimedia Services on a TDMA-Based Satellite Network. *IEEE Communications Magazine*, July, 1997.

[43] H.S. Chang, B.W. Kim, C.G. Lee, S.L. Min, Y. Choi, H.S. Yang, D.N. Kim, C.S. Kim. Performance Comparison of Static Routing and Dynamic Routing in Low Earth Orbit Satellite Networks. *IEEE Vehicular Technology Conference*, vol.2, pp.1240-1243, 1996.

[44] H.S. Chang, B.W. Kim, C.G. Lee, S.L. Min, Y. Choi, H.S. Yang, C.S. Kim. Topological Design and Routing for LEO Satellite Networks. *Proc. Of GLOBECOM*, pp.529-235, 1995.

[45] H.S. Chang, B.W. Kim, C.G. Lee, S.L. Min, Y. Choi, H.S. Yang, D.N. Kim, C.S. Kim. FSA-Based Link Assignment and Routing in Low Earth Orbit Satellite Networks. *IEEE Transactions on Vehicular Technology*, Vol.XX, No.Y, 1997.

[46] H. Uzunalioglu, W. Yen. Managing Connection Handover in Satellite Networks. *Proc. IEEE Globecom*, 1997.

[47] H. Uzunalioglu, W. Yen, F. Akyildiz. A Connection Handover Protocol for LEO Satellite ATM Networks. *Proc. ACM/IEEE MOBICOM*, 1997, pp.204-214.

[48] H. Uzunalioglu. Probabilistic Routing Protocols for Low Earth Orbit Satellite Networks. *Proc. IEEE ICC*, 1998.

[49] P. T. S.Tam, J. C. S.Lui, H. W.Chan, C. C. N.Sze, C. N.Sze. An Optimized Routing Scheme and a Channel Reservation Strategy for a Low Earth Orbit Satellite System. *IEEE VTC'99*, Vol.5, 1999.

[50] H. Perros. *Queueing Networks with Blocking: Exact and Approximate Solutions.* Oxford University Press, 1994.

[51] D.Hong, S.S. Rappaport. Traffic model and performance analysis for cellular mobile radio telephone systems with prioritized and nonprioritized handoff procedures. *IEEE Transactions on Vehicular Technology*, VT-35(3):77-92, August 1986.

[52] S.Choi, K.G. Shin. Predictive and adaptive bandwidth reservation for hand-offs in QoS-sensitive cellular networks. *ACM SIGCOMM*, 155-166, September 1998.

[53] S.Choi, K.G. Shin. Comparison of connection admission control schemes in the presence of hand-offs in cellular networks. *ACM/IEEE MOBICOM*, October 1998.

[54] D.A.Levine, I.F.Akyildiz, M.Naghshineh. A resource estimation and call admission control algorithm for wireless multimedia networks using the shadow cluster concept. *IEEE/ACM Transactions on Networking*, 5(1):1-12, February 1997.

[55] M.Naghshineh, M.Schwartz. Distributed call admission control in wireless/mobile networks. *IEEE JSAC*, 14(4):711-716, May 1996.

[56] D.Mitra. Some Results from an asymptotic analysis of a class of simple, circuit-switched networks. *Teletraffic Analysis and Computer Performance Evaluation*, 47-61, 1986.

[57] E.Gelenbe, I.Mitrani. *Analysis and Synthesis of Computer Systems.* Academic Press, 1980.